EFFECT OF INTERFACE ON DEFORMATION AND FRACTURE BEHAVIOUR OF METALLIC MATRIX FIBRE-REINFORCED COMPOSITES

SHOJIRO OCHIAI

1977

Effect of Interface on Deformation and Fracture Behaviour of Metallic Matrix Fibre-Reinforced Composites

by

SHOJIRO OCHIAI

A Thesis Submitted to
Kyoto University
for the Partial Requirements of
the Degree of Doctor of Engineering
1977

CONTENTS

Chapter I

General Introduction

It is well known that strength of pure metals can greatly be enhanced by introducing a high density of dislocations, although pure metals are soft in their purest conditions. The introduction of foreign atoms and fine particles also obstracts dislocation movements and raises the strength of metals. Thus the strengthening mechanisms are directly connected with the restriction of dislocation motion.

In the last fifteen years, an alternative strengthening mechanism "fibre-reinforcement" has been introduced. The basic concept is the production of two or more phase composite structure in which externally applied stress is transferred to embedded fibres with high strength by means of shear traction of matrix. The concept of composite materials has its origin in nature. For instance, some biological materials such as wood and bone are natural composites. The current interest in metallic matrix composites is the result of (i) the discovery that short fibres or whiskers are very strong and (ii) the observation that the properties of fibre-reinforced composites are essentially the same for continuous and discontinuous fibres. High-specific-strength materials such as whiskers and ceramic fibres, which are brittle and therefore notch-sensitive, and also cannot be used in the as-prepared conditions, become available when embedded in ductile matrix, which transferres applied stress to fibres and arrests cracks formed by earlier fracture of the weaker fibres.

A large number of experiments have been carried out to

produce high-specific-strength composites. Many experimental results, however , showed that the strength of composites behaved very erratically and did not obey the simple basic theory. Much of the above erratical results was based on the difficulty to obtain suitable interfacial conditions, with a resulting premature failure of composites.

Composites, by difinition , are heterophase materials and therefore interfaces are an inherent feature of their structure. The constituents have to be compatible with each other both mechanically and chemically. The mechanical compatibility problems, concerning with stress transfer mechanisms, mechanical interactions between the constituents and fracture mechanisms, are associated with differences of Young's modulus, Poisson's ratio, bulk modulus, rigid modulus, ductility and thermal coefficient between fibres and matrix. It should be noted that mechanical compatibility is strongly affected by interfacial conditions. For instance, interfacial conditions affect stress transfer mechanisms since stress transfer from matrix to fibres is carried out through interfaces. Also mechanical interactions between the constituents take place through interfaces and, under certain interfacial ccnditions, these interactions make mechanical behaviour of composites much different from that expected by each property of the constituents. Thus, mechanical compatibility problems should be discussed in accordance with interfacial conditions. The chemical compatibility problems relate to interfacial bonding and interfacial chemical reactions. In "in-situ" composites which are fabricated by unidirectional solidification of eutectic alloy, the two phases are in thermodynamic equilibrium at the fabrication temperature and therefore they are stable. In artificial composites, the two phases are not in the

thermodynamic equlibrium and chemical reaction takes place at interfaces. When fibres do not wet to matrix, as is often found in ceramic fibre/metal matrix composites, consolidation is very difficult. For this case, interfacial reaction yields a good wetting. However, in most cases, interfacial reaction degrade composite's properties, even if good bonding can be obtai

Up to date, mechanical and chemical compatibility problems have been widely investigated. However, there still exsist man uncertainties about deformation and fracture behaviour of composi concerning with the compatibility problems. As the above compatibility problems are closely related with interfacial conditions, a detailed investigation of effects of interfacial conditions on mechanical behaviour is needed.

The purpose of this paper is to understand, more precisely, the effects of interfacial conditions on deformation and fracture behaviour of composites by solving above uncertainties. For the above purpose, some single fibre-composites, together with multi fibre-ones, were used, since effects arising from existenc of other fibres,(such as complex triaxial stresses arising from long-range interactions between the components, propagation of cracks formed by failure of weaker fibres and cumulative fracture of fibres), could be eliminated by employing single fibre-composites. This approach will make it possible to understand the independent role of interfaces on mechanical behaviour of composites.

In chapter II, deviations of composite's behaviour from the rule of mixtures, which of course are affected by interfacial conditions, are considered. The present work deals with two positive deviations, strengthening effects of brittle zones on ductile fibre-composites and multiple necking of fibres,both o

which are derived from mechanical interactions between the constituents. In chapter III, interfacial shear stress and critical aspect ratio, which are the most important parameters for stress transfer from matrix to fibres, are measured by using a multiple-fracture test and a pull-out test for various types of interfacial conditions. The effects of interfacial conditions on stress transfer mechanisms are clearly described. In chapter IV, the investigation of effects of interfacial reaction on mechanical behaviour of composites is presented. Deformation and fracture behaviour of composites is discussed in detail for various types of reaction. In chapter V, the study of cold rolling characteristics of ductile fibre-composites with and without reaction zones at interfaces is presented. The role of reacted interfaces is also discussed. In chapter VI, the conclusions of this thesis are summarized.

Finally let's review the outline of theory of reinforcement.

(1)Stress-strain behaviour

McDanels et al[1] showed first that rule of mixtures (hereafter described as ROM) is valid for tensile strength by using W/Cu composites and subsequently extended the same rule to relate the yield strength and the mudulus of elasticity. The ultimate tensile strength (UTS) of continuous fibre-composite, σ_c ,is represented by

$$\sigma_c = \sigma_{fu}V_f + \sigma_m^* V_m \qquad \text{for } V_f > V_{min} \qquad (1)$$

where σ_{fu} is the UTS of the fibre, σ_m^* is the stress on the matrix at fracture strain of the fibre, V_f and V_m are volume fractions of the fibre and the matrix, and V_{min} is the minimum fibre volume fraction necessary to reinforce the matrix material, which will be explained later. The stress-strain behaviour of composites has been [illegible]d of four stages. For low strain below the

onset of plastic deformation of the matrix, both the components deform elastically (stage I). As composites are strained further, the matrix becomes plastic while the fibre is still elastic (stage II). With further strain, both the fibre and the matrix undergoes plastic deformation (stage III). Finally, both the fibre and the matrix begin failing (stage IV). Deformation behaviour in each stage is described as follows.

(1)-(I)Stage I

On the basis of ROM, the Young's modulus E_c^I of composites is represented by

$$E_c^I = E_f V_f + E_m V_m \qquad (2)$$

where E_f and E_m are Young's moduli of the fibre and the matrix respectively. However, eq.(2) is not strictly precise since the mechanical interactions between the fibre and the matrix are not taken into consideration. Paul[2] obtained a lower- and a upper bounds of E_c^I by using the theorem of least work and that of minimum potential energy,respectively. Hashin and Shtrikman[3] applied variational approach and obtained more close bounds. Hill[4] considered that the two basic properties of the composite are the bulk mudulus and the shear modulus, the other moduli being defined in terms of these. Their solutions showed deviation from ROM, though the deviation is relatively minor.

(1)-(II)Stage II

As the matrix undergoes plastic deformation, the secondary modulus E_c^{II} is represented by

$$E_c^{II} = E_f V_f + (d\sigma_m/de) V_m \qquad (3)$$

where $d\sigma_m/de$ is the slope of the stress-strain curve for the matrix. The work-hardening capacity of most metals is such that the term $(d\sigma_m/de)V_m$ is negligible in comparison to E_fV_f. Thus eq.(3) is approximated to

$$E_c^{II} = E_fV_f \qquad (4)$$

Deviations from eqs.(3) and (4) have been reported[5][6]. Also theoretical analyses have been carried out by many authors.[5]-[12] Two factors causing the devistions have been pointed out : constraint effect arising from the different lateral contractions between the fibre and the matrix[5]-[8] and the pile-up of dislocations on the fine fibres (dispersion hardening effect).[9]-[12] Up to date, these factors have been discussed in detail but not have been made clear yet.

(1)-(III)Stage III

Both the components deforming plastically, σ_c is expected to obey ROM relation, since Poisson's ratio become 0.5 in both the fibre and the matrix. However, actual deformation mode often deviates from the performance of the constituents with respect to necking or other inhomogeneous plastic flow.[13]-[15] Piehler[15] showed that necking of the fibre is arrested if the interfacial bonding is strong enough. Mileiko[16], and Garmong and Thompson[17] applied the plastic instability approach to the composites with strong interfacial bonding in order to describe the UTS and elongation , and obtained good results.

(1)-(IV)Stage IV

During this stage, the fibres contained in composites fail successively in some cases.[18]-[20] On the other hand, in other cases, the cracks formed by fracture of weaker fibres propagate into matrix and no successive fracture of fibres occurres.[21]-[24] Fracture of composites has been studied by applying the fracture

mechanics theory[21]-[24] and statistical one.[25][28] However, there still exist much uncertainties since fracture behaviour is very complex associated with fracture of fibres and matrix, debonding of fibres from the matrix, pull-out of fibres and mechanical interaction between the constituents.

(2)Strength based on ROM

At lower volume fraction, the matrix can work-harden sufficiently after fracture of the fibre to bear the applied load alone.[18] In such a case strength of composites cannot be represented by eq.(1). The σ_c is given by

$$\sigma_c = \sigma_{mu} V_m \qquad (5)$$

where σ_{mu} is UTS of the matrix. Therefore V_f should be greater than a certain value, V_{min} , to give rise to reinforcement. V_{min} is given by

$$V_{min} = \frac{\sigma_{mu} - \sigma_m^*}{\sigma_f + \sigma_{mu} - \sigma_m^*} \qquad (6)$$

If the fibre is ductile, when contained in composites , it can be elongated beyond the strain at which it starts to neck and subsequently fail when tested alone.[13]-[15][29] In such a case V_{min} does not appear. The above situations are illusted in Fig.

(3)Stress-transfer mechanism

(i)Continuous fibre-composites

When the fibre is continuous throughout the whole length of the specimen, load can be applied directly to it. Only a little stress is transferred by the matrix.

(ii)Discontinuous fibre-composite

Cox[30] presented a theory for the case of the fibre and the matrix in the elastic state on the assumption that (1)interfacial bond is perfect and that (2)lateral contractions of the components

are equal. The applied stress is transferred by shear in the matrix through the interface. The theoretical variations of tensile stress in the fibre σ_f and shear stress at the interface τ are established. Dow[31] and Rosen[25] presented the different treatments, which give the result similar to that of Cox.

Perhaps a much more significant case for metallic matrix composites includes that the fibre deforms elastically and the matrix plastically. Kelly[32] considered this case. The stress of σ_f in the fibre at a distance x from the end of the fibre is given by

$$\sigma_f = 4\tau x/d \qquad (7)$$

where τ and d are the shear stress at the interface and fibre diameter, respectively. If the fibre is longer than a critical length $\underline{l}_c$ given by

$$\underline{l}_c/d = \sigma_{fu}/2\tau \qquad (8)$$

where σ_{fu} is UTS of the fibre and $\underline{l}_c/d$ is so-called "critical aspect ratio", the shear stress builds up sufficient tensile stress to break the fibre.

(4)UTS of discontinuous fibre-composites

To continuous fibre-composites, eq.(1) is applicable as described already. For discontinuous fibre-composites, two regions must be considered according with the fibre length $\underline{l}$.

(i) $\underline{l} > \underline{l}_c$; The UTS of the fibre can be utilized and hence eq.(1) is modified to

$$\sigma_c = \bar{\sigma}_f V_f + \sigma_m^* V_m \qquad (9)$$

$\bar{\sigma}_f$ is average stress in the fibre and is calculated by

$$\bar{\sigma}_f = (1 - \underline{l}_c/2\underline{l})\sigma_{fu} \qquad (10)$$

(ii) $\underline{l} < \underline{l}_c$; The UTS of the fibre is not achieved. $\bar{\sigma}_f$ is represented by

$$\bar{\sigma}_f = \tau\underline{l}/d \qquad (11)$$

The UTS of composites is known by substituting eq.(11) into eq.(9).

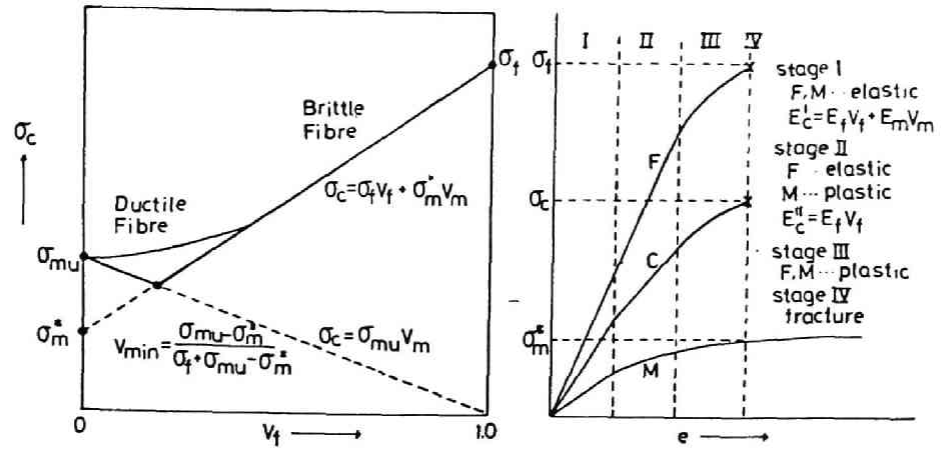

Fig.1 Theoretical variations of UTS of composites composed of both brittle and ductile fibres with fibre volume fraction and schematic illustration of four stages of deformation and fracture of composites

References

(1)D.L.McDanels, R.W.Jech and J.W.Weeton:Trans. Met. Soc. AIME 233(1965),636.

(2)B.Paul:Trans. Met. Soc. AIME, 218(1960),36.

(3)Z.Hashin and S.Strickman:J. Mech. Phys. Solids,10(1962),235.

(4)R.Hill:J. Mech. Phys. Solids,12(1964),199.

(5)A.Kelly and H.Lilholt:Phil. Mag.,20(1969),311.

(6)A.Kelly:Strengthening Methods in Crystals, Ed. by A.Kelly and R.B.Nicholson, Elsevier (1971), p.439.

(7)A.J.M.Spencer:Interna. J. Mech. Sci.,7(1965),197.

(8)J.F.Mulhern, T.G.Rogers, and A.J.M.Spencer:J. Inst. Maths. Applics.,3(1967),21.

(9)G.Garmong and A.Shepard:Met. Trans.,2(1971),175.

(10)B.J.Shaw:Acta Met.,15(1967),1169.

(11)H.E.Cline and D.F.Stein:Trans. Met. Soc. AIME, 345(1969),841.

(12)E.R.Thompson and F.D.Lemkey:Met. Trans.,1(1970),2799.

(13)R.M.Vennett, S.M.Volf and A.P.Levitt:Met. Trans.,1(1970),1569.

(14)C.Schoene and E.Scala:ibid.,3466.

(15)H.R.Piehler:trans. Met. Soc. AIME,233(1965),12.

(16)S.T.Mileiko:J. Mat. Sci.,4(1969),974.

(17)G.Garmong and R.B.Thompson:Met. Trans.,4(1973),863.

(18)A.Kelly:Proc. Roy. Soc.,282A(1964),63.

(19)F.D.Lemkey and E.R.Thompson:Met. Trans.,2(1971),1537.

(20)P.W.Heitman, L.A.Shepard and T.H.Courtney:J. Mech. Phys. Solids, 21(1973),75.

(21)M.R.Piggot:J. Mat. Sci.,5(1970),669.

(22)W.W.Gerberich:ibid.,283.

(23)W.W.Gerberich:J. Mech. Phys. Solids,19(1971),71.

(24)D.C.Phillips:J. Mat. Sci.,7(1972),1175.

(25)B.W.Rosen:Fiber Composite Materials, ASM,Ohio, (1965),p.37.

(26)D.E.Gücer and J.Gurland:J. Mech. Phys. Solids,10(1962),365.

(27)C.Z.Weben and B.W.Rosen:J. Mech. Phys. Solids,18(1970),189.

(28)V.R.Riley and J.L.Reddaway:J. Mat. Sci.,3(1968),41.

(29)I.Ahmad and J.M.Barranco:Met. Trans.,1(1970),989.

(30)H.L.Cox:Br. J. Appl. Phys.,3(1953),72.

(31)G.S.Holister:Fibre Reinforced Materials, Elsevier, (1966),p.14.

(32)A.Kelly and W.R.Tyson:J. Mech. Phys. Solids,13(1965),329.

Chapter II

Deviations of Mechanical Behaviour of Composites from the Rule of Mixtures

II -(1) Introduction

In almost all composites, deviations of mechanical behaviour from ROM exist, even if they are so small that they are not able to be detected. Some factors that could conceivably produce deviations are following : mechanical interaction between the fibres and matrix,[1)-(13)] interfacial reaction,[14)-(28)] thermal expansion effects,[29)-(36)] size effects,[13)(37)-(39)] and probably other effects. The above factors are relevant to interface. For instance, mechanical interaction between fibres and matrix is derived from the difference of Poisson's ratio between them[1),(2)-(6)] if the interfacial bonding is strong enough. If the interfacial bonding is weak, tensile stress exerted on the interface in multi-fibre-composites[6)(9)] will break the interface and therefore the mechanical interaction will disappear. Interfacial reaction is literally related to changes of interface. Thermal expansion effects also change interfacial conditions since the thermally induced stresses due to the difference of thermal coefficient between fibres and matrix are exerted at interfaces. The size effects are concerning with the pil-up of dislocations on fine fibres. For the effects,strong interfacial bond is necessary, otherwise interfaces might be sinks of dislocations. Thus, interfacial conditions are closely related with the deviations.

If deviations are positive from the rule of mixtures, they are not only interesting but also available for developments of practical composites. This chapter deals with two positive deviations, i.e. strengthening effect of the brittle zones on ductile fibre-composites and multiple necking phenomenon of fibres in composites in the former and the latter parts, respectively. In this work, single fibre-composites were used to eliminate the complex effects of the triaxial stresses and fracture mechanisms due to existence of many other fibres.

II-(2) Strengthening Effects of Brittle Zones on Ductile Fibre-Composites

II-(2)-1 Introduction

Chemical reactions at the fibre/matrix interface are known to be one of the factors reducing the strength of composites.[14]-[27] The formation of brittle zones by chemical reaction weakens the composites through multiple fracture of zones, since the fractured zones cannot carry the applied load. Thus the tensile strength of composites decreases with increasing volume fraction of brittle zones.[21][24][27] On the other hand, in some composite systems, brittle zones of an appropriate thickness improve the strength of composites[23]-[26]. This has been interpreted either as an increase of the interfacial bonding strength[23][25], or as a high strength of the brittle zones.[26][28] But it is found that composites which have cracked brittle zones show a higher strength than identical composites lacking zones and therefore neither of the above interpretations has proved applicable.

Recently Thornton and Thomas[40] have discussed the strengthening effects of brittle zones in theory and by experiment, using an aluminium-alumina composite. However, their theoretical treatment is not complete since it does not take into account those surface regions of the fibres exposed by fracture of the brittle zones. It ought to show that a large contribution to the strength of the sample is due to these exposed regions, and it needs to apply the idea of the constraint effect well-known in notched materials.[41][42] In fact, a high measured value of uniaxial tensile strength could not be explained if this contribution were neglected, since an

externally applied load is carried only by the aluminium fibre in these regions.

The purpose of this part is to present another strengthening mechanism of brittle zones on ductile fibre-composites; and to make clear the conditions under which the constraint effect well-known in notched materials[41][42] can exist.

The experiment was carried out using a single fibre-composite with two components : a brittle outer component and a ductile core. Therefore no effects due to neighbouring fibres or to numenrous components[9][36][43] need enter discussion of the mechanical behaviour of the present fibre-composites.

II-(2)-2 Experimental Procedure

Two kinds of brittle elastic-case/ductile-core composites were used in this experiment : An aluminium composite and a stainless steel one.

The aluminium composite was obtained by anodic oxidation of electropolished 1100 aluminium fibres with a nominal diameter of 800μm. The thickness of the oxide(alumina) coating was controlled by varying the anodizing times. The anodizing condition was 20 V at 0 °C and the electrolyte was 20 wt % sulphuric acid solution.

The stainless steel composite was prepared by extracting stainless steel fibres coated with a ternary (Fe,Cr)Al intermetallic brittle zone[27] from hot-pressed and annealed austenitic steel (nominally 200μm)-aluminium composites. Various thicknesses of coating were obtained by changing the annealing times at 600°C.

The mean UTS and normal elongation were 9.0 kg/mm^2 and 32.5%

for aluminium fibre, and 87 kg/mm^2 and 67% for stainless steel fibre, respectively. Both fibres were considered to be insensitive to a notch effect since they were ductile. Load-elongation curves were obtained for both bare and coated fibres. The strain rate was controlled to 5% per min.

The crack densities in the brittle zones were measured micrographically during deformation and after fracture of the composites. The surface of the composites was examined by a scanning electron microscope.

II-(2)-3 Results

II-(2)-3-(i) Aluminium-Alumina Composites

The appearance of the alumina film away from the fracture surface is shown in Photo.1(a)-(d) for various initial volume fractions of the brittle alumina zones, V_b^o. Crack density becomes lower as the thickness of alumina film increases. Longitudinal defects were clearly discerned in the thicker alumina film (Photo.1(d)). These were, however, formed not during the tensile test but during specimen preparation, as was ascertained micrographically. The number of cracks per mm, N , was measured as a function of elongation, as shown in Fig.1. The number of cracks, N′, after the fracture of composites was also measured as a function of V_b^o as shown in Fig.2. The value of N′ decreased with increasing V_b^o. The changes of σ_c and e_c with V_b^o are shown in Fig.3, where σ_c is the UTS of composites and e_c is the normal elongation at σ_c.

When multiple cracking occurs in the alumina film before the fracture of aluminium fibres, σ_c must follow the rule of mixtures

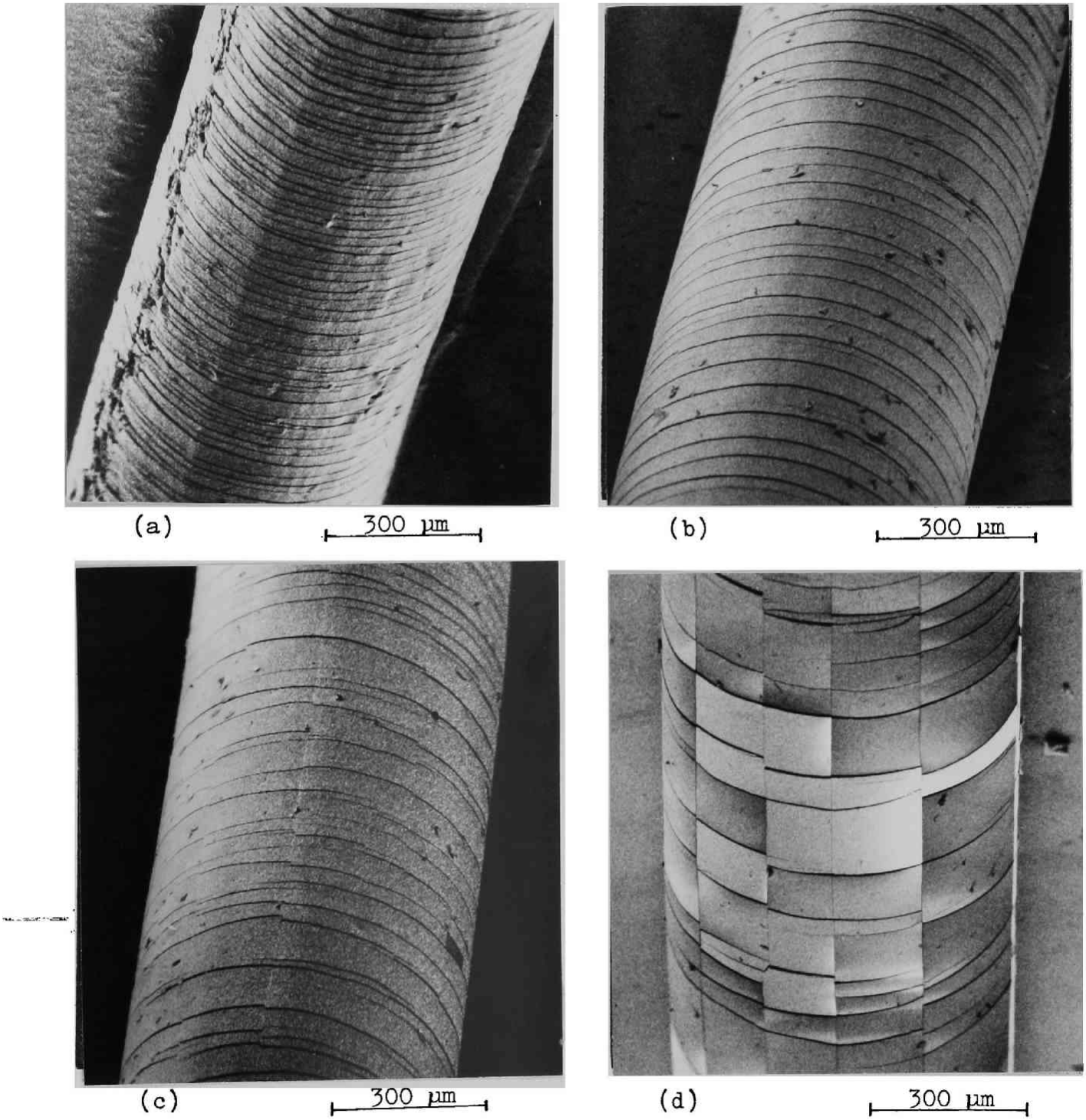

Photo.1 Appearance of alumina films away from fracture surfaces. V_b^o = (a) 0.012, (b)0.040, (c) 0.076, (d)0.229.

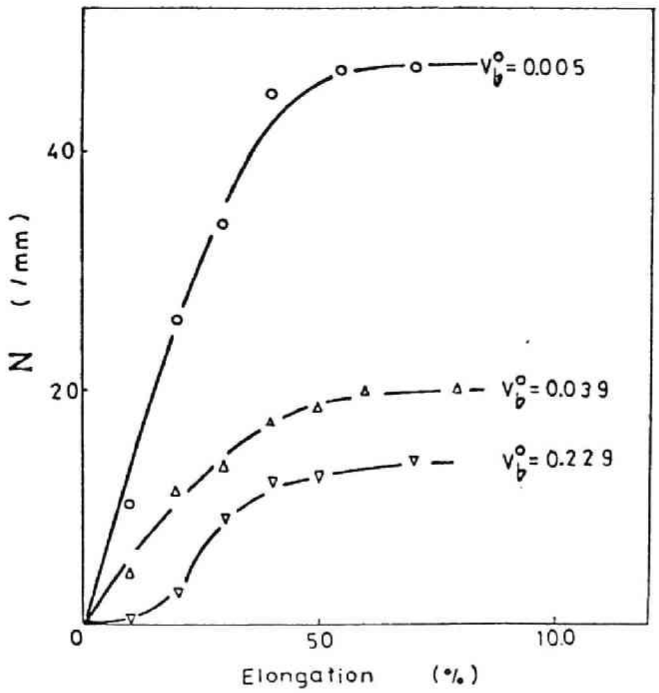

Fig.1 Number of cracks per mm in deformed Al-alumina composites as a function of elongation.

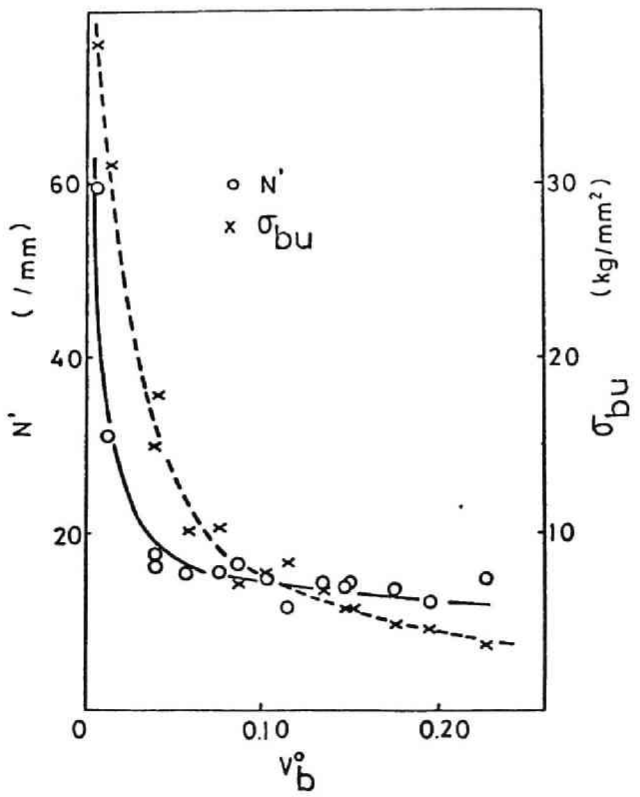

Fig.2 Number of cracks per mm in fractured Al-alumina composites and calculated strength of alumina film, σ_{bu} , as a function of V_b^o.

(ROM) : [44][45]

$$\sigma_c(\mathrm{ROM}) = \sigma_{fu} V_f^o \qquad (1)$$

where σ_{fu} is the UTS of Al fibre measured on unnotched sampls. However, the measured values of σ_c were higher than σ_c(ROM). The tensile stress of an Al fibre is given by σ_c/V_f^o on the basis of the original cross-section of the Al fibre. This is also presented in Fig.3. The values of σ_c/V_f^o were higher than σ_{fu}. Thus, the strengthening of the Al fibre by the alumina film is evident even though multiple crackings occured in the alumina film.

II-(2)-3-(ii) Stainless Steel-Intermetallic Compound Composites

Photo.2(a)-(c) are micrographs of the surface of brittle intermetallic zone 47.5μm thick, taken at various stages of elongation. The brittle zone began spalling at 6-7% elongation. The curves of UTS, σ_c and $\sigma_{5\%}$(normal stress at 5% elongation) versus V_b^o are shown in Fig.4, together with σ_c/V_f^o and $\sigma_{5\%}/V_f^o$. The measured values of $\sigma_{5\%}$ and $\sigma_{5\%}/V_f^o$ were higher than those predicted by ROM, just as with the aluminium- alumina composite(Fig.3). However, σ_c decreased linearly with increasing V_f^o, following ROM (eq.(1)), and σ_c/V_f^o showed a constant value equal to the UTS of the samples with $V_b^o=0$ and to that of unnotched samples. No positive deviation from ROM was found, indicating that the strengthening effect had vanished after spalling (or fracture, as shown later) of the brittle zone.

II-(2)-4 Discussion

If the fibres are brittle, and hence notch-sensitive, the formation of notches by multiple cracking of the coatings will

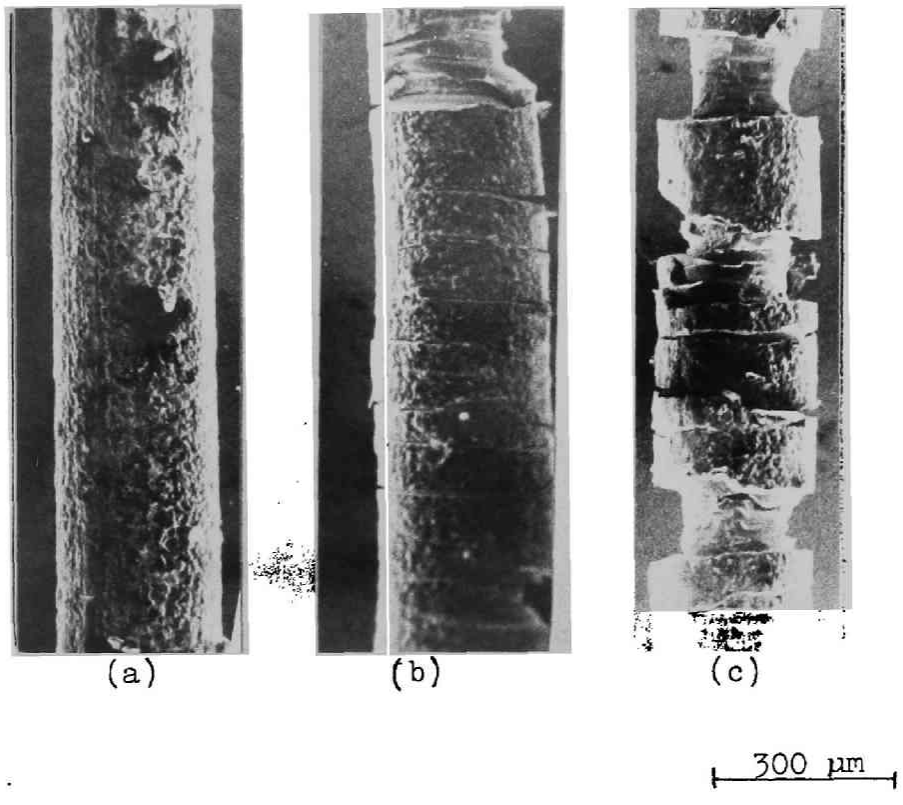

Photo.2 Appearance of intermetallic compound zone 47.5 μm thick at (a)0%, (b)6%, (c)20% elongations.

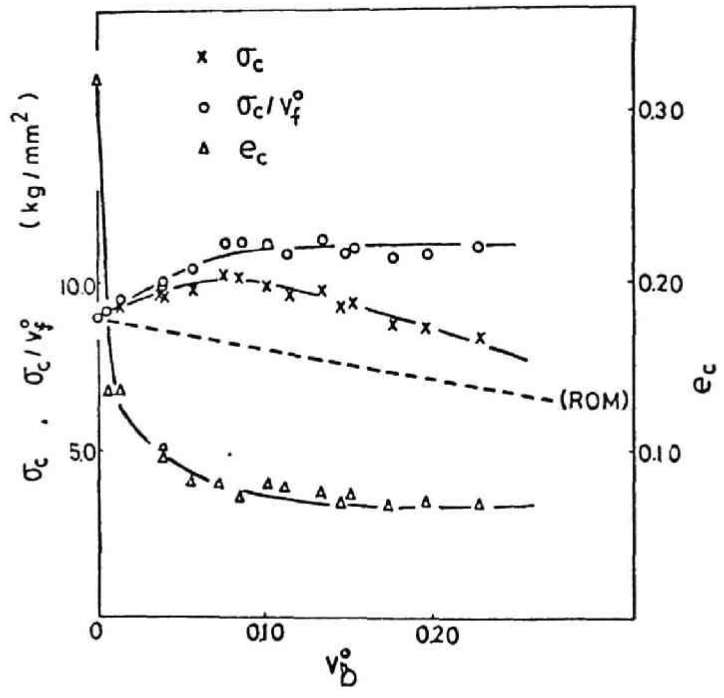

Fig.3 Measured values of σ_c and e_c of Al-alumina composites versus V_b^o.

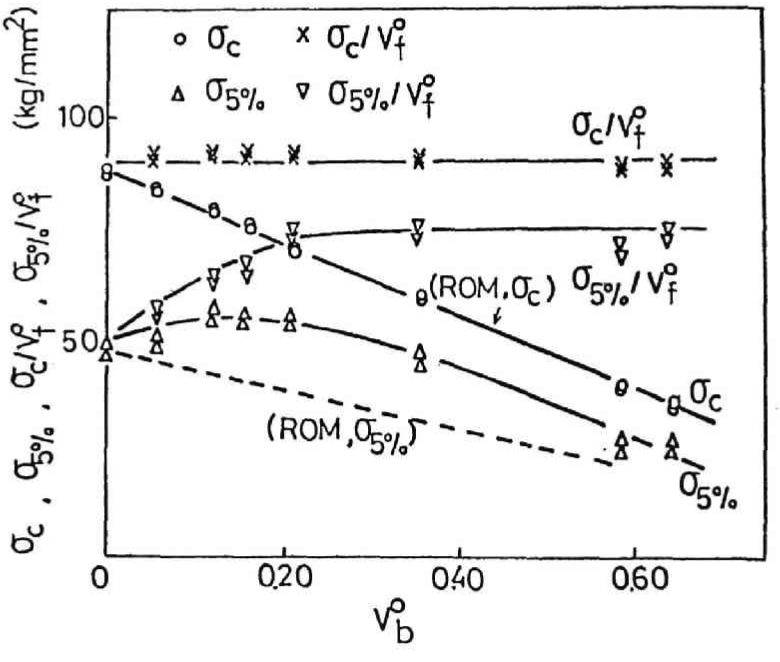

Fig.4 Measured values of σ_c, $\sigma_{5\%}$, σ_c/V_f^o and $\sigma_{5\%}/V_f^o$ of stainless steel-intermetallic compound composites versus V_b^o.

hasten a fracture of the fibres. Because of a high stress concentration at the notches, the fibres cannot support loads up to their full strength and the UTS of such composites will be lower than that of composites without brittle zones.[24][46][47]

Conversely, for ductile fibres the formed notch plays a role in strengthening the composite under certain conditions.

II-(2)-4-(i) Theory

A model, shown schematically in Fig.5, was employed to analyse the strengthening effects of brittle zones on ductile fibre-composites. The composite consists of two regions : Region I composed of an inner core of ductile fibre (`f´ in the figure) and outer sleeve of the brittle zone (`b´): Region II formed by the microcrackings of the brittle zone. ε_I is the true axial strain in the fibre in I, and r_f and r_b are radii of the fibre and the composite, respectively, with a strain ε_I. P is the true radial stress at the fibre/zone interface.

When notches are formed on a ductile fibre surface by multiple cracking in the brittle zone, they will introduce a constraint effect in Region II, which should raise the yield- and tensile strengths of the fibre. The conditions under which the constraint effect can exsist will be equal to those under which composites can be strengthened. The micro-fractured brittle zone in Region I, however, should adhere to the fibre in order to produce this effect. Otherwise the fibre bears the same load as that measured by the unnotched sample. Furthermore, a compressive transverse stress will be exerted on the brittle zone in Region I. When this compressive stress exceeds the compressive endurance of the brittle zone, the zone will be fractured in a transverse direction. In such a case, the constraint effect in Region II will fall off.

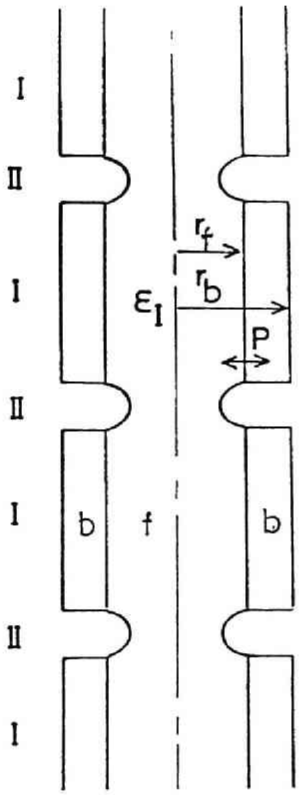

Fig.5 Model for thiaxial stress analysis.

As shown later, the constraint effect remains until the brittle zone is spalled or fractured by the compressive stress. The important parameters associated with this effect in Region II will be P and the maximum compressive stress, $\sigma_{\theta,max}$, in the brittle zone in Region I. These can be calculated as follows.

Assuming a uniform axial stress and strain in Region I, an equilibrium equation for I is

$$\frac{d\sigma_r}{dr} + \frac{\sigma_r - \sigma_\theta}{r} = 0 \qquad (2)$$

where r is the radius and σ_r and σ_θ are radial and transverse stresses, respectively. To solve eq.(2), we employ the following boundary conditions, which are similar to those used by Thornton and Thomas[40]: (i)the radial stress is zero at the outside surface of `b′; (ii)the radial stresses in `f′and `b′ are equal at the interface; (iii)the axial strain of `f′ is ε_I , where the subscript I refers to Region I, and the fracture strain of `b′ in an axial direction is ε_{bu}.

We can obtain σ_r, σ_θ, and the axial stress σ_z for both components as follows :

$$\begin{aligned}
\sigma_r(f) &= P \\
\sigma_\theta(f) &= P \\
\sigma_z(f) &= \sigma_f + P \\
\sigma_r(b) &= - PV_f/V_b(1-r_b^2/r^2) \\
\sigma_\theta(b) &= - PV_f/V_b(1+r_b^2/r^2) \\
\sigma_z(b) &= \varepsilon_{bu}E_b - 2\nu_b PV_f/V_b
\end{aligned} \qquad (3)$$

where σ_f is the axial true stress of the fibre tested separately with a strain ε_I ; V_f and V_b are real volume fractions of `f′ and `b′ in I at the strain ε_I; E_b is the Young′s modulus of `b′; and

ν_b is the Poisson's ratio of `b'. To evaluate P, no loss of adhesion at the fibre/zone interface is assumed. If there are no longitudinal defects (Photo.1(d)) in the coating film, the transverse strain in `f' and `b' are equal at their interface. However, if such defects do exsist, the transverse strain in `b' will be nearly zero until they close. Under these conditions, on the assumption that the volume of `f' is conserved, $\varepsilon_\theta(b)$ can be written as follows :

$$\varepsilon_\theta(b) = -(\varepsilon_I - \varepsilon')/2 \qquad (4)$$

where ε' is a strain in `f' when the defects in `b' are the closed forms. Also P is expressed by

$$P = \frac{E_b\{(\varepsilon_I - \varepsilon')/2 - \varepsilon_{bu}\nu_b\}V_b}{(1 + \nu_b)\{(1 - 2\nu_b)V_f + 1\}} \qquad (5)$$

As the compressive transverse stress in `b' is highest at the interface from eq.(3), $\sigma_{\theta,max}$ is given by

$$\sigma_{\theta,max} = -\frac{E_b\{(\varepsilon_I - \varepsilon')/2 - \varepsilon_{bu}\nu_b\}(1 + V_f)}{(1 + \nu_b)\{(1 - 2\nu_b)V_f + 1\}} \qquad (6)$$

Equations (3)-(5) and (6) contain V_f and V_b which are not equal to the initial volume fractions of V_f^o and V_b^o, respectively, but change their values with ε_I. For a small ε_I, the terms V_f^o, V_b^o, V_f and V_b are expressed as follows :

$$V_f^o = (r_f^o/r_b^o)^2$$

$$V_b^o = 1 - (r_f^o/r_b^o)^2$$

$$V_f = (r_f/r_b)^2 = \left\{\frac{r_f^o(1 - \varepsilon_I/2)}{r_f^o(1 - \varepsilon_I/2) + (r_b^o - r_f^o)(1 + \bar{\varepsilon}_r)}\right\}^2$$

$$= \frac{V_f^o(\,1 - \varepsilon_I\,)}{1 + 2\bar{\varepsilon}_r - \sqrt{V_f^o}\,(\varepsilon_I + 2\bar{\varepsilon}_r)}$$

$$V_b = 1 - V_f \qquad (7)$$

where $\bar{\varepsilon}_r$ is the mean radial strain in `b'. The radial strain in `b', ε_r, is a function of r and is represented by eq.(8), applying the Hooke's law :

$$\varepsilon_r = 1/E_b[\sigma_r(b) - \nu_b\{\sigma_\theta(b) + \sigma_z(b)\}]$$

$$= PV_f(1 + \nu_b)(2\nu_b - 1 + r_b^2/r^2)/E_bV_b - \varepsilon_{bu}\nu_b. \qquad (8)$$

Therefore $\bar{\varepsilon}_r$ is calculated by

$$\bar{\varepsilon}_r = \frac{1}{r_b - r_f}\int_{r_f}^{r_b} \varepsilon_r dr$$

$$= \frac{\{(\varepsilon_I - \varepsilon')/2 - \varepsilon_{bu}\nu_bV_f\{2\nu_b - 1 + 1/\sqrt{V_f}\}}{(1 - 2\nu_b)V_f + 1} - \varepsilon_{bu}\nu_b \qquad (9)$$

From eqs.(7) and (9) we can calculate V_f, V_b and $\bar{\varepsilon}_r$ for a given ε_I. By substituting those into eqs.(5) and (6) we can evaluate P and $\sigma_{\theta,max}$ as a function of ε_I.

II-(2)-4-(ii) Application to Composites Investigated

The foregoing treatment was also applied to the aluminium-alumina composites. In Fig.6, P and $\sigma_{\theta,max}$ were plotted as a function of ε_I. ν_b and E_b were assumed to be 0.25 and 5250 kg/mm^2 as used by Thornton and Thomas[40] in their work, and ε_{bu} was calculated by σ_{bu}/E_b, where σ_{bu} is the UTS of `b'. As σ_{bu} was not known, it was deduced to a first approximation by the same method as Thornton and Thomas, who used the stress build-up model for discontinuous fibre in ductile matrix proposed by

Kelly.[48] The value of ε' is less than 0.030 since every composite is sufficiently strengthened up to 3% elongation. Calculation was performed for the cases of $\varepsilon' = 0.000$ and 0.030. Fig.6 shows that P increases with V_b^o or equivalently with the thickness of `b', whereas $\sigma_{\theta,max}$ is independent of $V_b^o$ in appearance. This calculation leads to the following interpretation. When `b' is thick, P can increase sufficiently to spall `b' even for a small $\varepsilon_I$ while $\sigma_{\theta,max}$ is not yet high enough to fracture `b' in a transverse direction. Thus, the spalling of `b' is dominant. On the contrary, when `b' is thin $\sigma_{\theta,max}$ can rise enough to fracture `b' before P acquires the stress necessary for the spalling of `b'. Clearly, the fracture of `b' in a transverse direction is to be expected.

Before turning to experimental verification, let us evaluate P and $\sigma_{\theta,max}$ at fracture of the aluminium-alumina composites. Normal tensile stress of the composites is given by

$$\begin{aligned}\sigma_c &= \{\sigma_z(f)\pi r_f^2 + \sigma_z(b)\pi(r_b^2 - r_f^2)\}/\pi r_b^2 \\ &= \sigma_f V_f^o(1 - \varepsilon_I) \\ &\quad + \varepsilon_{bu}E_b\{V_b^o + V_f^o\varepsilon_I + 2\bar{\varepsilon}_r - \sqrt{V_f^o}(\varepsilon_I + 2\bar{\varepsilon}_r)\} \\ &\quad + P\left[V_f^o(1-\varepsilon_I) - 2\nu_b V_f/V_b\{V_b^o + V_f^o\varepsilon_I + 2\bar{\varepsilon}_r - \sqrt{V_f^o}(\varepsilon_I + 2\bar{\varepsilon}_r)\}\right]\end{aligned} \tag{10}$$

By inserting the measured values of UTS into σ_c, first ε_I and then P and $\sigma_{\theta,max}$ can be obtained from eqs.(5) and (6). In Fig.7 the curves of P and $\sigma_{\theta,max}$ versus V_b^o are shown. P at first increased with V_b^o but for large V_b^o it remained nearly constant. On the contrary, $\sigma_{\theta,max}$ was high for small V_b^o but low for large V_b^o.

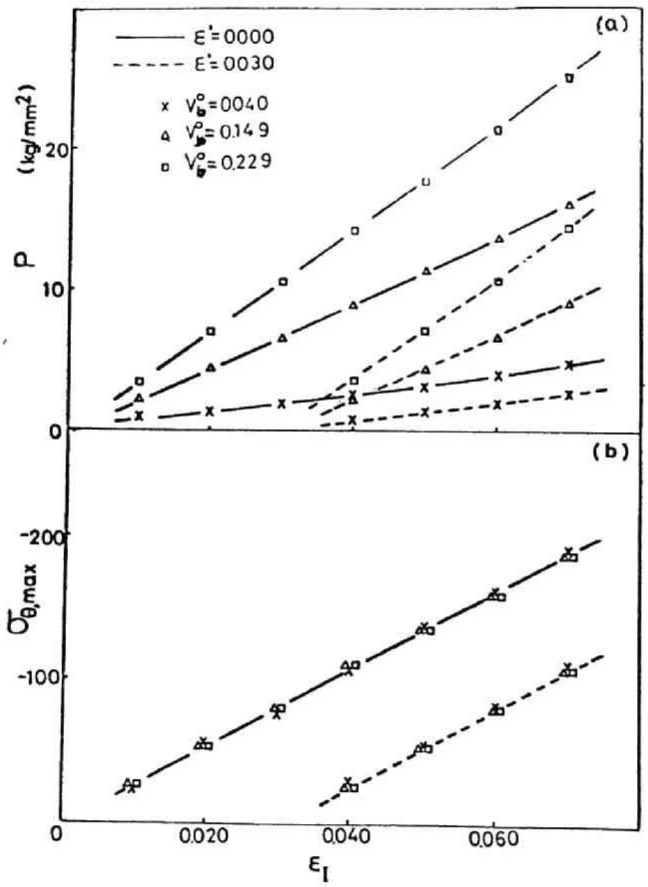

Fig.6 P and $\sigma_{\theta,max}$ calculated as a function of ε_I for Al-alumina composites.

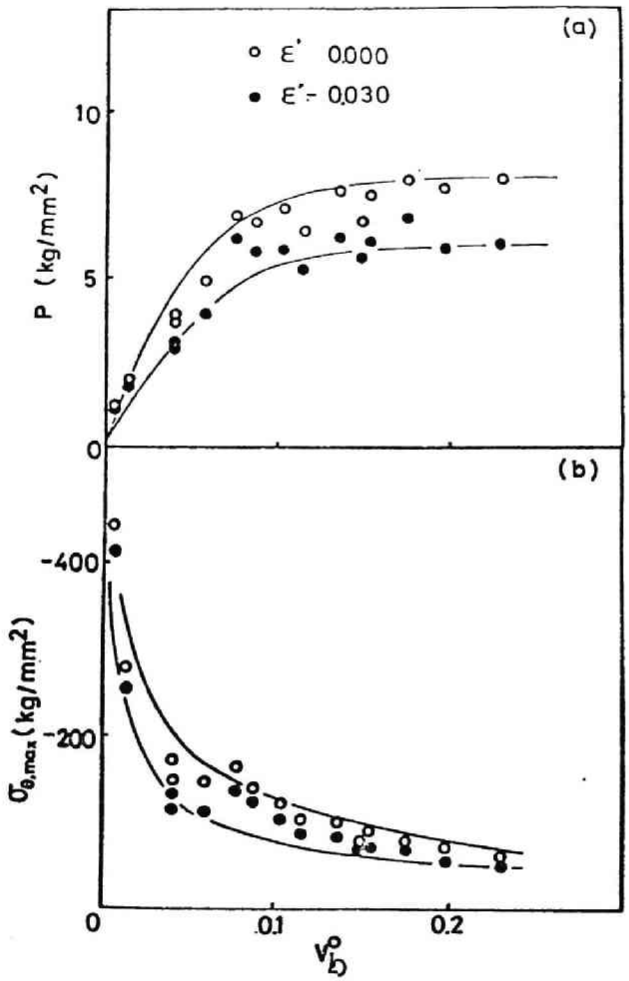

Fig.7 Calculated values of P and $\sigma_{\theta,max}$ at fracture of Al-alumina composites.

As the constraint factor will increase with V_b^o, σ_c/V_f^o is expected to increase with V_b^o. The measured values of σ_c/V_f^o actually increased with V_b^o for $V_b^o < 0.10$, but remained nearly constant for $V_b^o > 0.10$ (see Fig.3). The calculated values of P showed the same trend for $V_b^o > 0.10$. These results indicate that there is a particular reason for the saturation of σ_c/V_f^o and P for $V_b^o > 0.10$. Most probably this is attributable to the spalling of `b´ ; namely, when P exceeds the bonding strength between `f´ and `b´,`b´ will be spalled. For $V_b^o < 0.10$, P is not high enough to spall `b´, and hence `b´ will be fractured by compression in a transverse direction, since $\sigma_{\theta,max}$ is sufficiently high. The calculation result that $\sigma_{\theta,max}$ decreases with increasing V_b^o can be explained by the fact that the thinner the film, the stronger it becomes, since it has fewer defects.

To examine the above speculations, the surface of the aluminium—alumina composite after fracture was observed. As shown in Photo.3, the thinner films((a) and (b)) were fractured by the compression in a transverse direction, whereas the thicker films ((c) and (d)) were spalled. It is notable that this composite fractured as a whole as soon as spalling or compressive fracture of the alumina film occured. The explanation is that the stress on the Al fibre in Region II is higher than UTS of the unnotched fibre, owing to the constraint effect before spalling or fracture of the alumina film ; but it decreases after spalling or fracture of the alumina film and cannot be higher than the UTS of the unnotched fibre. The stainless steel-intermetallic compound composites after 7% elongation showed the similar tendency, as illustrated in Photo.4. The thin film (a) was fractured

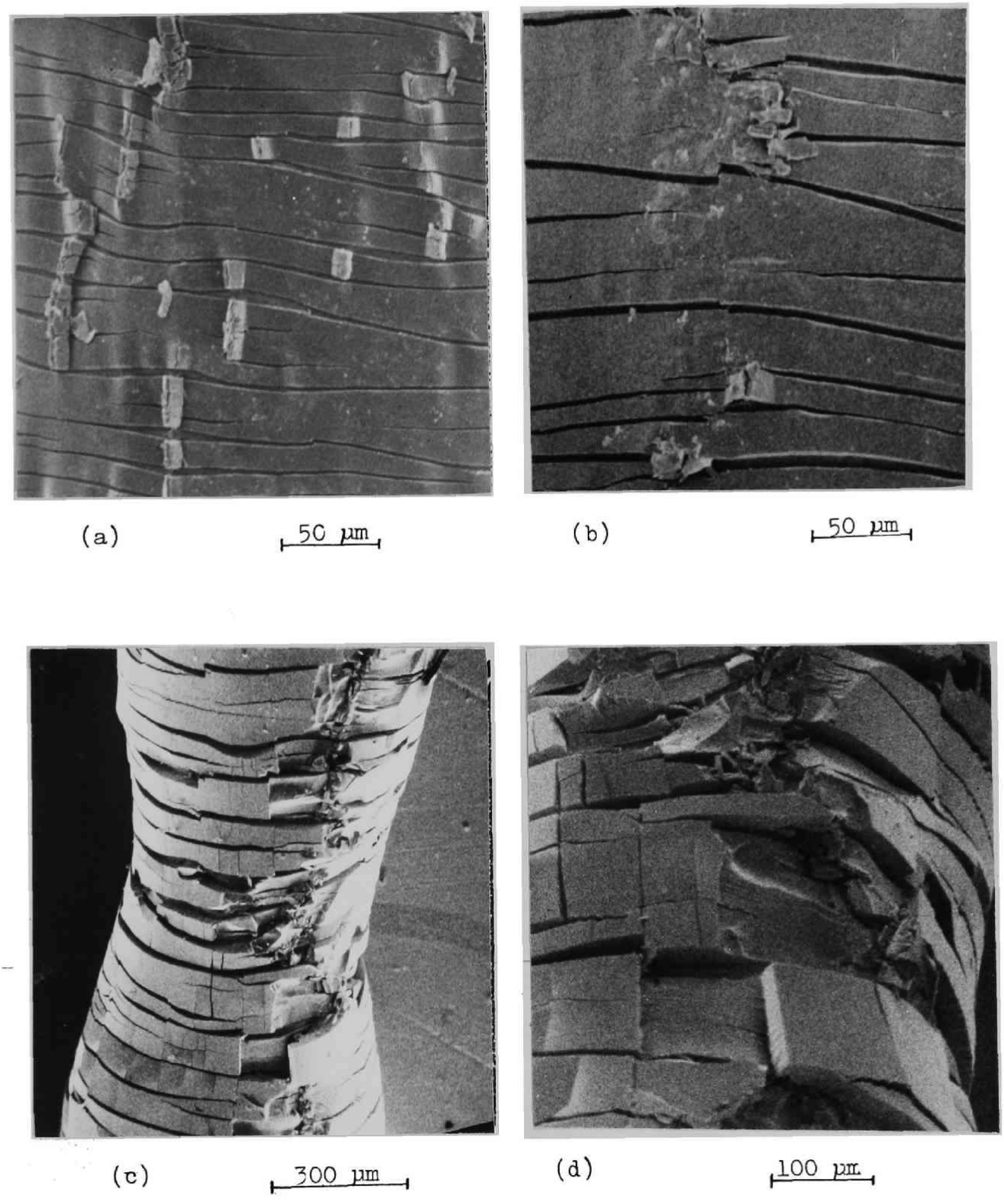

Photo.3 Appearance of Al-Alumina composites at fracture.
V_b^o = (a) 0.005, (b) 0.040, (c) and (d) 0.149.

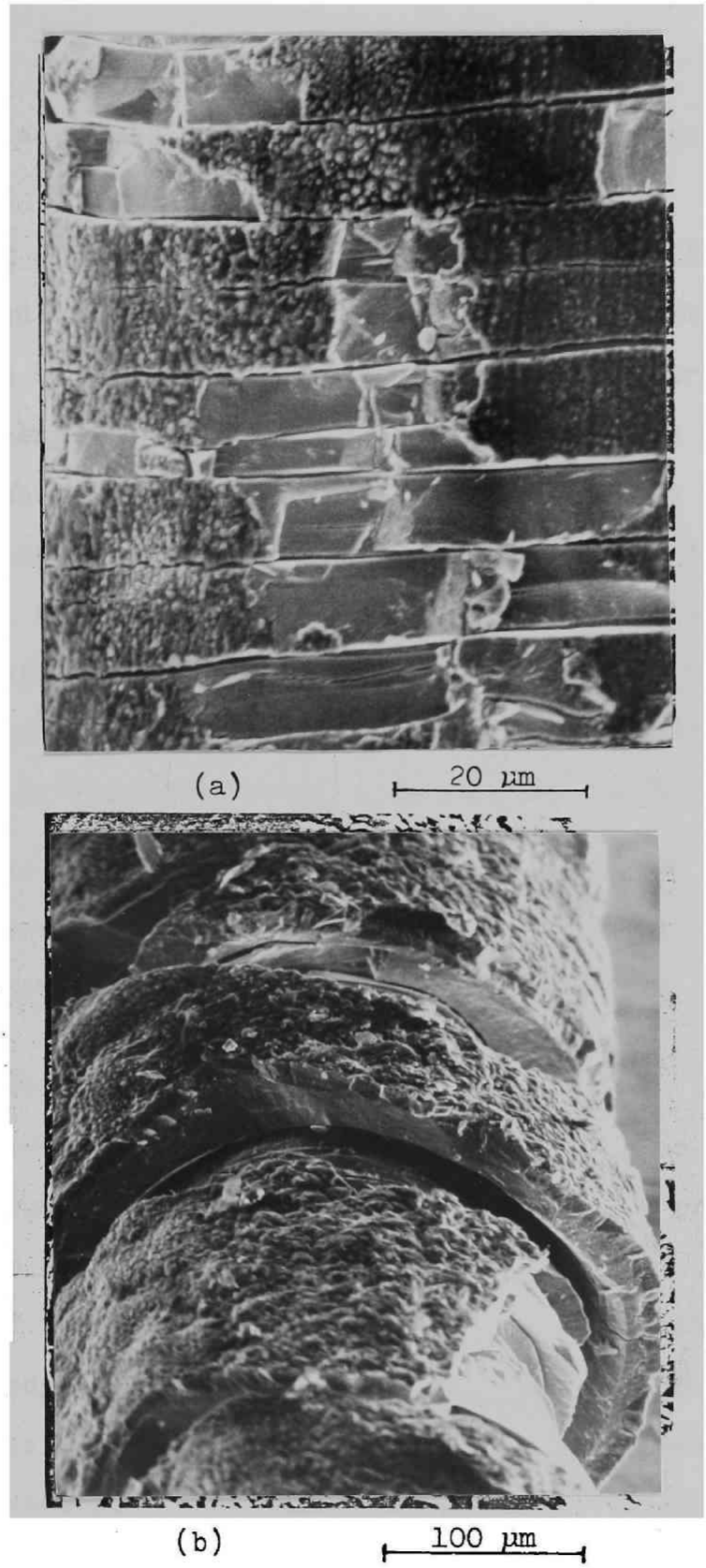

Photo.4 Appearance of stainless steel-intermetallic compound composites (thickness (a) 13.2μm, (b) 47.5 μm) after 7% elongation.

by the compression but the thick film (b) was detached from the fibre.

So long as the brittle zones adhered to the fibres and were not fractured by the compression, the constraint effect raised the strength of the fibres. However, once the brittle zones had been spalled or fractured by compressive stress, this effect vanished and the strength of the fibre fell to that of unnotched samples. When $c\sigma_f V_f^o$ is greater than σ_f, namely when $cV_f^o > 1$ (where c is a constraint factor), the strength of composites with brittle zones is higher than that of composites without zones. The measured σ_c of the aluminium-alumina composite and the $\sigma_{5\%}$ of stainless steel-intermetallic compound composite correspond to this case. On the other hand, the σ_c for the stainless steel-intermetallic compound composites corresponds to the case of c=1.

II-(2)-5 Conclusions

The strengthening effects of brittle zones on ductile fibre-composites were investigated and a new model was proposed on the basis of the constraint effect of notched ductile fibres. It was found that the strength of the fibres is raised by this effect as long as the brittle coating zones with multiple cracks adhere to the fibre and are not fractured by compressive transverse stress. The constraint effect vanished after the spalling or failure of the brittle zones. This strengthening theory was verified satisfactorily by a series of experiments.

II-(3) Multiple Necking of Fibre in Single Tungsten Fibre Composites

II-(3)-1. Introduction

Ductile fibres embedded in composites exhibit uniform elongation[9][43]-[46] or multiple necking[11][12] when the composites are elongated beyond ε_{fu}, the strain at which the fibres start to neck and subsequently fail when tested alone. For uniform elongation of the composites, it is maintained that a strong interfacial bond between fibre and matrix is necessary to prevent separation of the interface against radial tensile stresses and thus to supress necking.[9][49] On the other hand, according to Vennett et al.,[11] and Schoene and Scala[12], multiple necking of fibres in composites requires no strong interfacial bond. Schoene and Scala have also pointed out that the UTS and elongation of composites which exhibited multiple necking in the fibres were greater than those predicted by the rule of mixtures. Their observations suggest that multiple necking is an important key to the ductility and deformation behaviour of composites.

The intensions of the present work are to clarify the mechanisms of multiple necking and to discuss the relationship between several parameters such as neck spacing, reduction of area at neck, elongation, and the volume fraction of fibre. The specimens used in this study were single tungsten fibre-composites, since these could be readily fabricated by a plating method and the effects of neighbouring fibres could be eliminated.[9][36][43]

II-(3)-2 Experimental Procedure

Fibre and matrix employed were commercially pure tungsten wire of 100μm diameter, and pure copper, respectively. Before nickel- or copper-plating, each fibre was boiled for 30 min in a saturated sodium hydroxide solution to remove graphite lubricant and oxides. Solutions and conditions for plating are shown in Table 1. The volume fraction of fibre in the composite was adjusted by varying the thickness of the copper layer. The nickel coating was controlled up to 10μm thickness. Both W/Cu and W/Ni/Cu composites were annealed in vaccum at 600°C for 30 min to remove possible residual stresses induced during plating. Since no interfacial bond existed in the W/Cu composites prepared similarly by Cooper[50], some of the W/Cu and W/Ni/Cu composites were heat-treated in vaccum at 900°C for 10 min in order to strengthen the bond. Tensile tests were performed in an Instron tensile machine at a constant crosshead speed of 2 mm/min, or a strain rate of 0.05/min. After testing, fibre was extracted from the composites by etching away the matrix. Subsequent examination of the fibre by optical microscope,as illustrated in Fig.9, was carried out to measure neck spacing (l), neck diameter (d), and the fibre diameter between necks(D), in a fibre with an initial diameter D_o. Each parameter was measured at more than 24 points for each fibre.

II-(3)-3 Results

II-(3)-3-(i) Tensile Strength and Elongation of Composites

Fig.8 shows UTS, σ_c , and elongation at σ_c, ε_{cu} , vs. the volume fraction of fibre,V_f, for the W/Cu and W/Ni/Cu composites

Table 1 The electrolyte compositions and operating conditions for nickel and copper plating

	Copper Plating	Nickel Plating*
Composition of Electrolyte	$CuSO_4$: 209.7g/l H_2SO_4 : 52.4g/l in Water	$NiSO_4$: 329.2g/l $NiCl_2$: 44.9g/l H_3BO_3 : 37.4g/l in Water
Temperature(°C)	20	60
Current Density mA/mm^2	0.5	0.5

* Mechanical Stirring

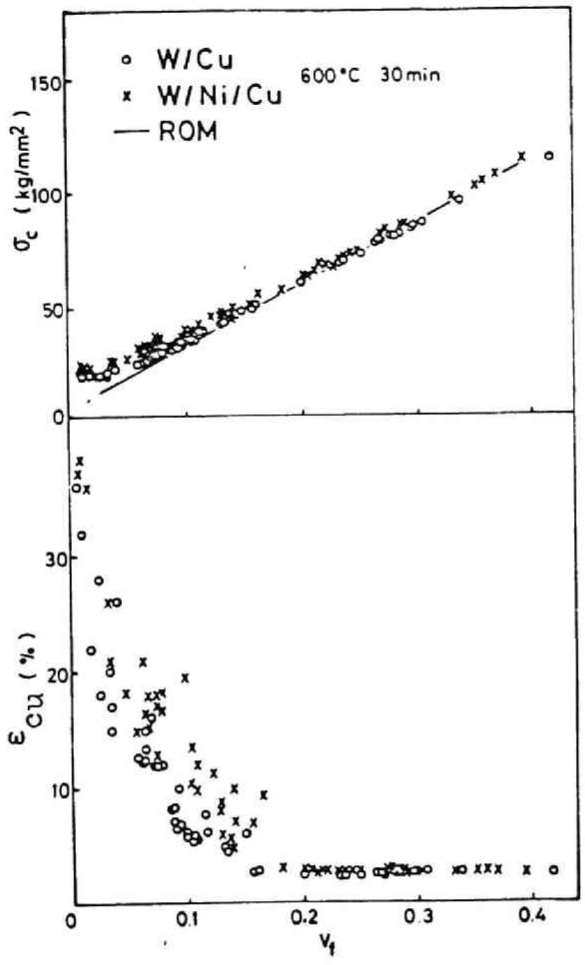

Fig.8 Measured values of (a)σ_c and (b)ε_{cu} of W/Cu and W/Ni/Cu composites annealed at 600°C for 30 min vs. V_f. ROM relationship between σ_c and V_f for W/Cu composite included for comparison.

annealed at 600°C for 30 min. According to the rule of mixtures(ROM), σ_c will be

$$\sigma_c = \sigma_{fu}V_f + \sigma_m^*V_m \qquad (11)$$

and eq.(11) is valid for $V_f > V_{min}$, where σ_{fu} is the UTS of the fibre ; σ_m^* is the tensile stress on the matrix elongated to ε_{fu}(a strain corresponding to σ_{fu}) ; V_m is the volume fraction of matrix ; and V_{min} is the minimum volume fraction of fibre to cause strengthening of the matrix material. The σ_{fu}, σ_m^*, and V_{min} in the W/Cu composites were determined as 270 kg/mm^2, 7.6 kg/mm^2, and 0.044, respectively. The solid line in Fig.8(a) is a prediction by ROM for W/Cu composites. At $V_f < 0.15$, the observed σ_c is larger than that predicted by ROM. While ROM predicts that composites with $V_f > V_{min}$(0.044 for W/Cu composite) will fail when the fibre fails, and that accordingly ε_{cu} will not exceed ε_{fu}, the observed ε_{cu} at $V_f < 0.15$ is in fact greater than ε_{fu}(2.0 %).

A deformed fibre in the composite at over 2 % elongation exhibited multiple necking, as shown in Fig.9(a) and (b). As clearly seen in Fig.9(b), the matrix flowed into a region around the necks with no apparent separation.

The W/Cu and W/Ni/Cu composites annealed at 900°C for 10 min showed similar tendency to those annealed at 600°C for 30 min, as shown in Fig.10(a) and (b).

II-(3)-3-(ii) Load-Elongation Curves

Fig.11 gives load-elongation curves for the W/Ni/Cu composite annealed at 600°C for 30 min. When V_f was large (V_f=0.228), the load-elongation curve seemed to follow the ROM prediction. However, when V_f was small (V_f=0.156 or 0.100), deviation from ROM was evident in spite of the condition $V_f > V_{min}$. At 2-6 %

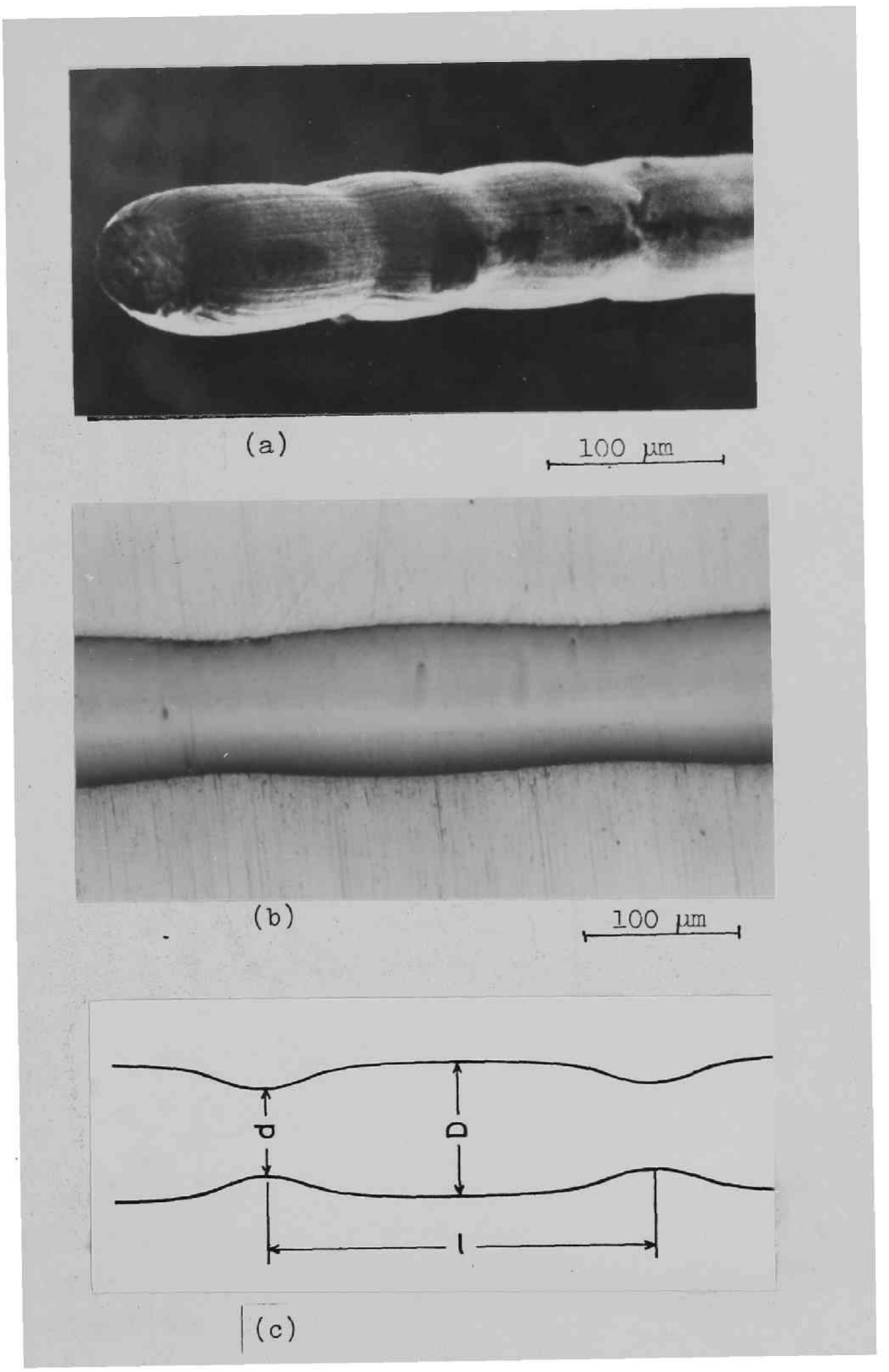

Fig.9 (a) Multiple necking of tungsten fibre extracted from fractured W/Cu composite. (b) Appearance of multiple necking in fibre and matrix adjacent to necks. (c) Schematic representation of D, d and l.

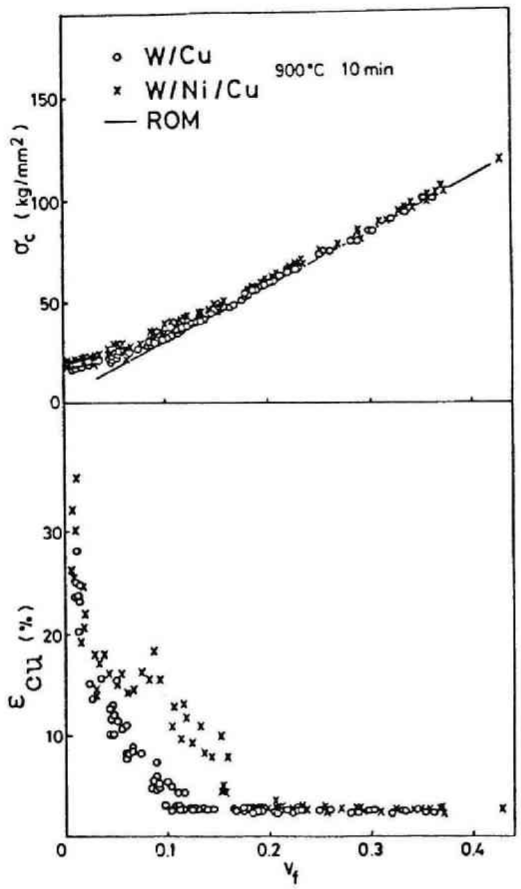

Fig.10 Measured values of (a)σ_c and (b)ε_{cu} of W/Cu and W/Ni/Cu composites annealed at 900°C for 10 min vs. V_f. ROM relationship between σ_c and V_f for W/Cu composite included for comparison.

elongation, surpassing ε_{fu} , the composite survived with little change in load.

The onset of multiple necking was found to be retarded in W/Ni/Cu composite annealed at 900°C for 10 min. This retarded necking may be explained in terms of the constraint of the matrix on the fibre due to strong interfacial bonding.[9][49]

II-(3)-3-(iii) Reduction in Area at Neck

Specimens used to study area reduction and neck spacing were annealed at 600°C for 30 min to eliminate strong interfacial bonding which might cause uniform elongation.

Reduction of area at necks in the fibre with elongation ε_c of the composites is shown in Fig.12(a) and (b). $1-(d/D_o)^2$ and $1-(d/D)^2$ denote, respectively, the reduction of area at necks with respect to an initial cross-sectional area of the fibre, and one with respect to a non-necked area. The greater the value of $1-(d/D)^2$, the larger is the difference in deformation between the necked and the non-necked parts, while $1-(d/D)^2=0$ means a completely uniform deformation of the fibre along the tensile axis. Thus $1-(d/D)^2$ is considered as a measure of uniformity of deformation in the fibre. It was observed that $1-(d/D_o)^2$ and $1-(d/D)^2$ in the W/Cu composite were greater than those in the W/Ni/Cu composite for given V_f and ε_c. This indicates that the fibre in the W/Cu composite deformed less uniformly than that in the W/Ni/Cu composite. It is also notable that $1-(d/D)^2$ becomes flattened for strains >10 %, indicating that the uniformity of the fibre does not appreciably change at large elongation, while $1-(d/D_o)^2$ increases with strain.

Reduction of area at necks vs. V_f at a given ε_c is shown

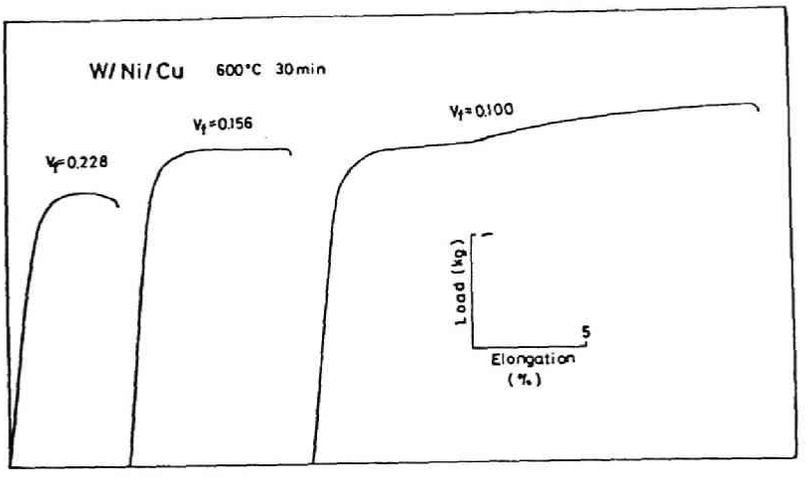

Fig.11 Typical load-elongation curves of W/Ni/Cu composite annealed at 600°C for 30 min.

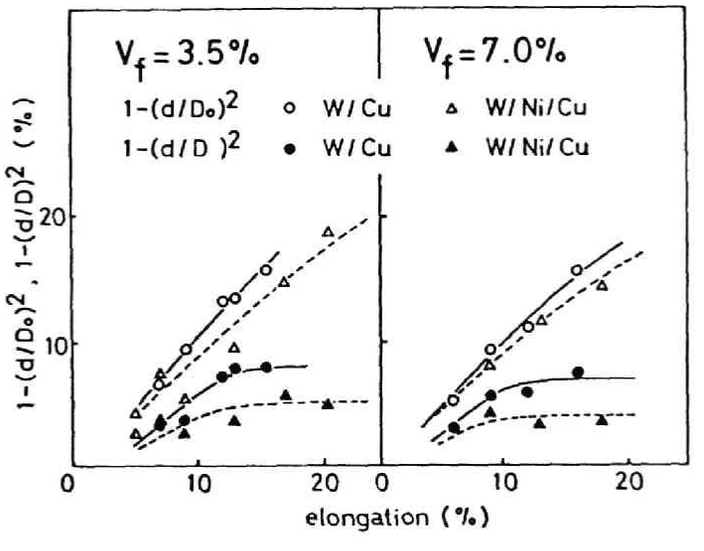

Fig.12 Measured values of $1-(d/D_o)^2$ and $1-(d/D)^2$ plotted against ε_c. Fibre volume fractions of W/Cu and W/Ni/Cu composites were (a)3.5 % and (b) 7.0 %, respectively.

in Fig.13. Little change in $1-(d/D_o)^2$ and $1-(d/D)^2$ with increasing V_f was apparent.

II-(3)-3-(iv) Neck Spacing

Neck spacing has been reported to be 3-5 times(Vennett et al.[11])or 5-6 times(Schoene and Scala[12])the fibre diameter. According to Vennett et al., neck spacing decreases as total elongation of the composites increases. Fig.14, however, indicates that while neck spacing decreases for 2-6 % elongation, beyond 6 % it then remains unchanged. V_f , as shown in Fig.15, has little effect on neck spacing.

II-(3)-4 Discussion

II-(3)-4-(i) Mechanism of Formation of Multiple Necking

One possible mechanism of forming multiple necking is that, when interfacial bonding is strong, a neck at a particular point can be inhibited by the matrix, causing necking to occur at some other locations where the stress states are more favourable. In this way, strong interfacial bonding may give rise to multiple necking. The validity of this mechanism, however, has been disputed.[11][12] It also fails to explain the observation in the present work that multiple necking of the fibres took place in composites with both weak and strong interfacial bonding and that fibres in composites with a degraded interfacial bond (i.e., carbon coating on fibres prepared by decomposing aceton at 800°C under argon atmosphere) exhibit multiple necking. From these results, it can be said that strength of interfacial bonding alone is not sufficient to explain the occurrence of multiple necking.

Another mechanism, proposed by Vennett et al.,[11] is concerned with the transfer of load from fibre to surrounding

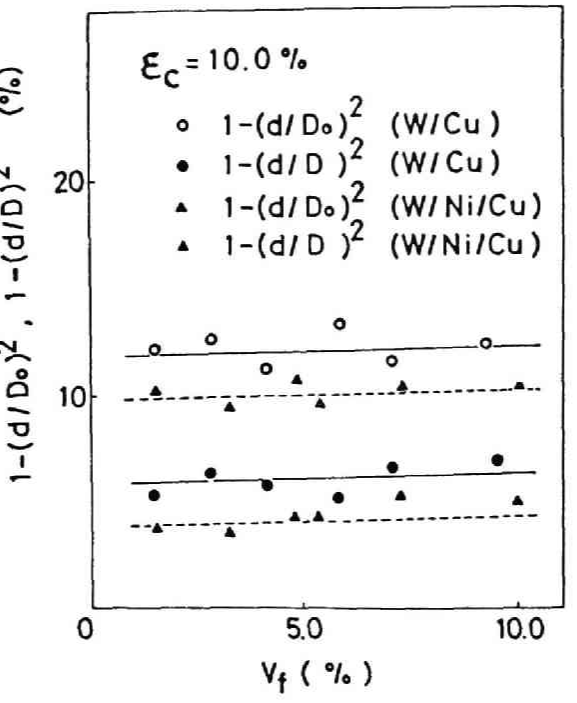

Fig.13 Measured values of $1-(d/D_o)^2$ and $1-(d/D)^2$ vs. V_f in W/Cu and W/Ni/Cu composites at 10 % elongation.

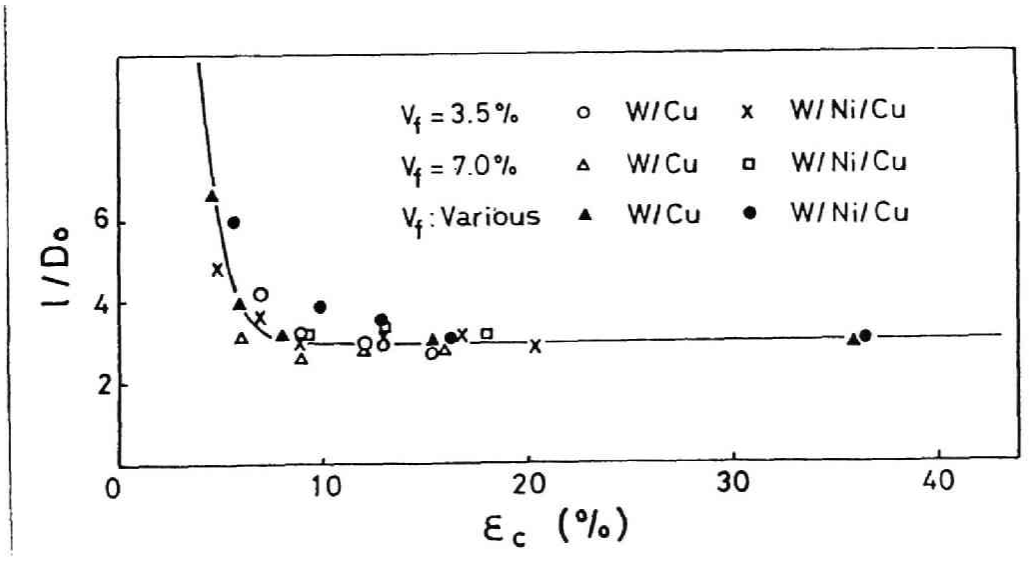

Fig.14 Relationship between neck spacing and ε_c.

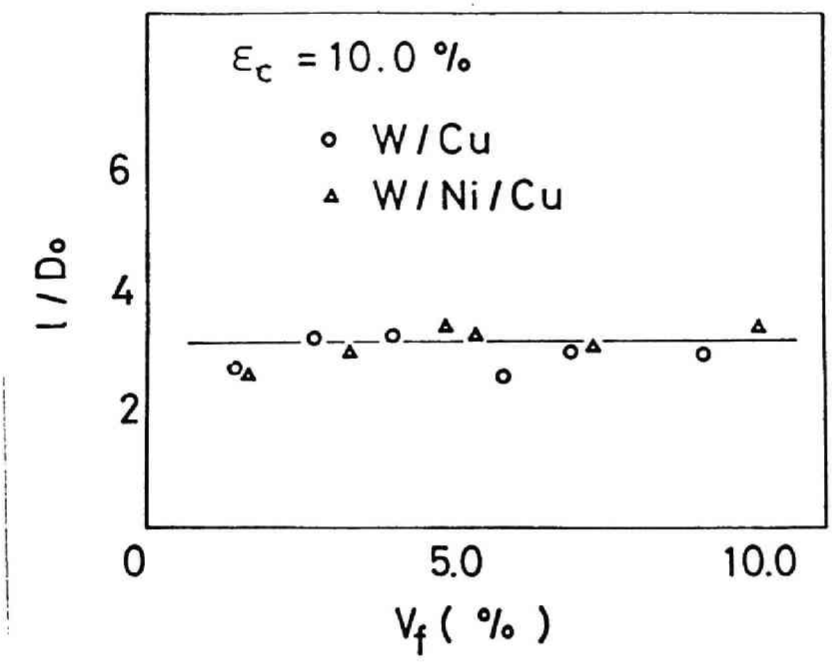

Fig.15 Relationship between neck spacing and V_f when ε_c was 10%.

matrix. When necking begins in the fibre with reduction of its cross-sectional area, the matrix will undergo increased localized deformation and be more strain-hardened in the vicinity of the neck than the rest of the matrix. An annular ring of the matrix around a neck, being strain-hardened, can support more load to resist further deformation. Thus necking in fibre will start to occur at other sections. The process of load transfer from fibre to matrix will be repeated along the entire length of the fibre. This mechanism seems consistent with the present observations in three respects. (i)It does not depend on strength of interfacial bond. (ii)The value of $1-(d/D)^2$ for the W/Ni/Cu composites was smaller than that for W/Cu composites at a given elongation and volume fraction of fibre. This implies that the load borne by a necked fibre can be shed more easily in the W/Ni/Cu composite than in the W/Cu composite, since, being stiffer, a nickel layer around the neck can support more load than copper. (iii)The weakness of the effect of V_f on $1-(d/D_o)^2$ and $1-(d/D)^2$ in both the W/Cu and W/Ni/Cu composites(Fig.13) suggests that it is the matrix adjacent to the neck, rather than the rest of the matrix away from the neck, that contributes to the shape of the multiple neck.

II-(3)-4-(ii) Deformation Process

The process of mechanical deformation in the composites can be described in three stages, as illustrated in Fig.16. Stage I is characterized by elastic deformation of both fibre and matrix.[1][44][45][51][52] At stage II, the matrix undergoes plastic deformation while the fibre still deforms in an elastic manner.[2][5][45][53]-[55] Most previous work has distinguished

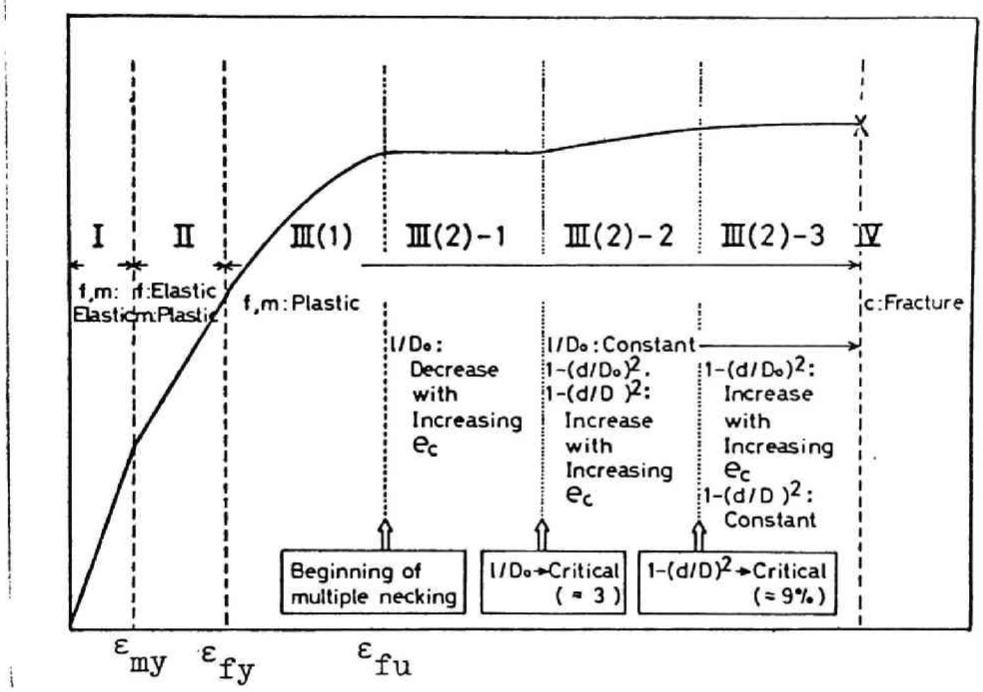

Fig.16 Deformation stages of composite accompanying multiple necking in fibre. ε_{my} and ε_{fy} are yield strains of matrix and fibre, respectively. Critical values of l/D_o (≈ 3) and $1-(d/D)^2$ ($\approx 9\%$) in this figure are for W/Cu composite annealed at 600°C for 30 min.

these two stages.

As deformation proceeds further, it reaches stage III where both fibre and matrix deform in a plastic manner. While previous studies have dealt little with stage III except for strongly bonded composites where the fibre deforms uniformly (9)(49)(56), this study focuses discussion on stage III with particular reference to composites exhibiting multiple necking of the fibre ; and for a better description of composite deformation, divides stage III into two substages, i.e., stages III(1) and III(2):

Stage III(1) : ranging from ε_{fy} , the onset of plastic deformation of fibre, to ε_{fu} , the deformation may be described by ROM since the Poisson's ratios of both components reach 0.5 at this stage and thus no difference in lateral contractions between fibre and matrix arises for constraint.

Stage III(2) : ranging from the end of stage III(1) to failure of the composite. Elongation of the composite exceeds ε_{fu} and thus ROM is not obeyed. For composites with multiple necking of fibre , stage III(2) now needs further differentiations :

Stage III(2)-1. With a repetition of the process of load transfer from fibre to matrix, necks are formed one after another. Neck spacing becomes smaller with increase in elongation (Fig.14). Additional elongation of the composite is not accompanied by increase in load (see Fig.11, V_f=0.100), since load on composite cross-section with the necked part of the fibre cannot exceed the load on the cross-section with the non-necked part. At the end of this stage, a critical number of necks will be formed on the fibre and a fixed neck spacing ($l \approx 3D_o$) will be attained.

Stage III(2)-2. Load carried by the composite again

rises since necks have already been formed at the end of stage III(2)-1 along the entire length of the fibre and therefore load-bearing capacity increases after stage III(2)-1. As elongation increases, both $1-(d/D_o)^2$ and $1-(d/D)^2$ become larger, indicating that uniformity of deformation in the fibre decreases.

Stage III(2)-3. With increase in elongation, $1-(d/D_o)^2$ becomes larger while $1-(d/D)^2$ remains constant. The uniformity of the fibre thus remains unchanged.

II-(3)-4-(iii) Critical Volume Fraction of Fibre for Multiple Necking.

Transfer of load from a necking fibre can be accommodated by strain-hardening of the matrix if a sufficient volume of matrix is present in the composite. Thus, the volume of matrix should be greater than a critical value. It is suggested that, if the volume fraction of fibre is smaller than a critical value, $V_{c,mn}$, the fibre embedded in the composite can exhibit multiple necking. When V_f is equal to or smaller than $V_{c,mn}$, the composite can be elongated at least to the end of stage III (2)-1 (6 % for W/Cu system). On the other hand, when $V_f > V_{c,mn}$, the composite will fail at ε_{fu}(2 %). It follows then that, as V_f decreases, ε_{cu} may increase not in a gradual manner but with a sudden jump at $V_{c,mn}$, as schematically represented in Fig.17. The results presented in Figs.8(b) and 10(b) may support this view, with a little uncertainty due to scattering of ε_{cu}. $V_{c,mn}$ is determined from Figs.8(b) and 10(b), and is listed in Table 2. Differences in $V_{c,mn}$ for each composite may stem from the varying extent of strain-hardening in the matrix, being different in annealing temperature, annealing time, and type of matrix material. A strong matrix seems to

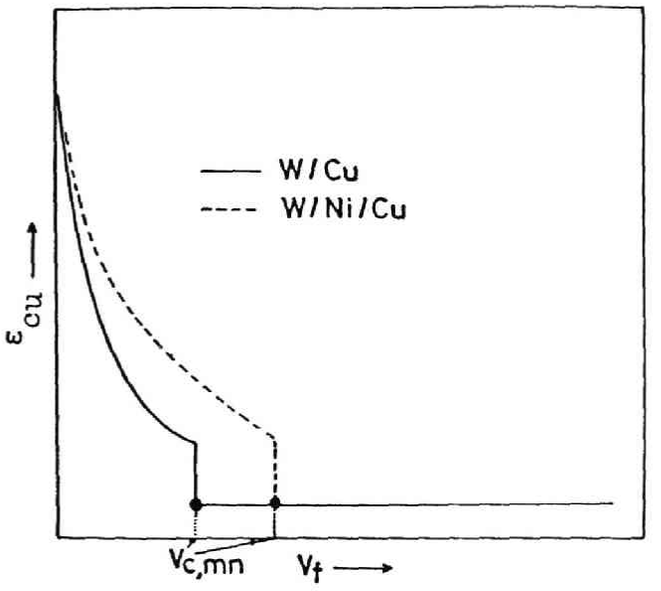

Fig.17 Schematic representation of suggested relationship between ε_{cu} and V_f.

Table 2 Critical fibre volume fraction $V_{c,mn}$ below which multiple necking occurs in fibre.

Composite	Heat-Treatment	$V_{c,mn}$
W/Cu	900°C 10 min	0.10
W/Ni/Cu	900°C 10 min	0.15
W/Cu	600°C 30 min	0.13
W/Ni/Cu	600°C 30 min	0.16

yield a large $V_{c,mn}$.

According to ROM, elongation of the composite at $V_f > V_{min}$ cannot exceed ε_{fu}. However, at $V_f < V_{c,mn}$ (but $> V_{min}$), the fibre exhibits multiple necking, and the composite can be elongated beyond ε_{fu}. Since the fibre in a composite with even a weak interfacial bond exhibits multiple necking, the deviation of the composite ductility from ROM may arise in a similar manner to that of a composite with a strong interfacial bonding.[9][49][56]

II-(3)-5 Conclusions

(1) The tensile strength and elongation of composites in which the fibres exhibited multiple necking were greater than those predicted by the rule of mixtures.

(2) The fibres in the W/Cu composite deformed less uniformly than those in the W/Ni/Cu composite. The uniformity of the deformed fibres in both composites did not change with elongation above a certain elongation.

(3) Neck spacing decreased with increasing elongation in the range 2-6 %, but became constant above 6 %.

(4) Multiple necking may be caused by local transfer of load from fibre to matrix.

(5) Stage III of deformation, where both fibre and matrix deform plastically, can be divided into two substages, III(1) and III(2). The latter stage can be further differentiated into three subdivisions.

(6) There existed a critical volume fraction of fibre for multiple necking. The critical value experimentally determined for each composite indicated that a strong matrix yielded a large critical value.

II-(4) Summary

In the former part of this chapter, the strengthening effect of the brittle zones on ductile fibre-composites was studied. The experiment was carried out using single fibre-composites with two components : a brittle outer component and a ductile core of fibre. It was suggested that the fibre can be strengthened by the constraining effect of the notched regions formed by micro-crackings of the brittle zone, as long as the brittle zone adheres to the fibre and is not fractured by the compressive transverse stress. The suggested theory satisfactorily explained the experimental results. After spalling or fracture by the transverse stress of the brittle zone, the constraint effect could not exist, and the usual rule of mixtures was applicable.

In the latter part of this chapter, mechanisms of multiple necking and deformation of fibre-composites were studied, using single tungsten fibre-copper matrix composites prepared by a plating method. It was concluded that multiple necking results from local transfer of load from fibre to surrounding matrix. Processes of plastic deformation of the composites at various stages were discussed,and the characteristics of each stage were described. Neck spacing with 2-6% elongation decreased with increase in elongation but remained constant above 6% elongation. Multiple necking occured when the volume fraction of fibre was smaller than a critical value. The critical value determined for each composite indicated that a strong matrix yielded a large critical value.

REFERENCES

(1)R.Hill : J. Mech. Phys. Solids, 12(1964),199.

(2)Ibid.,213

(3)B.Paul:Trans. Met. Soc. AIME,218(1960),36.

(4)Z.Hashin and S.Shtrickman : J. Mech. Phys. Solids,10(1962),235.

(5)A.Kelly and H.Lilholt:Phil. Mag.,20(1969),311.

(6)A.Kelly:Strengthening Methods in Crystals, Ed. by A. Kelly and R. B. Nicholson, Elsevier (1971), p.439.

(7)A.J.M.Spencer:Interna. J. Mech. Sci., 7(1965),197.

(8)J.F.Mulhern, T.G.Rogers, and A.J.M.Spencer : J. Inst. Maths. Applics.,3(1967),21.

(9)H.R.Piehler:Trans. Met. Soc. AIME, 233(1965),12.

(10)I.Ahmad and J.M.Barranco:Met. Trans., 1(1970),989.

(11)R.M.Vennett, S.M.Volf, and A.P.Levitt: ibid.,1569.

(12)C.Schoene and E.Scala: ibid.,3466.

(13)G.Garmong and A.Shepard:Met. Trans.,2(1971),175.

(14)P.W.Jackson and J.R.Majoram:J. Mat. Sci.,5(1970),9.

(15)R.B.Barclay and W.Bonfield:J. Mat. Sci.,6(1971),1076.

(16)W.I.Stuhrke:Metal Matrix Composite, ASTM,(1969) p.76.

(17)P.W.Jackson:Metals Eng. Quarterly, ASM,9(1969),22.

(18)D.W.Petrasek and J.W.Weeton:Trans. Met. Soc. AIME,230(1964),977

(19)S.Ochiai, M.Mizuhara and Y.Murakami:J. Japan Inst. Metals, 37(1973),208.

(20)D.M.Braddick, P.W.Jackson and P.J.Walker:J. Mat. Sci., 6(1971),419.

(21)D.W.Petrasek:Trans. Met. Soc. AIME,236(1966),887.

(22)Y.Umakoshi, K.Nakai and T.Yamane:Met. Trans.,5(1974),1250.

(23)W.H.Sutton and E.Feingold:General Electric Space Sci. Lab. Rep. R65SD39, (1965), p.54.

(24)P.W.Heitman, L.A.Shepard and T.H.Courtney:J. Mech. Phys. Solids, 21(1973),75.

(25)K.Akamatsu and K.Kamei:Read at the Autumn Meeting of Japan Inst. Metals, 1975.

(26)E.Friedrich and W.Pompe:J. Mat. Sci.,9(1974),1911.

(27)A.Pattnaik and A.Lawley:Met. Trans.,5(1974),111.

(28)Y.Umakoshi and T.Yamane:Trans. JIM,17(1976),25.

(29)J.O.Outwater,Jr:Mod. Plast.,33(1956),156.

(30)L.Holliday and J.Robinson:J.Mat.Sci.,8(1973),301.

(31)D.A.Koss and S.M.Copley:Met. Trans.,2(1971),1557.

(32)G.Garmong:Met. Trans.,5(1974),2183.

(33)Ibid.,2191.

(34)Ibid.,2199.

(35)K.G.Krieder and V.M.Patarini:Met. Trans., 1(1970),3431.

(36)K.Nakazawa, M.Otsuka and S.Umekawa:J. Japan Inst. Metals, 36(1972),1168.

(37)B.J.Shaw:Acta Met.,15(1967),1169.

(38)H.E.Cline and D.F.Stein:Trans. Met. Soc. AIME, 345(1969),841.

(39)E.R.Thompson and F.D.Lemkey:Met. Trans.,1(1970),2799.

(40)J.S.Thornton and A.D.Thomas, Jr : Met. Trans., 3(1972),637.

(41)R.Hill : Mathematical Theory of Plasticity, Chap.9. Oxford(Clarendon Press), (1950)

(42)A.S.Tetelman and A.J.McEvily, Jr : Fracture of Structural Materials, New York, John Wiley and Sons, (1967), p.125.

(43)Chapter IV-(4)

(44)D.L.McDanels, R.W.Jech and J.W.Weeton : Trans. Met. Soc. AIME, 233(1965),636.

(45)A.Kelly and W.R.Tyson : J. Mech. Phys. Solids, 13 (1965),329.

(46)Chapter IV-(3)

(47)Chapter IV-(5)

(48)A.Kelly and G.J.Davies : Met. Rev., 10(1965),1.

(49)S.T.Mileiko : J. Mat. Sci., 4(1969),974.

(50)G.A.Cooper : J. Mat. Sci., 2(1967),409.

(51)H.L.Cox : Brit. J. Appl. Phys., 3(1953),72.

(52)B.W.Rosen : Fibre Composite Materials, Ohio, ASM (1964), p.37.

(53)M.R.Piggot : Acta. Met., 14(1966),1429.

(54)A.J.M.Spencer : Internat. J. Mech. Sci., 7(1965), 197.

(55)J.F.Mulhern, T.G.Rogers, and A.J.M.Spencer : J. Inst. Maths. Applics., 3(1967),21.

(56)G.Garmong and R.B.Thompson : Met. Trans., 4(1973),863.

Chapter III

Effects of Interfacial Conditions on Stress Transfer Mechanisms

III-(1). Introduction

When fibres are continuous throughout the whole length of the specimen, stress can be applied directly to them.[1)-(3)] In this case, interfacial bonding is not necessary. On the other hand, when the fibres are discontinuous, externally applied load is transferred from matrix to fibres only through the interface. Therefore it is important to know the relation between the interfacial conditions and stress transfer mechanisms. Up to date, little has been known about the relation.

The most important parameters for stress transfer through the interface are interfacial shear stress τ and critical aspect ratio l_c/d. There are some methods for measurement of the above parameters.[4)(5)] Among them, the two methods are employed in this work : multiple-fracture test and pull-out one, since the other methods employing the composites with many discontinuous fibres suffer at least one serious disadvantage that many short fibres should be aligned unidirectionally and uniformly. The characteristics of the methods employed are as follows.

(i) Multiple-fracture test.

Below a minimum fibre volume fraction to cause strengthening of the matrix material, V_{min} , the matrix can work-harden sufficiently to bear the further applied load after the contained fibre breaks. Therefore, an initially continuous brittle fibre breaks continually into shorter lengths, finally into

$l_c/2$, which is a half of the critical length. Knowing the l_c/d and σ_{fu} where d is a diameter of the fibre and σ_{fu} is the UTS of the fibre, interfacial shear stress τ can be calculated by Kelly's equation;[5]

$$\sigma_{fu}/2\tau = l_c/d \qquad (1)$$

(ii) Pull-out test

Fibres embedded in a composite should be longer than a critical length for them to be stressed to fracture, otherwise, they are pulled-out from the matrix. Namely the fibres show either pull-out or fracture as a function of embedded length divided by a diameter. Therefore, τ and l_c/d can be directly measured by embedding one end of a fibre in the matrix into various depths and applying load through the other end. The aspect ratio at the transition point from pull-out to fracture corresponds to twice the critical aspect ratio, since , in the real composites, load is applied at both ends of the fibres.

The results of the multiple-fracture and pull-out tests will be described in the former part of (2) and the latter part of (3) in this chapter, respectively. Effects of interfacial conditions on stress transfer mechanisms will be discussed in detail.

III-(2) Study on Stress Transfer Mechanisms by Multiple-Fracture Test.

III-(2)-1 Introduction

Many investigations have been made on the deformation and fracture behaviour of tungsten fibre-reinforced copper matrix composite[5]-[8] (hereafter described as W/Cu composite).

According to these reports, this composite fabricated by the vaccum infiltration method has strong interfacial bonding between the fibre and the matrix, and consequently Young's modulus, yield strength and UTS of the composite nearly obey the rule of mixtures. Since all of these works have shown that desired interfacial bonding can be achieved by the treatment such as cleaning of graphite lubricant and oxides in the surface of the fibres, it was not necessary in this analysis to consider the effects of interfacial conditions on the deformation and fracture behaviour of this composite. In this investigation, the effects of the interfacial conditions (which are changed by coating carbon, boronnitride powder and nickel on the surfaces of tungsten fibres) on critical aspect ratio and interfacial shear stress will be clarified by using multiple-fracture test. The aims of coating of carbon, boronnitride powder and nickel[9] are to weaken the interfacial bonding, to reduce the bonding area, and to strengthen the interfacial bonding, respectively. The reasons why single fibre-composites are used instead of multi-fibre-ones in this work are as follows.

(1) In multi-fibre-composites, the weakest fibre among the fibres contained in the composites fails in the early stage of deformation of the composites, which often causes fracture of the neighbouring fibres.[8][10][11] In such a case, it is impossible to know the effects of the interfacial conditions directly from the experimental results.

(2) Kelly[5] considered a stress transfer mechanism from matrix to fibre in a model which consists of a central rod of fibre surrounded by a sleeve of matrix during the deformation stage where the fibre deforms elastically and matrix plastically

(stage II). To apply the Kelly model for this work, it is better to use single fibre-composites.

(3) In single fibre-composites with the volume fraction of fibre smaller than V_{min} which is the minimum fibre volume fraction to reinforce the matrix material, the number of breaks of the originally continuous fibre can be measured easily.

III-(2)-2 Experimental Procedure

Tungsten wire of 100μm diameter was selected as the reinforcing fibre material in the matrix of pure copper. The tungsten fibre as-supplied, which is ductile at room temperatuer, was made brittle by annealing in vaccum at 1300°C for 100 min.[12] All fibres used in this work were cleaned to remove graphite lubricant and oxides by boiling in a saturated sodium hydroxide solution for 30 min prior to coating or copper plating. Carbon coating on the fibres was done by decomposing aceton at 800°C under an argon atmosphere. Boronnitride (BN) powder coating was done by immersing the fibres in a water suspending BN particles and drying up them in air. As the tensile strength of the interface between tungsten and copper in the electroformed W/Cu composites was reported to be not so much different from zero,[13] a binding agent which binds the fibre and the matrix tightly was sought for. Nickel was selected as a third coating material by the following considerations:

(a) Electroformed W/Ni composite have a strong interfacial bonding when annealed in vaccum at 900°C for 1-10 min.[9]

(b) As nickel and copper form a homogeneous solid solution in the Ni-Cu phase diagram,[14] an interfacial bonding between nickel

and copper is expected to be strong when a counter diffusion occurs slightly.

The electrolyte compositions and the operating conditions for nickel and copper plating are shown in Table 1. The thickness of a nickel layer was restricted to be 5 μm in all the specimens. As the volume fraction of nickel is only about 1/10 of that of tungsten, it can be neglected compared with those of tungsten and copper, especially when the volume fraction of the matrix is large. Nickel plays a role only as a binder between tungsten fibre and copper matrix. Fibre volume fraction was varied by changing the thickness of copper layer. Hereafter, carbon, BN powder and nickel coated tungsten fibre-copper matrix composites will be described as W/C/Cu, W/BN/Cu and W/Ni/Cu composites, respectively.

All the specimens except W/Ni/Cu composites were annealed in vaccum at 550°C for 30 min. W/Ni/Cu composites were annealed in vaccum at 900°C for 5 min.

Room-temperature tensile tests were carried out with an Instron tensile machine at a constant cross-head speed of 2 mm per min, corresponding to a strain rate of 0.05 per min, to obtain load-elongation curves.

Observation of the fractured specimens was made by a photomicroscope.

III-(2)-3 Results

Fig.1 shows typical load-elongation curves of W/Cu composites containing initially continuous brittle tungsten fibres. When the fibre volume fraction (V_f) is large (V_f=0.165 or 0.578), an initial drop in load due to fracture of a fibre occurres and subsequently the load increases slightly because of the work-

Table 1 The electrolyte compositions and operating conditions for nickel and copper plating

	Copper Plating	Nickel Plating*
Composition of Electrolyte	$CuSO_4$: 209.7g/l H_2SO_4 : 52.4g/l in Water	$NiSO_4$: 329.2g/l $NiCl_2$: 44.9g/l H_3BO_3 : 37.4g/l in Water
Temperature(°C)	20	60
Current Density mA/mm^2	0.5	0.5

* Mechanical Stirring

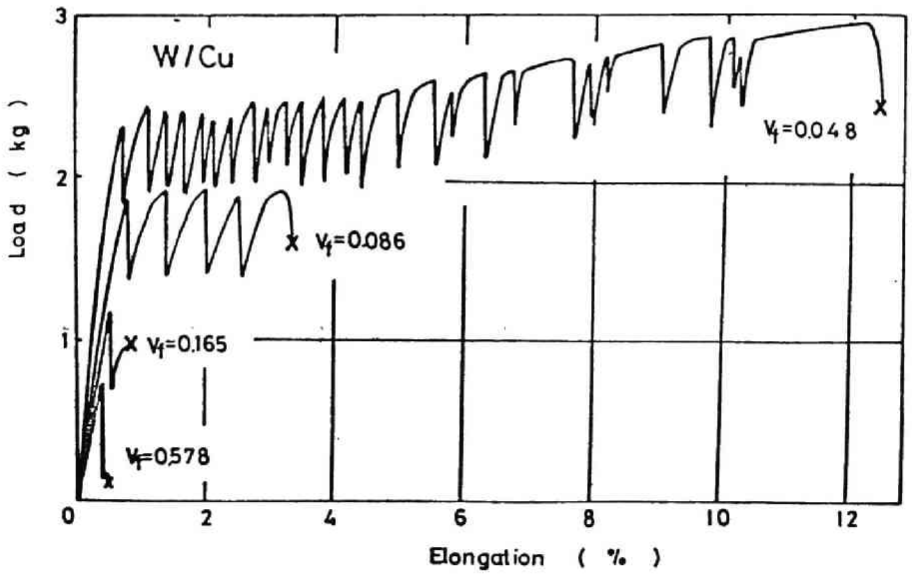

Fig.1 Typical load-elongation curves of W/Cu composites containing initially continuous brittle tungsten fibres.

hardenability of the copper matrix. In this case the maximum load of the composites is found at the fracture strain of the fibre. When V_f is small (V_f=0.048 or 0.086), the breakdown of a fibre in one cross-section causes a drop in load borne by the composite. In this cross-section, however, the matrix work-hardens and the load bearing capacity of this cross-section rises again so that the fibre once fractured fails in another cross-section. With a repetion of this process, the fibre fractures continually into shorter lengths and finally reaches $l_c/2$ which is half of the critical length. This process is similar to that reported by Kelly[15] in detail.

Fig.2 shows a relationship between elongation at maximum load of W/Cu composites and V_f. In the range of $V_f > 0.09$, the elongations are nearly constant, whereas in the range of $V_f < 0.09$, the elongations increase with decrease in V_f. Below V_{min} given by[15]

$$V_{min} = \frac{\sigma_{mu} - \sigma_m^*}{\sigma_{fu} + \sigma_{mu} - \sigma_m^*} \qquad (2) \quad ,$$

the matrix can work-harden sufficiently to bear the further applied load. σ_{mu}, σ_{fu} and σ_m^* in eq.(2) are UTS's of the matrix and fibre, and the stress on the matrix when the fibre reaches its UTS, respectively. Substituting the values measured in this work, σ_{mu}=20 kg/mm^2, σ_{fu}=140 kg/mm^2 and σ_m^*=5 kg/mm^2 into eq.(2), V_{min} for W/Cu composites is calculated to be 0.10. From Fig.2, V_{min} is found to be 0.09 experimentally, agreeing well with the calculated value of 0.10.

The numbers of drops in load-elongation curves, namely, the number of breaks of the initially continuous fibres are plotted against V_f in Fig.3. In the range of $V_f < V_{min}$, the fibre fractures continually, and this agrees with the theory of reinforcement.

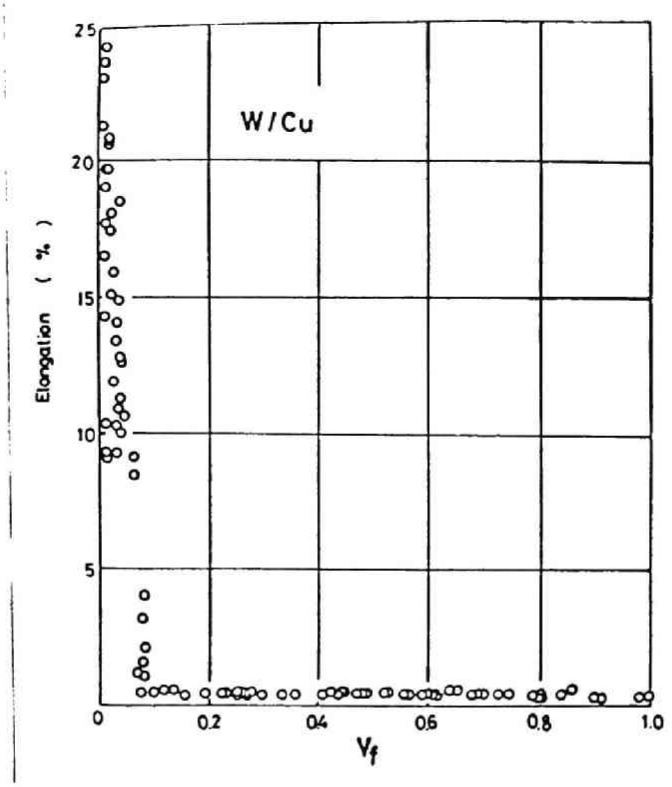

Fig.2 Relationship between elongation at maximum load and V_f in W/Cu composites.

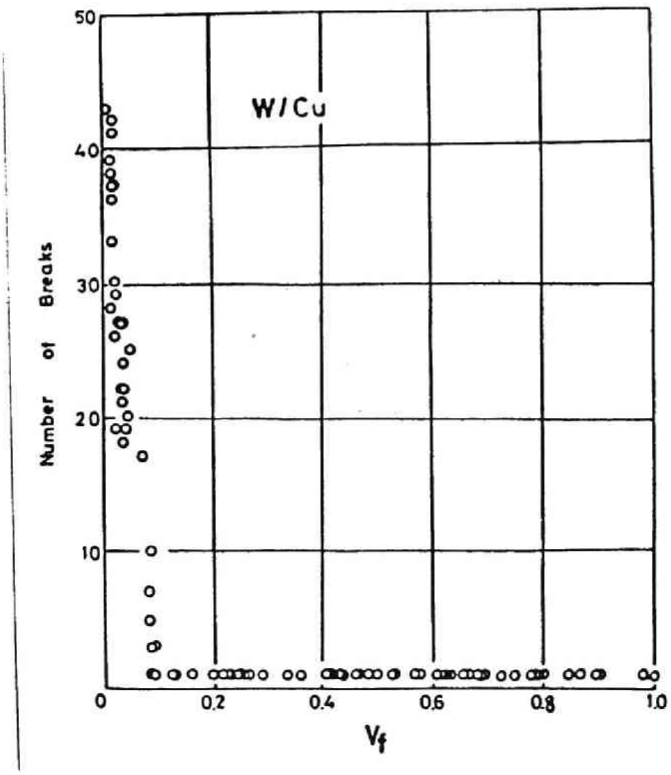

Fig.3 Numbers of breaks of the initially continuous fibres versus V_f.

Fig.4 is a histogram of lengths of the fractured fibres measured from the photomicrographs of the fractured composites containing 1.0 % of the initially continuous brittle fibres, where d is a diameter (100 μm in this case) and $\bar{l}$ is the measured length of the segments. Measured values of $\bar{l}/d$ are scattered to some extent, perhaps due to flaws or imperfections in the fibres.

Fig.5 shows $\bar{l}/d$ plotted against V_f in W/Cu composites. There is a tendency for $\bar{l}/d$ to decrease with decrease in V_f.

Photo.1 shows the appearances of the fractured W/Cu composites... In the specimen (a) with V_f =0.040 which is smaller than V_{min}, an initially continuous tungsten fibre in the composite fractures continually with drops in load in the load-elongation curve as shown in Fig.1. As the fibre breaks at many cross-sections, the matrix deforms especially in these cross-sections , and therefore, the specimen shows an apparently multiple necking-like shape as a whole. The length of the segments decreases with increase in V_f, as shown in (a) and (b). This result agrees with that of Fig.5. As a result of continuous fracture of the fibre, voids are formed between the fractured segments, but the matrix does not flow into such voids, (c). This fact indicates that in this experiment we can apply Kelly model in which the stress transfer across the end plane of the fibre is not considered.

As the stress transfer from the matrix to the fibre takes place at the interface, if the interfacial condition is altered, the degree of stress transfer and hence the number of breaks of an initially continuous fibre will be varied. Numbers of breaks of the fibres in W/C/Cu, W/BN/Cu, W/Cu and W/Ni/Cu

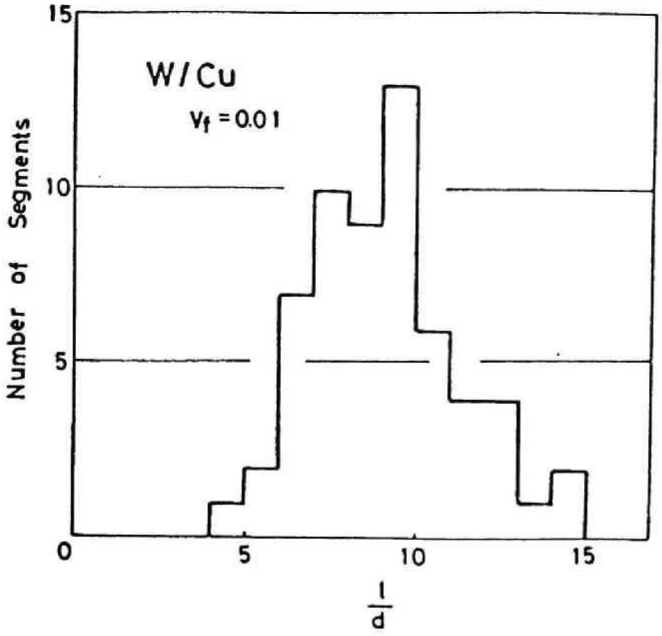

Fig.4 Histogram of lengths of the fractured fibres measured from the photomicrographs of the fractured W/Cu composites containing 1.0% of the initially continuous tungsten fibres.

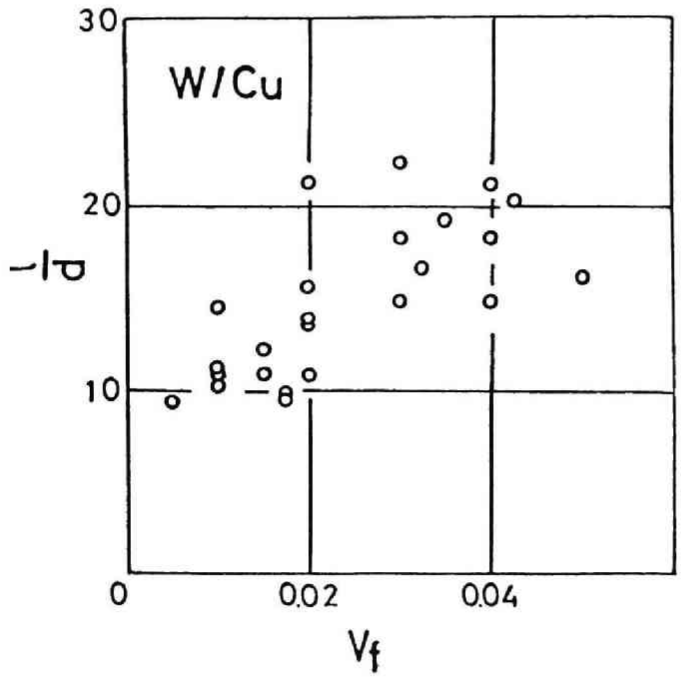

Fig.5 Measured values of $\bar{l}/d$ plotted against V_f in W/Cu composites..

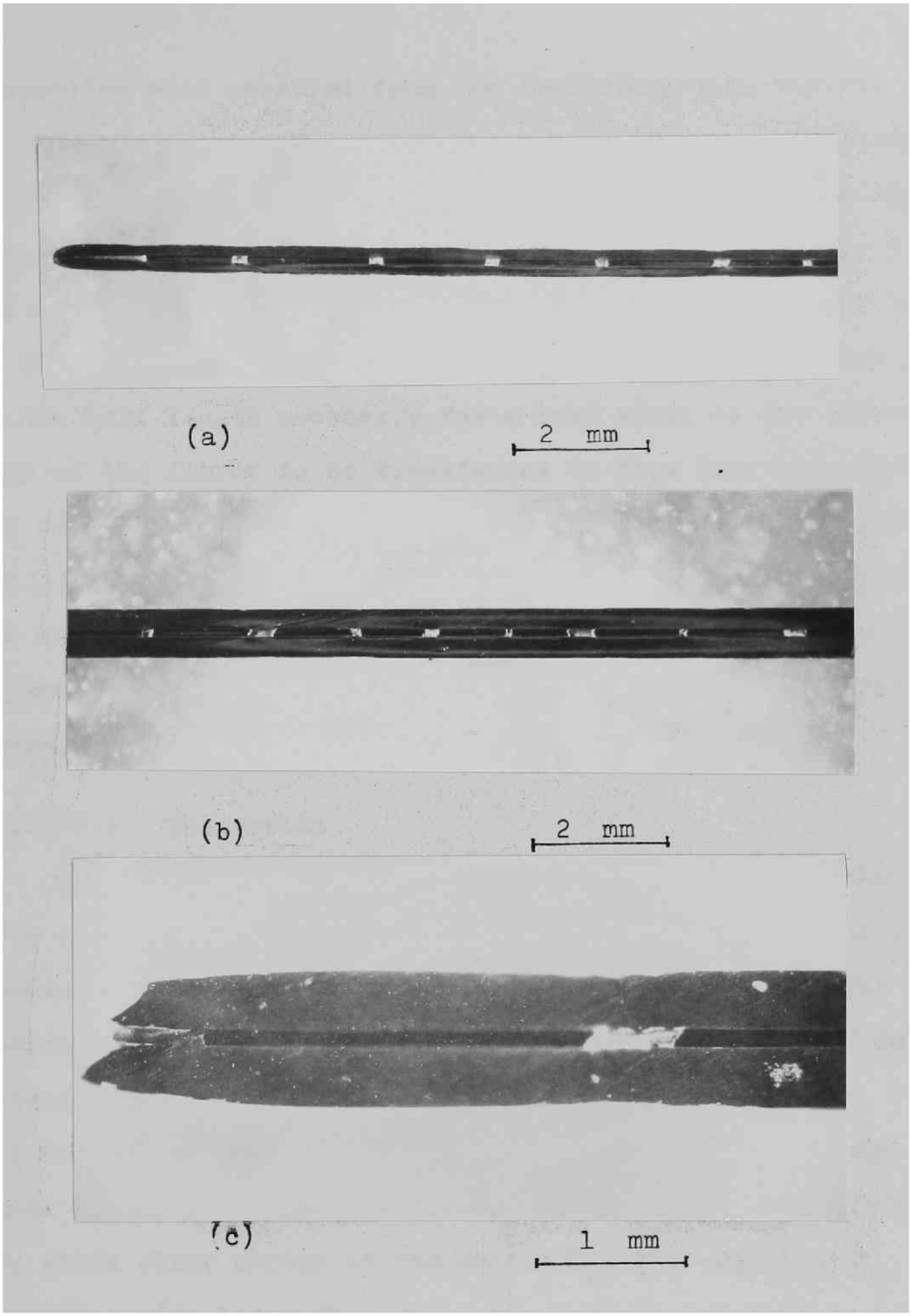

Photo.1 Appearances of the fractured W/Cu composite containing initially continuous fibre.

ccmposites were measured from the load-elongation curves. In this experiment, V_f of all the composites was restricted to be 2.0 %, because the number of breaks of the fibres is dependent upon V_f as stated above. The result is shown in Table 2. The critical length l_c is given by eq.(1). The average length of the fractured fibres is considered to be $l_c/2$, because $l_c/2$ is the half length necessary for a load equal to the breaking load of the fibres to be transferred to them from the matrix. The values of l_c/d and τ calculated according to Kelly model[5] are also summarized in Table 2. This result indicates that the measured values of l_c/d become smaller and the calculated values of τ become larger as the interfacial bonding becomes stronger.

III-(2)-4 Discussion

At the beginning , which values must be taken as the value of τ should be mentioned, if we do not take into account (a) residual stresses and (b) triaxial stresses caused by the differences in the mechanical properties and amounts of deformation between the fibre and the matrix.

(i) When the interfacial bonding is strong enough, namely, the shear strength of the interfacial bonding, τ', is higher than the yield shear stress of the matrix τ_m, τ is equal to τ_m.

(ii) When τ' is lower than τ_m , the interfacial bonding breaks during deformation in stage I, and never returns to its original state once it has broken. Therefore, τ' is equal to zero in stage II. According to the above consideration, τ also should be zero. In the case of (ii), the stress cannot be transferred from matrix to the fibre.

Now, let us discuss on the results shown in Table 2.

Table 2 Effects of the interfacial conditions on the number of breaks, critical aspect ratio and interfacial shear stress.

Specimen	Number of Breaks (average)	l_c/d	τ (kg/mm^2)
W/C/Cu	17	47.1	1.5
W/BN/Cu	20	40.0	1.8
W/Cu	27	29.6	2.4
W/Ni/Cu	72	11.1	6.3

Although τ' is unknown in all the specimens used in this experiment, we can deduce that τ' is lower than τ_m in W/Cu, W/C/Cu, and W/BN/Cu composites, based on the following reasons:
(A) Tensile strength of the interface has been reported to be almost zero in the electroformed W/Cu composites.[13]
(B) If τ' is higher than τ_m in W/Cu composites, τ of these composites must be equal or nearly equal to that of W/Ni/Cu composites, namely τ_m. However, such a result is not obtained as shown in Table 2. In view of the fact that carbon and BN powder are used as coating materials which lower the interfacial bonding strength, it is more reasonable to consider that τ' is equal to zero in stage II in W/Cu, W/C/Cu and W/BN/Cu composites. Table 2 shows that stress is transferred from the matrix to the fibre although τ' is equal to zero. Here, let us discuss the following three points :
(I) Why and how is the stress transferred in spite of zero interfacial bonding ?
(II) Why are the values of τ evaluated by the Kelly model different from each other in W/Cu, W/C/Cu and W/BN/Cu composites ?
(III) Why do τ and l_c/d depend upon V_f ?
It appears that these problems lie in the stand-point that τ is controlled only by the interfacial bonding strength and the effects of residual stresses and triaxial stresses on stress transfer are not taken into consideration. Two stress transfer mechanisms can be suggested when the interfacial bonding strength is zero.

(a) Effects of Residual Stress

As W/Cu, W/C/Cu and W/BN/Cu composites were annealed in vaccum at 550°C for 30 min and then slowly cooled in a furnace to relieve residual stresses introduced during plating, compressive

stress, even if small, may be built up at the interface during cooling process since the coefficient of thermal expansion of copper is larger than that of tungsten.[16] The effect of residual compressive stress on stress transfer was investigated in the fibre-reinforced plastics by Outwater.[17] However, as, in such composites, both the fibre and plastics deform elastically, Outwater's model cannot be applied to our results which indicate that the stress is transferred during stage II. Since it is now clear that the maximum residual stress is not higher than the yield stress of the matrix, the residual stress which exists in stage I may be relieved in stage II where the matrix deforms plastically. Therefore, we cannot explain our results only by considering the effect of residual stress.

(b) Effects of Compressive Stress Arising from the Different Contractions and the Difference in Deformation Amounts between the Fibre and the Matrix

Poisson's ratio of tungsten is 0.28[18], while that of copper is 0.34[18] and 0.50 in stage I and in stage II, respectively. Also the deformation amount of the matrix will be larger than that of the fibre after debonding occurs at the interface. Therefore, the differences in Poisson's ratio and deformation amount between the fibre and the matrix will cause the matrix to exert an appreciable compressive stress P on tungsten fibre in the present specimens which consist of a cetral rod of tungsten fibre surrounded by a sleeve of copper matrix. When a composite is reinforced with a continuous fibre, this compressive stress can be calculated according to Kelly[19], if interfacial bonding is strong enough for both the fibre and the matrix to be subjected to the same axial strain. However, no solution has been found for such

a case where the interfacial bonding is not strong enough and the matrix slides relating to the fibre. Then following treatment similar to that of Kelly[19], we can derive eq.(3) as a clue to deduce the value of P (see Appendix) :

$$P = \frac{e_m(1 - 2\nu_f e_f/e_m)V_m}{V_f/K_m + 1/G_m + V_m/k_f} \qquad (3)$$

where e, ν, K, G, and k are strain in the axial direction, Poisson's ratio, bulk modulus, rigid modulus and plane strain bulk modulus respectively, and the subscripts f and m refer to the fibre and matrix respectively. If e_f is equal to e_m, eq.(3) becomes the same form as that obtained by Kelly[19]. However, eq.(3) is not correct for discontinuous fibre-reinforced composites because it is applicable only for continuous fibre-reinforced composites. Here, we use eq.(3) only as a tentative equation to deduce the magnitude of P.

The magnitude of P is a function of e_f and e_m. Since our consideration is being restricted to the stage where the fibres fracture continually, e_f is taken to be a fracture strain of tungsten fibres. However, as e_m has not been measured in this work, we must calculate P by using appropriate values of e_m. Substituting V_f=0.020, e_f=0.0033, ν_f=0.28, K_m=11500 kg/mm^2, G_m=4100 kg/mm^2 and k_f=37300 kg/mm^2, P is calculated to be 12.2 kg/mm^2 and 8.2 kg/mm^2 for e_f/e_m=0.60 and 0.80, respectively. Shear stress τ_f caused by friction between the fibre and the matrix is represented by

$$\tau_f = \mu P \qquad (4)$$

where μ is a coefficient of friction between the fibre and the matrix. Now, μ is unknown for all the specimens. If we assume μ is equal to 0.3, τ_f is calculated to be 3.7 and 2.5

kg/mm^2 for e_f/e_m=0.6 and 0.8, respectively. If we assume μ is equal to 0.1, τ_f is calculated to be 1.2 and 0.8 kg/mm^2 for e_f/e_m= 0.6 and 0.8, respectively. These calculated values of τ_f agree fairly well with those shown in Table 1. From the tentative calculation described above, the fact that stress can be transferred from the matrix to the fibre in the composites with zero interfacial bonding strength could be verified, even if tentatively, although the exact values of e_f/e_m and μ in all the specimens are not known. It is probably due to the differences in μ and e_f/e_m that the values of τ calculated by the Kelly model[5] are different from each other in W/Cu, W/C/Cu and W/BN/Cu composites.

Next, let's consider the relationship between l_c/d and V_f. The values of τ were calculated by using the Kelly model and plotted against $V_f(< V_{min})$, in Fig.6. It is evident from the figure that values of τ are dependent upon V_f. This result is explained as follows. As the drop in stress due to a fracture of the fibre is $\sigma_f V_f$, the matrix must work-harden by $\Delta\sigma_m$ which satisfies eq.(5) to compensate the drop in stress, $\sigma_f V_f$.

$$\Delta\sigma_m(1-V_f) = \sigma_f V_f \qquad (5)$$

If the matrix can compensate for the drop in stress by work-hardening, the fibre can be fractured continually. From eq.(5), we obtain

$$\Delta\sigma_m = \sigma_f V_f/(1-V_f) \qquad (6)$$

Eq.(6) indicates that a larger amount of deformation of the matrix is necessary to compensate for the drop in stress in the composite with larger V_f. Once an initially continuous fibre had fractured continually to some extent along the length of the

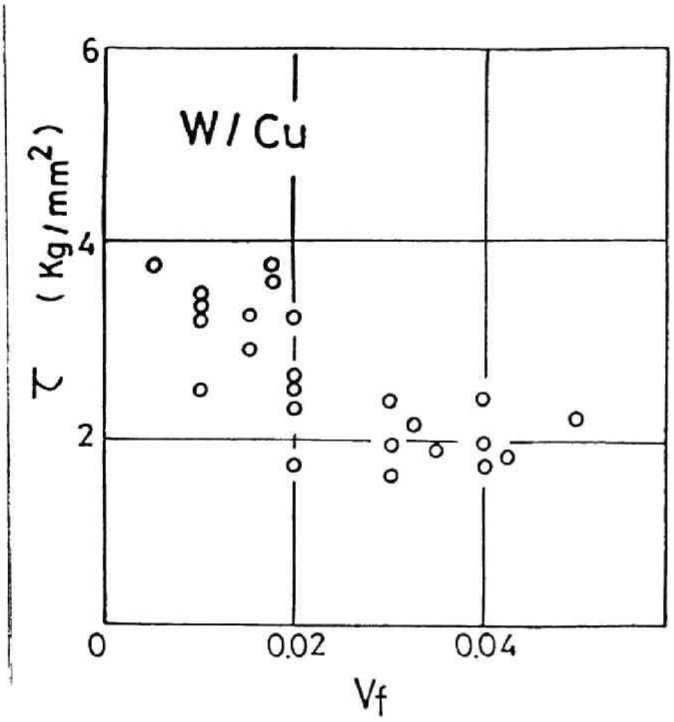

Fig.6 Calculated values of τ plotted against V_f in W/Cu composites.

composite, whether or not this fibre continues to fracture into shorter lengths is dependent upon the following two factors. One is the ability of the matrix for further deformation prior to the fracture of the composite at the cross-section where the fibre has fractured already. The other is that for further increase in τ at the cross-section where the fibre has not fractured yet. When V_f ($< V_{min}$) is large, the matrix fails prior to the increase in τ enough to break further the fibre once fractured, because the ability for further deformation prior to its failuer is not large. On the contrary, when V_f is small, τ can be increased as the matrix has a larger ability for further deformation prior to its failure. Therefore the broken fibres can be fractured further and l_c/d becomes smaller. The increase in τ arises from work-hardening of the matrix and from the increase in compressive stress due to the differences in contraction and the amount of deformation between the fibre and the matrix, for $\tau' > \tau_m$ and $\tau' < \tau_m$, respectively. The increase in τ of the W/Cu composites is the latter case. The three points in question may be explained as discussed above.

Various methods to obtain the critical aspect ratio have been reported.[5] The method to obtain it from the fracture behaviour of the initially continuous fibre in the single fibre-composites with V_f smaller than V_{min} is the simplest. However, there is a difference in the stress condition between in the single fibre-composites and in the multi-fibre-ones. Especially when V_f is large ($> V_{min}$) in multi-fibre-composites, tensile stress is caused at the interface.[20] Therefore, the values of l_c/d obtained in the single fibre-composites cannot be applied directly to the multi-fibre-ones. Although this

method has some disadvantages, it is useful because an experimental estimation of the effects of interfacial conditions on stress transfer from the matrix to the fibre can be readily made if V_f is made constant in all the specimens.

III-(2)-5 Conclusions

Single fibre-composites containing initially continuous brittle fibres were prepared by a plating method. Load-elongation curves , critical aspect ratios and interfacial shear stressses were obtained. Effects of interfacial conditions on stress transfer mechanisms were discussed. The results obtained are as follows.

(1) When V_f is smaller than V_{min}, as the initially continuous fibres in the composites fracture continually into shorter lengths and finally reach $l_c/2$. Therefore, we can obtain the critical aspect ratio and interfacial shear stress according to the Kelly model. The values of critical aspect ratio and interfacial stress were found to depend upon V_f and the interfacial conditions.

(2) The external stress was found to be transferred from the matrix to the fibre even though the interfacial bonding strength is zero. This result was explained in terms of the frictional shear stress arising from the compressive stress caused by the difference in contraction and deformation amount between the fibre and the matrix.

III-(2)-6 Appendix

When a composite is reinforced with a continuous fibre, compressive stress P at the interface between the fibre and the matrix can be calculated by using Kelly's treatment[19] if the

interfacial bonding is strong enough for both the fibre and the matrix to be subjected to the same axial strain. However, no solution has been found yet for such a case where the interfacial bonding is weak for the matrix to slide relating to the fibre. Then, following the treatment similar to that of Kelly, we shall try to derive P for such a case. The stress equilibrium equation for an axially symmetric state in stage I is written as

$$\frac{d\sigma_r}{dr} + \frac{\sigma_r - \sigma_\theta}{r} = 0 \qquad (A1)$$

where r is the radius, and σ_r and σ_θ are radial and transverse stresses, respectively. As Hooke's law provides the relation

$$\sigma_r + \sigma_\theta = \text{const.}, \qquad (A2)$$

σ_r , σ_θ and the longitudinal stress σ_z can be obtained in both the fibre and the matrix when their strains are e_f and e_m, respectively

$$\sigma_r(f) = A - B/r^2$$

$$\sigma_\theta(f) = A + B/r^2$$

$$\sigma_z(f) = e_f E_f + 2\nu_f A$$

$$\sigma_r(m) = C - D/r^2$$

$$\sigma_\theta(m) = C + D/r^2$$

$$\sigma_z(m) = e_m E_m + 2\nu_m C \qquad (A3)$$

where A, B, C and D are the constants and f and m in the parentheses refer to the fibre and the matrix, respectively. To evaluate A, B, C and D, we can use the following conditions :

(a) If $B \neq 0$, $\sigma_r(f)$ and $\sigma_\theta(f)$ are infinite. B must be zero.

(b) ν_m is larger than ν_f and also the deformation amount of the matrix is larger than that of the fibre. Therefore, the

transverse strain of the fibre is equal to that of the matrix at the interface.

(c) The radial stresses in the fibre and the matrix are equal at the interface.

(d) The radial stress in the matrix is zero at the outside surface.

From the constant A, P can be obtained as eq.(A4) if it is taken as positive when the fibre is under compression :

$$P = \frac{2(e_m \nu_m - e_f \nu_f)V_m}{V_f/k_m + 1/G_m + V_m/k_f} \qquad (A4)$$

In stage II, eq.(A4) becomes

$$P = \frac{e_m(1 - 2\nu_f e_f/e_m)V_m}{V_f/K_m + 1/G_m + V_m/k_f} \qquad (A5)$$

by setting $\nu_m=0.5$ and $k_m=K_m$ [19].

III-(3) Study on Stress Transfer Mechanisms by Pull-Out Test

III-(3)-1 Introduction

In this work, pull-out test is used to measure τ and l_c/d. Effects of (1)irregularities on the fibre surface, (2)preparation method, (3)coating, (4)interfacial reaction and (5) thermal cycling on τ and l_c/d are clarified experimentally.

In order to check the pull-out test results, the fracture surfaces of single fibre-composites with identical interfacial conditions are examined.

The values of τ measured by the pull-out and multiple-fracture tests are compared, which will give suggestions on stress transfer mechanism. The values of τ measured by the multiple-fracture test are taken from Table 2 in the former part in this chapter.

III-(3)-2 Experimental Procedure

Tungsten wire of 500μm diameter was used as the fibre material in the matrix of pure copper. Specimens were prepared mainly by the plating method (P method). The supplied fibres were boiled in a saturated sodium hydroxide solution for 30 min to remove the graphite lubricant on their surfaces (B treatment). After this surface treatment, the fibres were coated when necessary and then plated with copper up to 500μm in thickness.

To know the effect of (1), some fibres after B treatment were electropolished in the dilute sodium hydroxide solution until the irregularities (die markings in this case) were removed (E treatment). Two types of the aforementioned surface treatments, B and E, will make clear the effect of the existence

of irregularities on τ and l_c/d. For (2), a vaccum infiltration method (I method)[8] was used as a preparation method, together with P method. For (3), graphite (G), boronnitride(BN), and nickel (Ni) were selected as the coating materials for the reasons stated already in the former part of this chapter. For graphite coating, the fibres were used under the as-supplied condition, since graphite adhered to the supplied fibres as lubricant. The thickness of each coating material was at most less than 1/50 of the fibre diameter. These specimens will be described as W/G/Cu, W/BN/Cu and W/Ni/Cu, respectively, and the specimens without coating as W/Cu. For (4), the results of W/Ni/Cu specimens annealed at 900°C for 10 min in vaccum were compared with those of the non-annealed ones. For (5), W/Cu and W/G/Cu specimens were thermally cycled 0-100 times between 0 and 300°C.

The pull-out test was carried out with an Instron tensile machine at a constant crosshead speed of 2 mm per min.

Observation of the fibre surfaces and the fractured composites was made by a scanning electron microscope.

III-(3)-3 Results and Discussion

At first, copper was plated on the polished surfaces of tungsten blocks and then tensile strength of the interface was measured. It was nearly zero. This result agrees well with that of Cooper.[13] With this fact in mind, the effects of the aforementioned factors were investigated.

III-(3)-3-(i) Results of Pull-Out Test.

III-(3)-3-(i)-(1) Effects of Irregularities on the Fibre Surface

Fig.7 shows the stress in the fibre at pull-out (open points) or fibre fracture(filled points) as a function of the embedded length, $\underline{l}$, divided by the diameter, d. From these results, τ and $\underline{l}_c/d$ were obtained according to Kelly model[5] as shown in Table 3. It should be noted that the shear strength of the interface was not zero although the chemical interfacial bonding strength was nearly zero. A similar result has been obtained by Cooper.[13] The apparent inconsistency of these results can be explained by the following results and consideration. Photo.2(a)(b) shows the surfaces of the fibre after B-and E-treatments, respectively. Irregularities(die markings) are found in the B-treated fibre but are scarcely observable in the E-treated fibre. Photo.2(c) shows the fracture surface of W(B-treated fibre)/Cu composite. It is found that, before the tensile test, copper had adhered to tungsten in accordance with the irregularities on the fibre surface. The value of τ of the specimens of B-treated fibres was greater than that of the specimens of the E-treated fibres as shown in Table 3. Then, τ is considered to be produced by the interlocking effect of the interface when the interfacial bonding is nearly zero.

III-(3)-3-(i)-(2) Effects of the Preparation Method

In the case of W/Cu specimens, τ was much greater when prepared by the I method than when prepared by the P method. To explain the high value of τ (21.2 kg/mm^2) by the I method, the existence of chemical bonding will be inevitable since the interlocking effect derived from the irregularities can produce only 2.4 kg/mm^2(P method).

III-(3)-3-(i)-(3) Effects of Coating

When graphite was coated, τ became small when compared

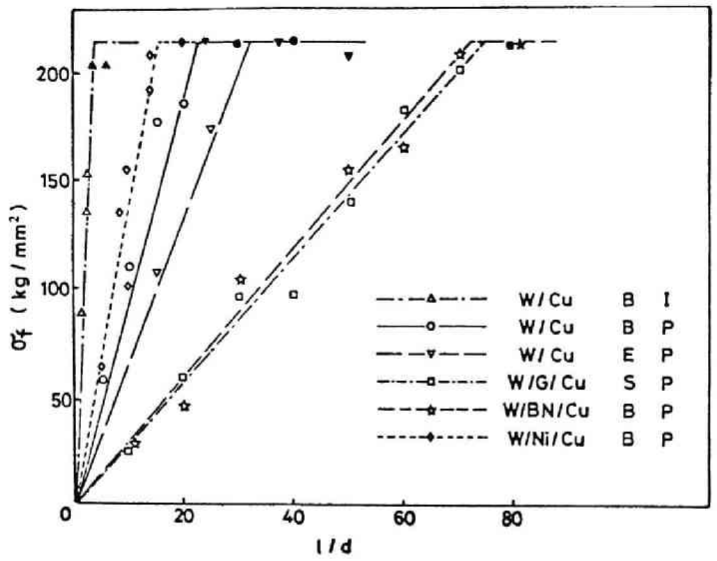

Fig.7 Fibre stress of W/Cu(I method), W/Cu(P method), W(E-treated)/Cu, W/G/Cu, W/BN/Cu and W/Ni/Cu specimens at pull-out(open points) or fibre fracture(filled points) as a function of the embedded length divided by the diameter. B and E, and I and P refer to the surface treatments and preparation methods,respectively. S refers to the as-supplied condition of the fibres.

Table 3 Effects of (1) irregularities on the fibre surface, (2) preparation method, (3) coating, (4) Interfacial reaction, and (5) thermal cycling on the shear strength and critical aspect ratio

(1) Irregularities on the fibre surface

Cleaning method	l_c/d	τ(kg/mm^2)
E	68.2	1.6
B	44.2	2.4

(2) Preparation methods

Preparation method	l_c/d	τ(kg/mm^2)
I	5.0	21.2
P	44.2	2.4

(3) Coating

Specimen	l_c/d	τ(kg/mm^2)
W/Cu	44.2	2.4
W/G/Cu	147.0	0.7
W/BN/Cu	147.0	0.7
W/Ni/Cu	31.2	3.4

(4) Interfacial reaction

Specimen	l_c/d	τ(kg/mm^2)
W/Ni/Cu, as plated	31.2	3.4
W/Ni/Cu, annealed	11.2	9.6

(5) Thermal cycling

Specimen	l_c/d	τ(kg/mm^2)
W/Cu, T0	44.2	2.4
W/Cu, T1	44.2	2.4
W/Cu, T5	44.2	2.4
W/Cu, T20	70.0	1.5
W/Cu, T100	148.0	0.7
W/G/Cu, T0	147.0	0.7
W/G/Cu, T100	185.0	0.6

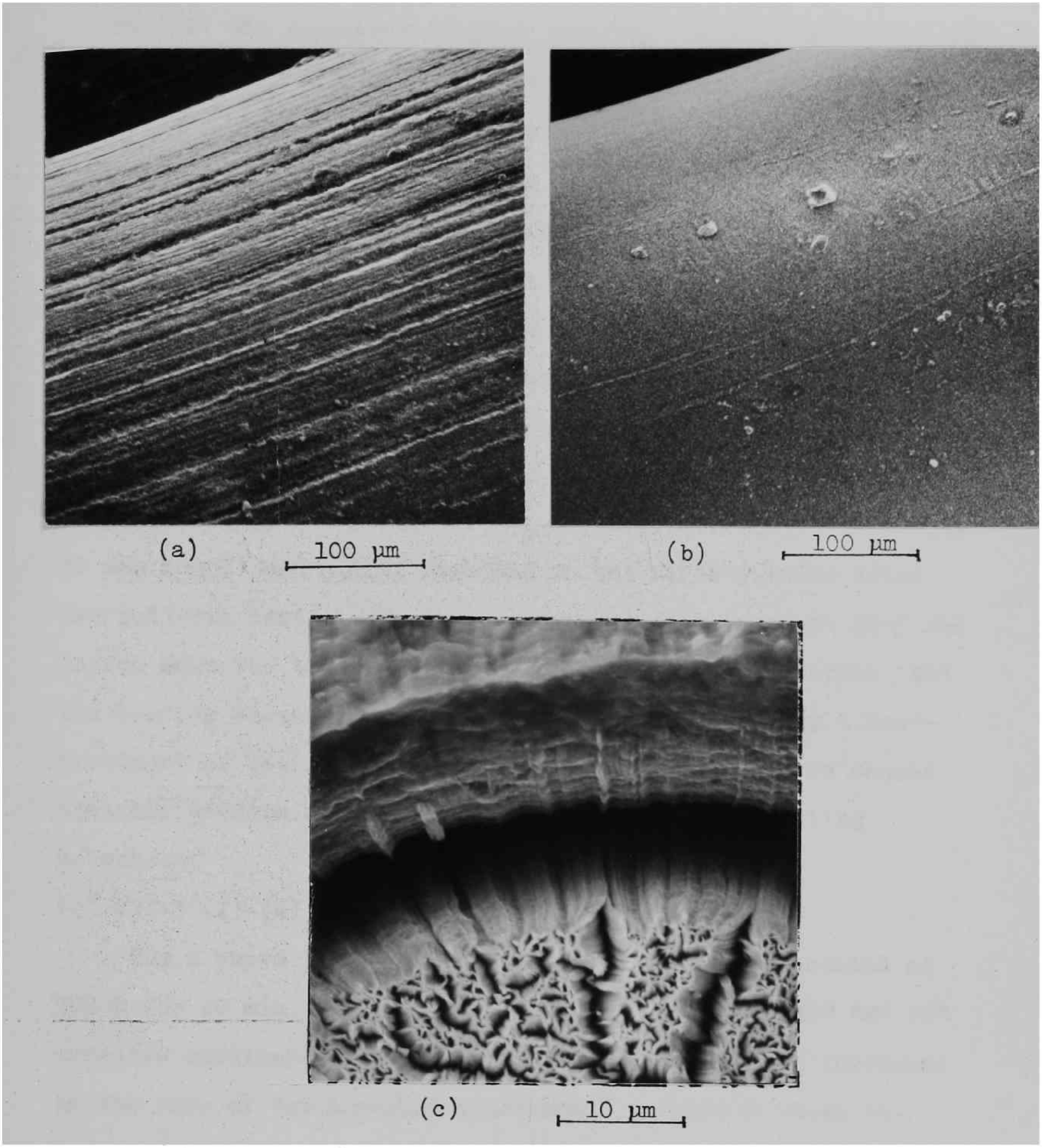

Photo.2 Scanning electron micrographs of the surfaces of B-(a) and E-(b) treated tungsten fibres and a fracture surface of W/Cu composite prepared by the P method (c).

to that of the specimens without coating. This is explained as follows:(a)graphite acts as a lubricant and (b)the hollows in the fibre surfaces are filled with graphite(lack of irregularities). When BN was coated, τ also became small, due to a reduction of the contact area between the fibre and the matrix. Contrary to graphite or BN coating, nickel coating produced a high value of τ than no coating. The value of τ of W/Ni specimens was measured for comparison. It was 10.3 kg/mm^2. This value was much greater than 3.4 kg/mm^2 of W/Ni/Cu specimens. This means that pull-out was caused by the shear fracture not at the tungsten-nickel but at the nickel-copper interface. Actually, it was found that nickel remained on the fibre surface after the pull-out test. In these specimens, the increase in τ was not so much due to weak bonding between nickel and copper, but the bonding strength between them can be enhanced by a heat-treatment if desired, as shown later. Therefore, we should consider effects of heat-treatment for selecting coating materials.

III-(3)-3-(i)-(4) Effects of Interfacial Reaction

Fig.8 shows the results of W/Ni/Cu specimens annealed at 900°C for 10 min, together with those of the as-plated and non annealed specimens for comparison. The value of τ increased in the case of the annealed specimens. Photo.3 shows the fracture surfaces of W/Cu(a), W/Ni(b) and W/Ni/Cu(c) composites annealed at 900°C for 10 min. In the W/Cu composite, the fibre is separated from the matrix. On the other hand, in the W/Ni and W/Ni/Cu composites, the fibres are not separated from the matrices, which indicates that the interfacial bonding is strong in these composites. Nickel is a useful coating

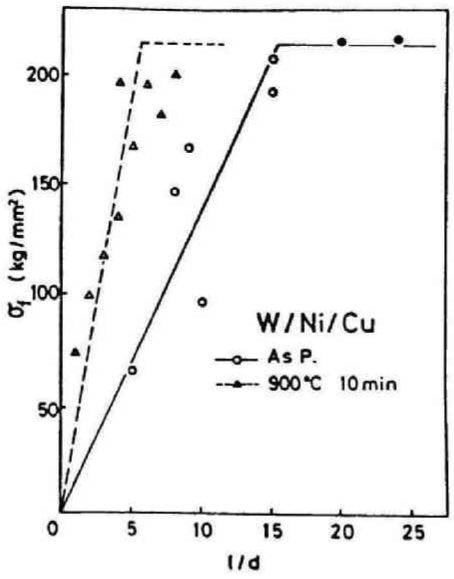

Fig.8 Fibre stress of as-plated and annealed W/Ni/Cu specimens at pull-out(open points) or fibre fracture(filled points) as a function of the embedded length divided by the diameter.

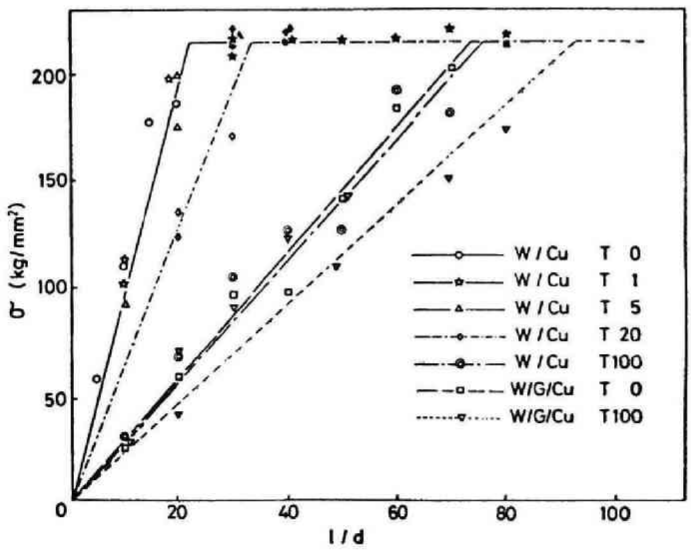

Fig.9 Fibre stress of the thermally cycled specimens at pull-out(open points) or fibre fracture(filled points) as a function of the embedded length divided by the diameter.

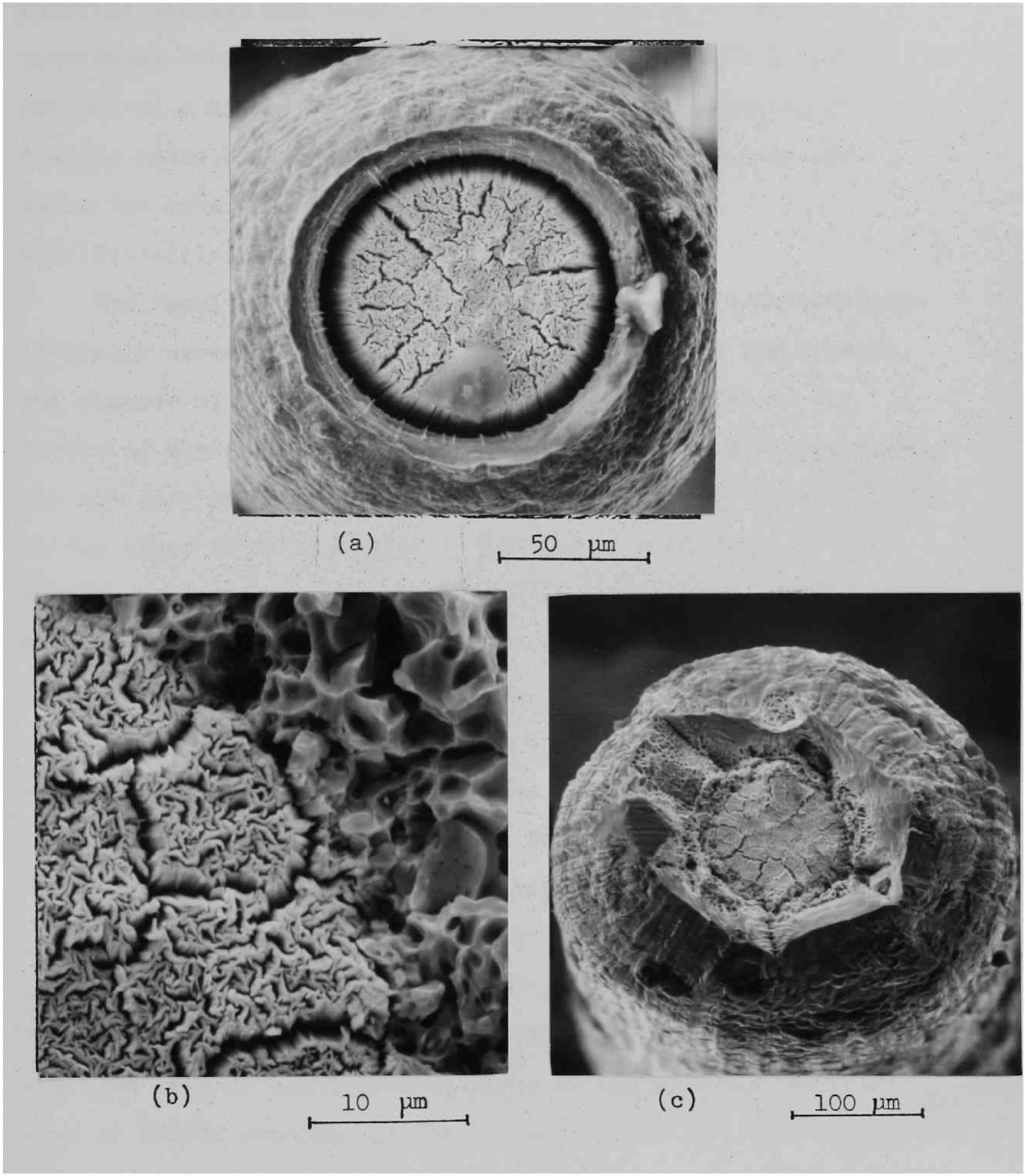

Photo.3 Scanning electron micrographs of the fracture surfaces of W/Cu (a), W/Ni annealed at 900°C for 10 min (b) and W/Ni/Cu annealed at 900°C for 10 min (c).

material because the tungsten-nickel and nickel-copper interfaces become strong when annealed, and therefore nickel can act as a binding agent. An appropriate selection of coating material and a favourable interfacial reaction can raise the interfacial shear strength.

III-(3)-3-(i)-(5) Effects of Thermal Cycling

The results of pull-out tests of W/Cu and W/G/Cu specimens thermally cycled between 0 and 300°C are shown in Fig.9 where the figures of 0, 1, 20 and 100 that follow T refer to the number of thermal cyclings. The value of τ of W/Cu specimens did not vary in the cases of T1 and T5 treatments but decreased in the cases of T20 and T100 treatments. The value of τ of W/G/Cu specimens was also decreased by the thermal cycling. When thermally induced stresses at the interface due to the difference in the thermal expansion coefficients of tungsten[21] and copper[16] become greater than the interfacial strength, the interface will fracture and then the values of τ will decrease.

III-(3)-3-(ii) Comparison of the Values of τ Measured by the Pull-Out Test and the Multiple-Fracture Test.

Table 4 shows the comparison of the values of τ measured by the pull-out test with those obtained by the multiple-fracture test. The value of τ measured by the multiple-fracture test of the W/G/Cu specimen is assumed to be equal to that of W/C/Cu specimen in the former part (2) of this chapter, since the effects of graphite and carbon coatings are considered to be not so much different from each other. In W/G/Cu, W/BN/Cu and W/Cu composites, the values of τ measured by the pull-out test are smaller than those measured by the multiple-fracture test. On the contrary, a reverse result is obtained in W/Ni/Cu

Table 4 Comparison of the values of τ (kg/mm^2) measured by pull-out test with those obtained by the multiple-fracture test.

Specimen	Pull-out test	Multiple-fracture test
W/G/Cu	0.7	1.5
W/BN/Cu	0.7	1.8
W/Cu	2.4	2.4
W/Ni/Cu*	9.6	6.3

* Annealed specimen

composites. This difference is explained as follows.

(A) In the cases of W/G/Cu, W/BN/Cu and W/Cu composites

In the multiple-fracture test, even if the interface breaks, the compressive stress caused by the different contractions and the difference of deformation amounts between the fibre and the matrix should be taken into consideration, when the shear strength of the interface is smaller than τ_m which is a shear stress in the matrix. This compressive stress can cause a frictional shear stress at the interface. Therefore external stress can be transferred from the matrix to the fibre through this frictional stress , and then the fibre can be fractured into shorter segments even once the interface has broken. Thus in the multiple-fracture test, the frictional shear stress at the interface is measured as τ , when the shear strength of the interface is weak and therefore the interface breaks prior to failure of the composites. On the contrary, in the pull-out test, the shear strength of the interface is measured as τ . In the case of W/G/Cu, W/BN/Cu and W/Cu specimens, the shear strength of the interface is very weak and therefore the values of measured by the multiple-fracture test are greater than those measured by the pull-out test.

(B) In the case of W/Ni/Cu composites annealed at 900°C for 10 min.

When the shear strength of the interface is high enough, the composites fail before the interface breaks in the case of multiple-fracture test. In such a case, the measured values of τ correspond to a shear stress in the matrix which is

smaller than the shear strength of the interface. The result of W/Ni/Cu composites annealed at 900°C for 10 min is considered to correspond to this case.

III-(3)-4 Conclusions

Effects of irregularities on the fibre surface, sample preparation method, coating, interfacial reaction and thermal cycling on shear strength of the interface and the critical aspect ratio were investigated by the pull-out test. The results of the pull-out test were checked with the observation of the fracture surfaces of single fibre-composites and compared with those of the multiple-fracture test. The main results obtained are summarized as follows.

(1) Even when the tensile strength of the interface was nearly zero, the shear strength of the interface was not zero. Shear strength of the interface was considered to be produced by the interlocking effect of the irregularities on the interface.

(2) Shear strength of the interface was affected by the factors such as the preparation method, coating, interfacial reaction and thermal cycling. Appropriate selections of the preparation method, or coating materials , and a favourable interfacial reaction produce high interfacial shear strength.

(3) In the pull-out test , the shear strength of the interface was measured. On the other hand, in the multiple-fracture test, the frictional shear stress caused by the differences of the deformation amount and Poisson's ratio between the fibre and the matrix was measured when the interfacial bond is weak,while shear stress in the matrix was measured when interfacial bond is strong.

III-(4) Summary

Two important parameters for stress transfer from matrix to fibre, i.e. shear stress at interface and critical aspect ratio were measured both by the multiple-fracture test and by the pull-out test on the composites with various interfacial conditions. The experimental results showed that whichever weaker between interfacial shear strength and shear stress in the matrix determines the stress transfer mechanism. If the latter is lower than the former , the effective interfacial shear stress for stress transfer corresponds to the latter. In this case, strong interfacial bonding exceeding shear stress in the matrix cannot be available. Strong interfacial bonding allows for cracks to propagate easily as shown later in chapter IV-(4). Thus, it can be concluded that extremely strong bonding is not necessary. If the interfacial bonding strength is weaker than the shear stress of the matrix , the interface fails (namely debonding occurs) when the exerted shear stress exceeds the shear strength. Thus efficiency of stress transfer of this case is lower than that of the aforementioned case of strong interfacial bonding. After failure of the interface, compressive stress is exerted on the fibre due to differences of Poisson's ratio and deformation amount between fibre and matrix. Then frictional shear stress is exerted on fibre. When the frictional shear stress is higher than the interfacial shear strength, critical aspect ratio can be decreased. In view of this point, coefficient of friction between the constituents plays a important role, since the frictional shear stress increases with increasing coefficient. Some factors can be mentioned as affecting ones on the coefficient. For instance, irregularities on fibre surfaces and appropriate coatings can raise it.

References

(1) G.S.Holister and C.Thomas : Fibre Reinforced Materials, Elsevier, London , (1966),p.14.

(2) S.Ochiai, M.Mizuhara and Y.Murakami : J. Japan Inst. Metals, (in press)

(3) Y.Murakami, S.Ochiai, K.Shimomura and S.Okuda : Read at the Autumn Meeting of Japan Institute of Metals, (1975).

(4) A.Kelly : Proc. Roy. Soc., 282A(1964),63.

(5) A.Kelly and W.R.Tyson : J. Mech. Phys. Solids, 13(1965),329.

(6) D.L.McDanels, R.W.Jech and J.W.Weeton : Trans. Met. Soc. AIME, 233(1965),636.

(7) A.Kelly and H.Lilholt : Phil. Mag., 20(1969),311.

(8) Chapter IV-(4)

(9) Chapter IV-(3)

(10) R.W.Hertzberg : Fibre Composite Materials, ASM, Ohio, (1964), p.77.

(11) S.Ochiai, M.Mizuhara, M.Kawasaki and Y.Murakami : Trans. JIM, 15(1974),66.

(12) F.O.Jones : Niobium, Tantalum, Molybdenum and Tungsten, Ed. by A.G.Quarrel, Elsevier, (1961), p.151.

(13) G.A.Cooper : J. Mat. Sci., 2(1967),409.

(14) M.Hansen : Constitution of Binary Alloys, McGraw-Hill, (1958), p.601.

(15) A.Kelly: Proc. Roy. Soc., 282A(1964),63.

(16) C.J.Smithells : Metals Reference Book, Vol.3, Butterworth, London, (1967), p.686.

(17) J.O.Outwater, Jr.: Mod. Plast., 33(1956),156.

(18) C.J.Smithells : Metals Reference Book, Vol.3, Butterworth, London, (1967), p.708.

(19) A.Kelly : Strengthening Methods in Crystals, Ed. by A.Kelly and R.B.Nicholson, Elsevier, (1971), p.439.

(20) L.J.Ebert and J.D.Gadd : Fiber Composite Materials, ASM, Ohio, (1964), p.89.

(21) C.J.Smithells : Metals Reference Book, Vol.3, Butterworth, London, (1967), p.687.

Chapter IV

Effects of Interfacial Reaction on Mechanical Behaviour of Composites

IV-(1) Introduction

In artificial composites, interfacial chemical reactions between fibres and matrix take place during preparation and/or application. Chemical reactions and their effects on mechanical properties of composites are very complex, since different interfacial reactions occur in different composite systems and therefore the mechanical behaviour is different among each composite. Chemical problems in fabrication, testing and evaluation of composite systems occur in both bonding of the two phases and direct reaction between the phases. If fibres do not wet to matrix, consolidation is very difficult and good mechanical properties cannot be obtained. For this case, interfacial reaction, at first sight, seems to play a role to bind the two phases. However, in most cases, interfacial reactions degrade properites of composites, even if good bonding can be obtained. Up to date, effects of interfacial reaction on mechanical properties of composites have been widely investigated[(1)-(27)], and the mechanical properties of several composites have been clarified in some detail. However, much uncertainties remain unsolved so that systematic explanation for the effects of interfacial reactions on properties of composites hasn't been constructed. In this chapter, the mechanical properties of some composites with interfacial reactions will be described and finally summarized systematically in view of characteristics

of the reaction zone, interfacial bonding, thickness of the zone and reaction time.

In (2) , effects of the brittle zone formed on the fibre surface on mechanical behaviour of ductile fibre-ductile matrix composites, which were investigated by using single- and multi-fibre/ductile matrix composite, will be discussed. In (3), the relationships between mechanical properties and the extent of interfacial reaction investigated by using single semi-ductile fibre/ ductile matrix composite will be described. In (4) , deformation and fracture behaviour of the multi- semi-ductile and ductile fibre/ ductile matrix composites with and without interfacial reaction will be discussed, together with some mechanical interactions between fibres and matrix. In (5) , tip radius of cracks formed by earlier fracture of the brittle zone will be calculated for the two cases : One is the case where the brittle zone is formed in the peripheral zone of the fibre and the other is the case where the zone is formed on the fibre surface. The calculated values of tip raduius will make clear the difference of fracture behaviour between the above two cases. In (6), effects of interfacial reaction on deformation and fracture behaviour of composites will be summarized in view of the aforementioned four points.

IV-(2) Deformation and Fracture Behaviour of Composites with Brittle Zones on Fibre Surfaces

IV-(2)-1 Introduction

Chemical reactions taking place at fibre-matrix interface have been known as one of the causes in reducing the strength of composites. When the formed zone is brittle, it gives rise to microcracks. In such a case, two types of degradation are found depending upon the ductility of fibres. If fibres are notch-sensitive, the formation of notches by the multiple crackings of the brittle zone hastens fracture of fibres. Then, as fibres cannot support the loads up to their full strengths, strength of composites fall below the value expected by the rule of mixtures.[2)(5)(12)] On the other hand, if fibres are ductile and notch-insensitive, degradation is relatively minor and strength of composites can be approximately predicted by the rule of mixture in which the contribution of the brittle zone is neglected.[5)(12)(16)]

However, in some cases, when fibres are ductile, strength of composites is raised in spite of multiple crackings of the brittle zone.[28)(29)] In chapter II-(2), to explain the strengthening mechanism of such cases, a new model was suggested and applied to some single fibre-composites composed of two components - a brittle outer case of the brittle zone and a ductile core of the fibre.[28)] The suggested model explained the experimental results satisfactorily.

In this place, an extension is needed in real composites containing three components - fibres, brittle zone and matrix. The aims of this work are (i)to apply the model to the experimental

results and (ii)to clarify the effects of the brittle zone on deformation and fracture behaviour of multi-ductile fibre-composites containing three components.

IV-(2)-2 Experimental Procedure

Two kinds of composites were used in this experiment : two components (aluminium-alumina)- and three components (stainless steel-brittle zone-aluminium)- composites.

IV-(2)-2-(i) Aluminium-Alumina Composite

The preparation method of aluminium-alumina composite was described already.[28] Two kinds of aluminium fibres with a nominal diameter of 800μm were used. One, also having been used in the previous work[28] was consisting of fine grains whose size was 50μm on an average (A-type) and the other of coarse bamboo-like ones (B-type). The mean UTS was 9.0 kg/mm^2 and 4.7 kg/mm^2 for A- and B-type fibres, respectively. Both types showed more than 20% elongation and were notch-insensitive.

IV-(2)-2-(ii) Stainless Steel-Brittle Zone-Aluminium Composite

The fibre and matrix materials were 18-8 stainless steel wire with a nominal diameter of 200μm and 99.99% aluminium,respectively. The fibres were wound over electropolished aluminium sheets. The wound samples and aluminium sheets were piled up alternatively. The assembly was hot-pressed in vaccum at 500°C for 30min under a pressure of 450 kg/cm^2. The length, width and thickness of the as-pressed composite were 60, 10 and 2.5 mm ,respectively. The initial fibre volume fraction V_f^o was 17.8%. The volume fraction V_b^o of the brittle zone formed at the fibre-matrix interface and V_f^o

were varied by changing the annealing times at 600°C in vaccum.

Two types of specimens for tensile test of multi-fibre composites were used : sheet-specimens for measurement of flow stress and UTS, and notched specimens both for observation of fracture behaviour and for measurement of UTS. Tensile test was carried out with an Instron tensile machine at a cross-head speed of 2 mm per min.

The appearance of the composites during deformation and after fracture was observed by a scanning electron microscope.

IV-(2)-3 Results

IV-(2)-3-(i) Aluminium-Alumina Composite

Tensile strength , σ_c , of aluminium-alumina composite is shown in Fig.1. Typical appearance of the alumina film after fracturing of the composite is such that as shown in chapter II-(2). As the multiple crackings occur in the alumina film prior to fracture of the composite , σ_c will follow the rule of mixtures (ROM) in which the contribution of the alumina film to composite strength is neglected, namely

$$\sigma_c(\mathrm{ROM}) = \sigma_{fu} V_f^o \qquad (1)$$

where σ_{fu} is the UTS of the aluminium fibre measured on un-notched sample (i.e. bare aluminium fibre). The measured values of σ_c , however, were higher than σ_c(ROM) represented by the dashed lines in Fig.1(b). Both A- and B-type composites were strengthened by the brittle zone though the brittle zone exhibited multiple crackings and therefore the zone could not carry the applied load. The strengthening efficiency is given by $\sigma_c/\sigma_c(\mathrm{ROM})$. It is clearly

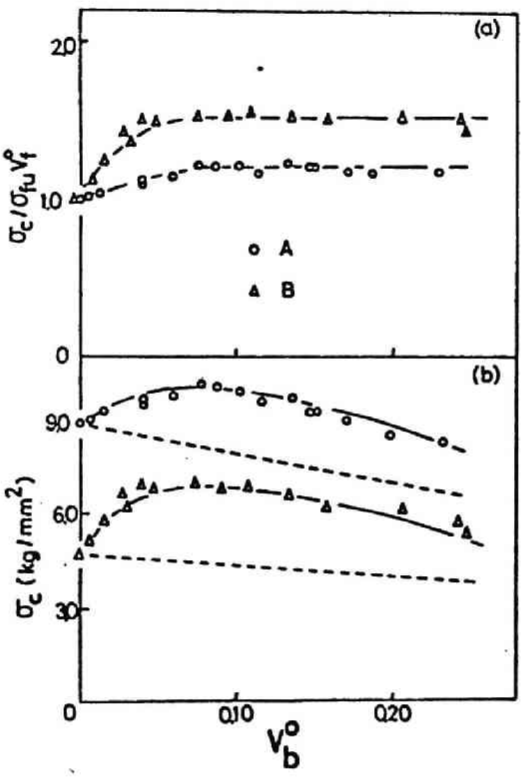

Fig.1 Measured values of σ_c and σ_c/σ_c(ROM) of the aluminium-alumina composite

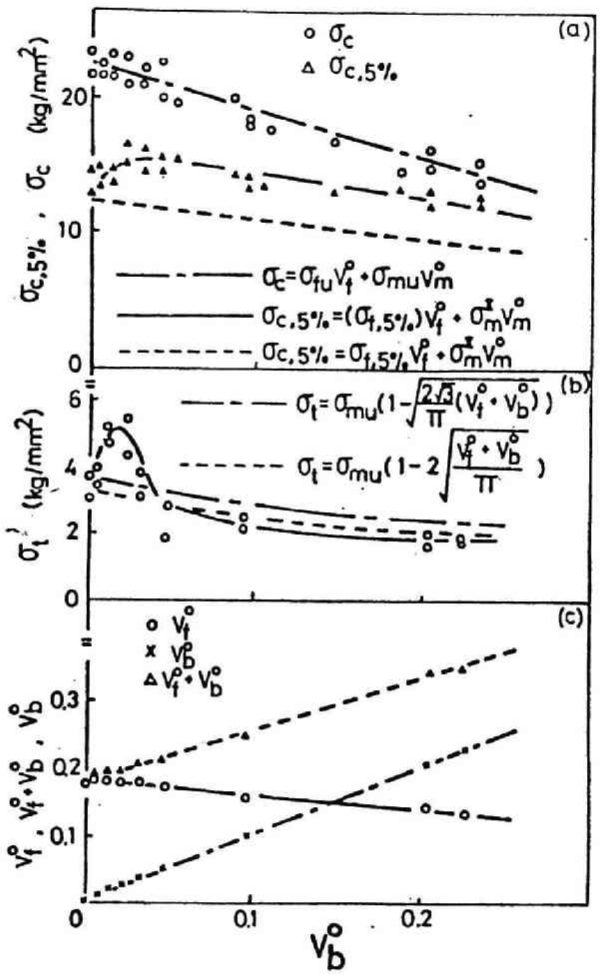

Fig.2 Measured values of σ_c, $\sigma_{c,5\%}$, σ_t, V_f^o and $V_f^o + V_b^o$ of the stainless steel-brittle zone-aluminium composite

seen in Fig.1(a) that the efficiency of B-type composite is much higher than that of A-type one.

IV-(2)-3-(ii) Stainless Steel-Brittle Zone-Aluminium Composite

Tensile test was carried out both on the sheet and notched specimens containing multi-fibres, brittle zone and matrix, and also on the fibres coated with the brittle zone extracted from the composite (hereafter described as the extracted fibres).

IV-(2)-3-(ii)-(a) Sheet Specimens

In Fig.2(a), the longitudinal (parallel to the alignment of the fibres) flow stress at 5% elongation , $\sigma_{c,5\%}$, tensile strength σ_c, and transverse (perpendicular to the fibres) tensile strength σ_t versus V_b^o are represented. The measured values of $\sigma_{c,5\%}$ increased at first and then decreased with increasing V_b^o , while those of σ_c decreased linearly with increasing V_b^o. As the brittle zone exhibiting multiple crackings cannot carry the applied load, $\sigma_{c,5\%}$ will be given by ROM as eq.(2).

$$\sigma_{c,5\%}(\mathrm{ROM}) = \sigma_{f,5\%}V_f^o + \sigma_m^* V_m^o \qquad (2)$$

where $\sigma_{f,5\%}$ and σ_m^* are tensile stresses of the bare fibre and the matrix at 5% elongation, and V_m^o is the volume fraction of the matrix. The measured values of $\sigma_{c,5\%}$, however, were higher than $\sigma_{c,5\%}(\mathrm{ROM})$ represented by the dashed line. As shown later, if $\sigma_{f,5\%}$ is replaced by ($\sigma_{f,5\%}$) which is the 5% flow stress of the extracted fibre, the calculated values of $\sigma_{c,5\%}$ (represented by the solid line) agree well with the measured ones. On the other hand, UTS of the composite σ_c is given approximately by

$$\sigma_c(\mathrm{ROM}) = \sigma_{fu}V_f^o + \sigma_{mu}V_m^o \qquad (3)$$

where σ_{fu} and σ_{mu} are respectively UTS's of the bare fibre and the matrix tested separately. The measured values of σ_c agreed well with the calculated ones. The fracture surfaces of the compoistes with various thicknesses of the brittle zone are shown in Photo.1. In the as-pressed composite, interfacial reaction was scarecely found, (a). In the composite with V_b^o=0.012(b), 0.049(c) and 0.205(d), the brittle zone was broken in numerous segments. The size of the segments was nearly identical for a given V_b^o, as in (d).

The result of the transverse tensile test is shown in Fig.2(b). The σ_t increased with increasing thickness of the brittle zone up to V_b^o=0.02, but decreased with further increasing V_b^o. Fracture surface of the composites with various V_b^o is shown in Photo.2. In the as-pressed composite, fracture occurred at the fibre-matrix interface. When V_b^o=0.02, the fibre-matrix interface was not clearly discerned, which might correspond to the increase in σ_t. When V_b^o was large, fracture occurred at the brittle zone-matrix interface but not at the fibre-brittle zone interface. The weak bond between the brittle zone and the matrix has been reported.[16][30][31] The reason has been explained in terms of the volume change occurring during the formation of the brittle zone.[31] Assuming no contribution of the brittle zone-matrix interface to σ_t, σ_t is dependent only upon the area fraction and UTS of the matrix and is given by

$$\sigma_t = \sigma_{mu}\left(1 - \sqrt{\frac{2\sqrt{3}}{\pi}\left(V_f^o + V_b^o \right)} \right) \qquad (4)$$

for hexagonal packing array of the fibres and

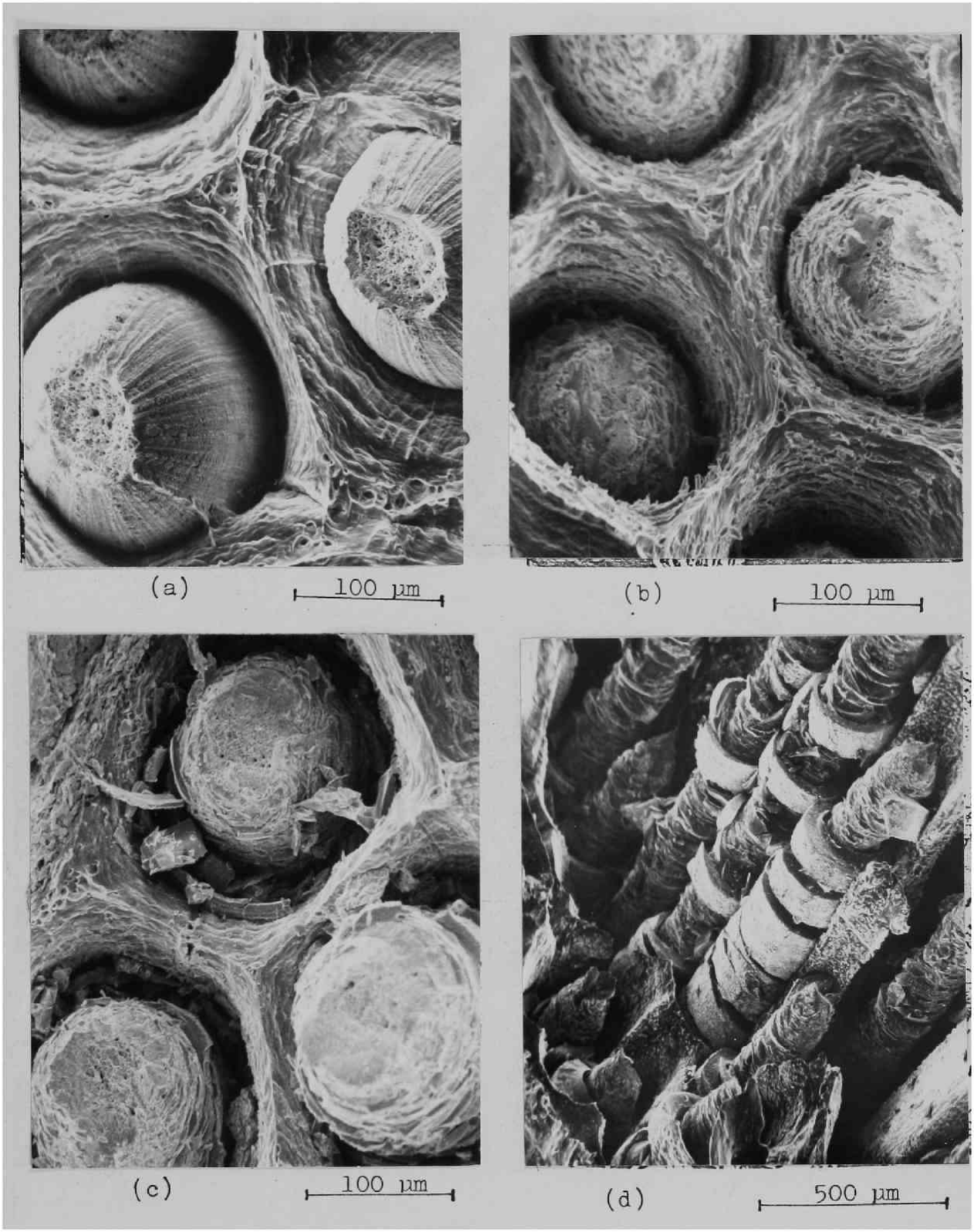

Photo.1 Fracture surface of the stainless steel-brittle zone-aluminium composite. (a)as-pressed (b)V_b^o=0.012 (c)V_b^o=0.049 (d)V_b^o=0.205

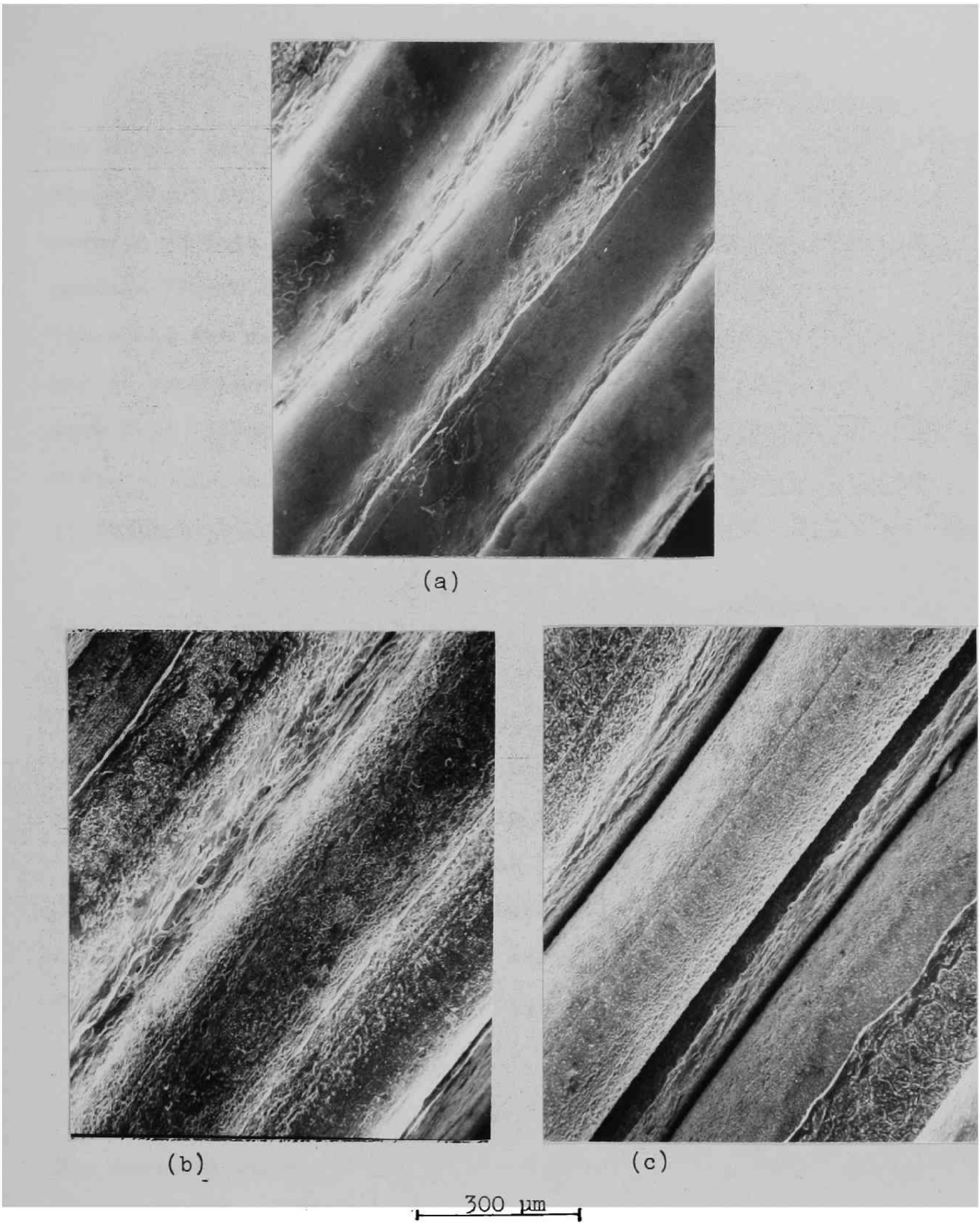

Photo.2 Fracture surface of the stainless steel-brittle zone-aluminium composite by a transverse tensile test. (a)as-pressed (b)V_b^o=0.020 (c)V_b^o=0.095.

$$\sigma_t = \sigma_{mu} \left(1 - 2 \sqrt{\frac{V_f^o + V_b^o}{\pi}} \right) \qquad (5)$$

for square packing array. The σ_t-V_b^o relations calculated by eqs.(4) and (5) are also shown in Fig.2(b). Judging from the results of this calculation and the observation of the fracture surface (Photo.2), it is known that the bond strength between the fibre and the matrix was very weak in the as-pressed condition and it increased by a slight interfacial reaction, but, due to weak bond between the brittle zone and the matrix, σ_t decreased with further increasing V_b^o.

IV-(2)-3-(ii)-(b) Extracted Fibre

In this and the follwing sections, parentheses will be used to descriminate the volume fractions of fibre, flow stress and UTS of the extracted fibre from those of the ternary stainless steel-brittle zone-aluminium composite.

The UTS (σ_{fu}) and 5% flow stress ($\sigma_{f,5\%}$) of the extracted fibre are shown in Fig.3 which is reproduced from chapter II-(2). (V_b^o) is the volume fraction of the brittle zone in the extracted fibre. The (σ_{fu}) and ($\sigma_{f,5\%}$) showed the similar tendencies to σ_c and $\sigma_{c,5\%}$ of sheet specimens, respectively. According to ROM, (σ_{fu}) and ($\sigma_{f,5\%}$) are given by

$$(\sigma_{fu})(\mathrm{ROM}) = \sigma_{fu}(V_f^o) \qquad (6)$$

$$(\sigma_{f,5\%})(\mathrm{ROM}) = \sigma_{f,5\%}(V_f^o) \qquad (7)$$

The measured values of (σ_{fu}) obeyed the ROM relation but ($\sigma_{f,5\%}$) showed positive deviation from the same relation. These results indicate that the brittle zone plays a role in the strengthening of the composites although the brittle zone does

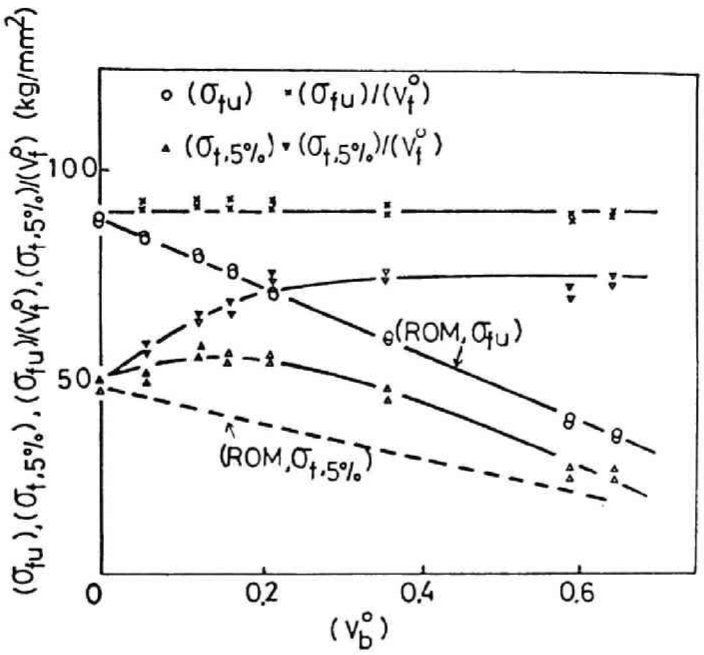

Fig.3 Measured values of (σ_{fu}) and $(\sigma_{f,5\%})$ versus V_b^o

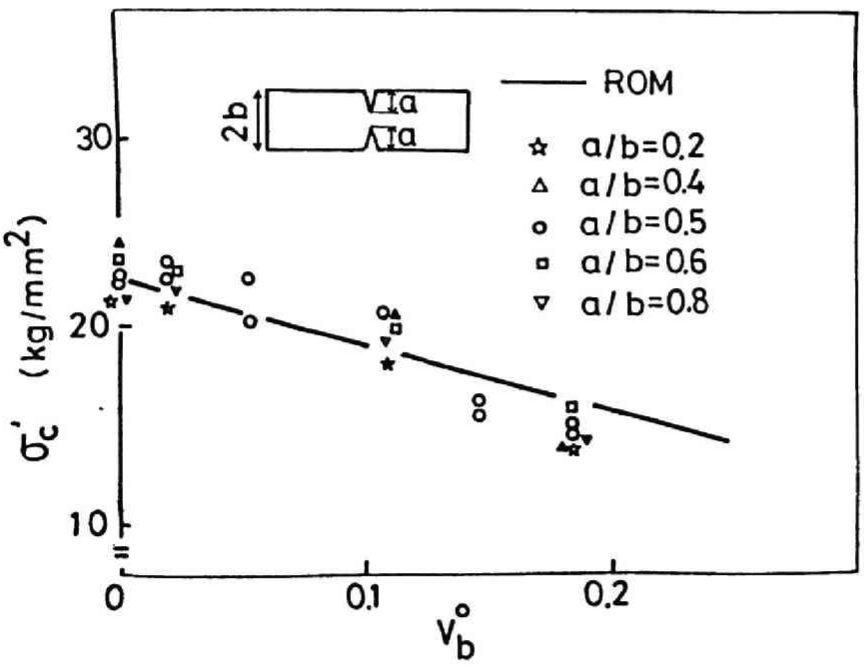

Fig.4 Measured values of σ_c' versus V_b^o

not carry the externally applied load. The appearance of the brittle zone at various stages of deformation was observed in chapter II-(2). The result showed that at 6-7% elongation, thick zone began spalling and thin zone being failed in a transverse direction by the compressive stress.

IV-(2)-3-(ii)-(c) Notched Specimens

Tensile strength σ_c' of the notched specimens composed of stainless steel fibres, brittle zone and matrix on the basis of the net (unremoved) cross-sectional area versus V_b^o is presented in Fig.4. It is found that σ_c' nearly obeyed the ROM relation (eq.(3)) as similarly as σ_c of the sheet specimens and the change of a/b did not affect on σ_c' where a is the depth of the notch and b is half the width of the specimen, as illustrated in Fig.4. In almost all specimens other than the as-pressed one, splitting occured. The as-pressed composite showed bridging of the fibres. Typical fracture behaviour, such as bridging and splitting, is shown in Photo.3.

IV-(2)-4 Discussion

IV-(2)-4-(i) Strengthening Mechanism by the Brittle Zone

IV-(2)-4-(i)-(a) Aluminium-Alumina Composite

It was suggested that ductile fibres can be strengthened by the constraining effect of the notched regions formed by micro-crackings of the brittle zone, as long as the brittle zone adheres to the fibres when it is thick and is not failed by the compressive transverse stress when it is thin.[28] The suggested theory satisfactorily explained the experimental results.[28] Accordi

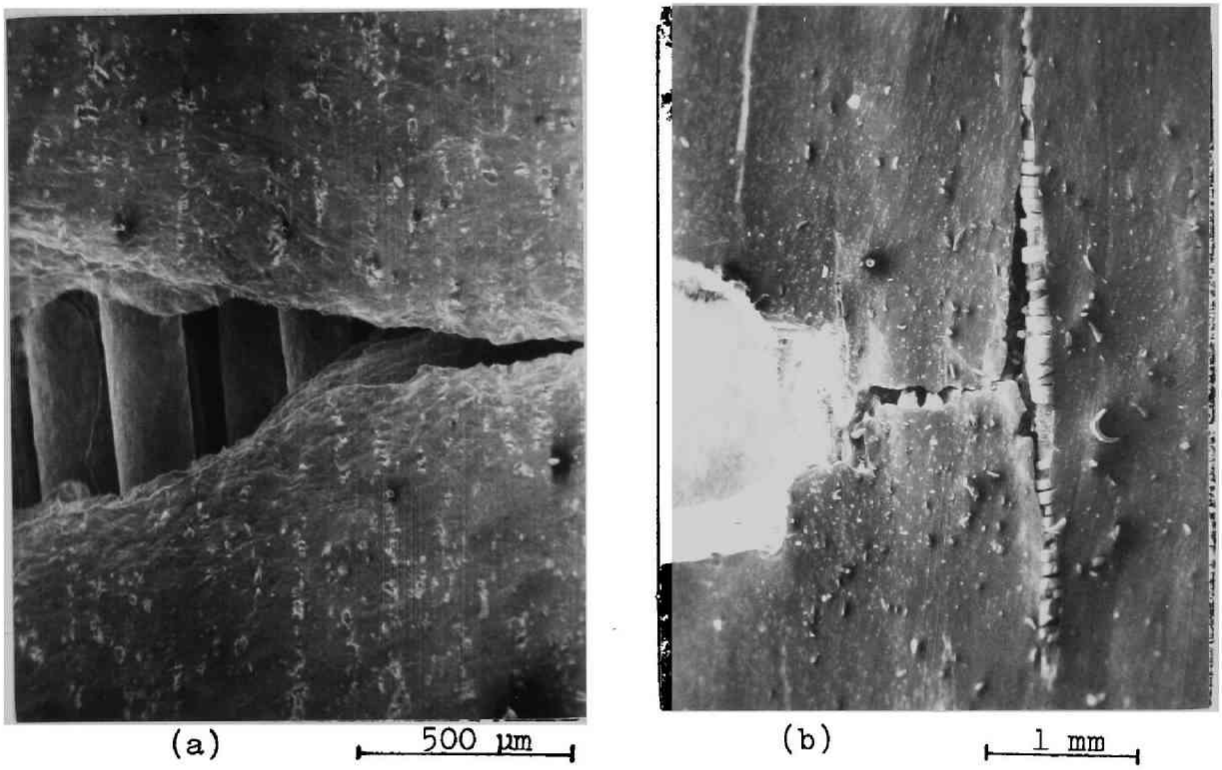

Photo.3 Fracture behaviour of the notched specimens of the stainless steel-brittle zone-aluminium composite (a)as-pressed (b)V_b^o=0.184

to the theory, two important parameters, the tensile stress exerted at the interface P and the maximum transverse compressive stress exerted on the brittle zone $\sigma_{\theta,max}$, were calculated for A- and B-type composites. The result is represented in Fig.5. The calculated values of P and $\sigma_{\theta,max}$ of A-type composite showed the similar tendencies to those of B-type one. This result indicates that a unique strengthening mechanism acts on both composites. The calculated values of P for both types of composites increased with V_b^o for $V_b^o < 0.10$, but ramained nearly constant for $V_b^o > 0.10$. When P exceeds the bond-strength between aluminium and alumina film, alumina film spalls. For $V_b^o < 0.10$, P is not high enough to spall alumina film, but $\sigma_{\theta,max}$ is so high that alumina film fails in the transverse direction. The appearance of the composites was observed also in this work and the result of calculation was affirmed just as in the previous work.[10] The result that P and $\sigma_{\theta,max}$ of A-type composite were nearly same as those of B-type one for a given V_b^o also means that the strengthening effect yields the same increase in strength for both composites, and that the smaller the value of σ_{fu}, the greater becomes the strengthening efficiency $\sigma_c/\sigma_c(ROM)$ i.e. $\sigma_c/\sigma_{fu}V_f^o$, as shown in Fig.1.

Next, let's consider the difference in deformation behaviour between A- and B-type composites. As stated already, one difference between A- and B-type fibres is the size of the grains: A- and B-type fibres consist of fine and coarse bamboo-like grains, respectively. When the B-type fibres are strained, a weakest grain deforms preferentially and the UTS is dependent upon the weakest grain. Then, the alumina film adhering to the weakest grain

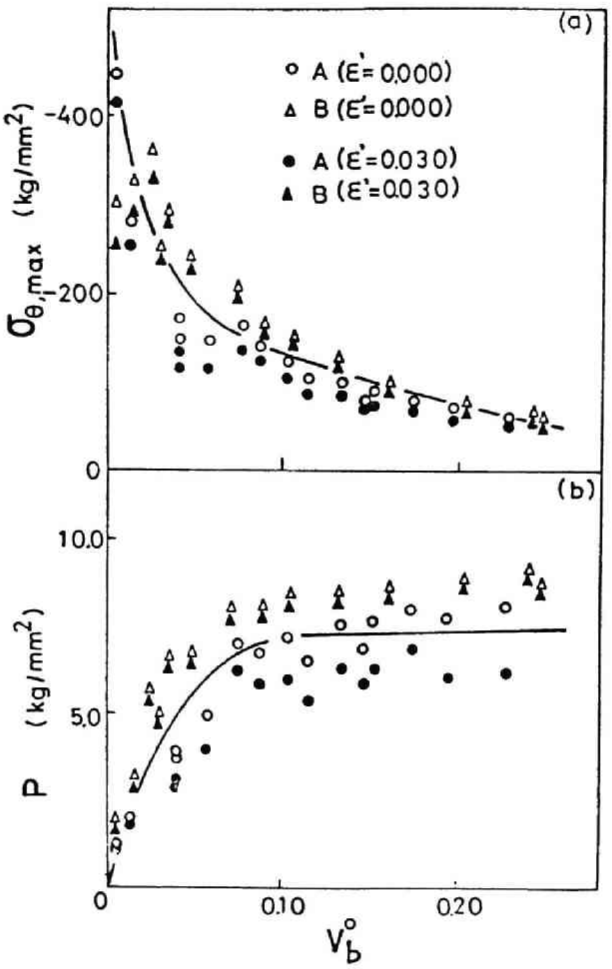

Fig.5 Calculated values of P and $\sigma_{\theta,max}$ at the fracture of the aluminium-alumina composites.

exhibits multiple crackings at an earlier stage of deformation. In such a case, the strengthening mechanism acts predominantly on the weakest grain. Such a situation is found in Photo.4 and Fig.6 where e_c is the elongation of the composite at maximum load, e_I, which is calculated by substituting σ_c into eq.(10) in chapter II-(2), is the axial elongation of the fibre in the Region I which is composed of the fibre and the alumina film and ε' is the elongation in the fibre when the longitudinal defects in the alumina film close (see chapter II-(2)). The calculated values of e_I exsist in the hatched range. They are greater than e_c for small V_b^o in B-type composite while they are smaller than e_c in A-type one. At first sight, as the axial elongation of the fibre in Region I is smaller than that in Region II formed by the cracking of the brittle zone (see chapter II-(2)), e_I should be smaller than e_c which means average axial elongation of the fibre in Region I and II. The result of B-type composite seems to be inconsistent with the above prediction. However, the apparent inconsistency can be explained as follows. In the weakest grain of the B-type fibre, P and $\sigma_{\theta,max}$ will develop and therefore the brittle alumina film will spall or will be failed preferentially to the one on the other grains. Therefore the calculated e_I corresponds to the axial elongation of the fibre in Region I in the weakest grain while e_c is the average axial elongation of the fibre in Region I and II in all the grains. Thus for B-type composite, e_I is greater than e_c. The above conception is affirmed by the appearance of B-type composite just before fracture showing that the weakest grain undergoes major deformation but the other grains minor one (Photo.4). When V_b^o becomes large,

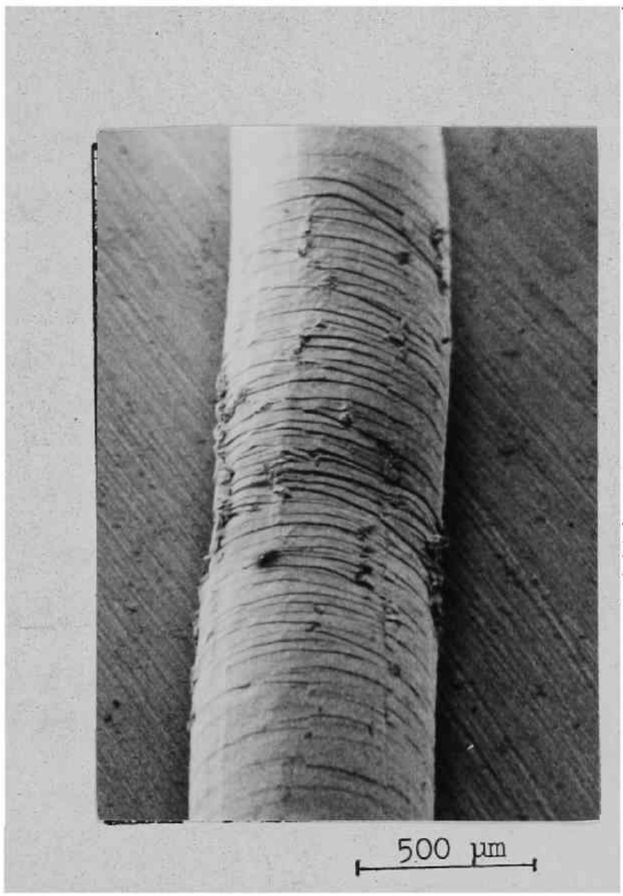

Photo.4 Appearance of the aluminium-alumina composite just before fracture. $V_b^o=0.024$

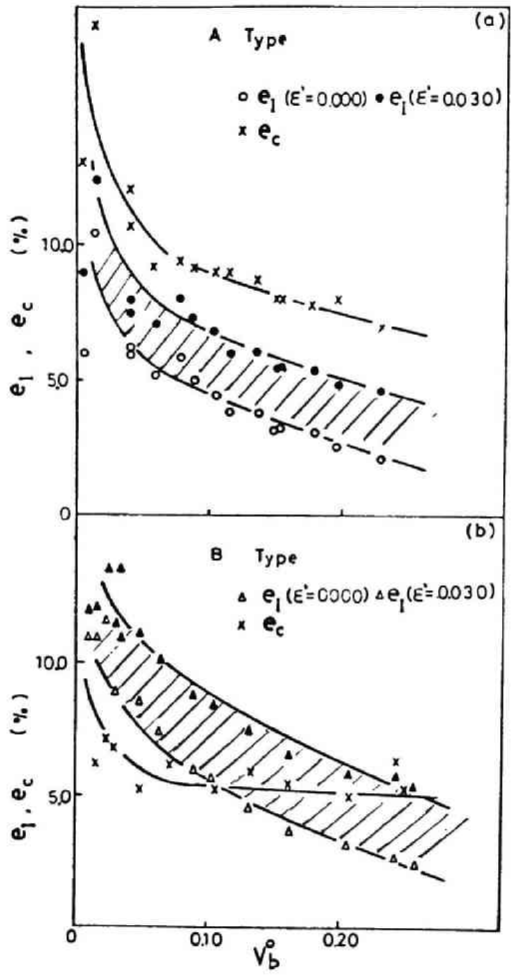

Fig.6 Measured e_c and calculated e_I for A- and B-type aluminium-alumina composites

the brittle zone spalls at small e_I (see Fig.6 in chapter II-(2)). Therefore, with increasing V_b^o , e_I reduces to e_c and finally it becomes smaller than e_c as similarly as e_I of A-type composite.

IV-(2)-4-(i)-(b) Stainless Steel-Brittle Zone-Aluminium Composite

The σ_c of multi-fibre composite obeyed ROM, but $\sigma_{c,5\%}$ showed positive deviation. Also (σ_{fu}) and $(\sigma_{f,5\%})$ of the extracted fibre showed the similar tendencies to σ_c and $\sigma_{c,5\%}$, respectively. As the strengthening effect by the brittle zone vanishes after spalling or fracture by compressive transverse stress of the brittle zone, the results of σ_c and (σ_{fu}) correspond to this case. On the other hand, the results of $\sigma_{c,5\%}$ and $(\sigma_{f,5\%})$ correspond to the case where strengthening effect exists. In this place, it is expected that the magnitude of the effect will be different to each other between the two- and three components composites when the brittle zone experiences constraint from outside as well as inside in the three components composite. If it is so, the measured values of $\sigma_{c,5\%}$ will not be same as the values calculated by

$$\sigma_{c,5\%} = (\sigma_{f,5\%})V_f^o + \sigma_m^* V_m^o \qquad (8)$$

since eq.(8) contains only the strengthening effect of the brittle zone on the fibres. The measured values of $\sigma_{c,5\%}$, however, agree well with the calculated ones. This fact means that, the strengthening effect of the brittle zone on the three components composite arises only from the effect of the brittle zone on the fibres, and the mechanical interaction between the brittle zone and the matrix is negligible. If the bonding strength between the brittle zone and the matrix is high enough, some mechanical

interaction between them will arise. In the composite used in this work, the bonding between the brittle zone and the matrix is very weak and weaker than the bonding between the fibre and the brittle zone as stated already. Therefore, the weak bonding between the brittle zone and the matrix is considered to have been broken under 5% elongation, since, in multi-fibre composites, tensile stress is exerted on the interface.[32][33] After failure of the brittle zone-matrix interface, only the interaction between the fibre and the brittle zone can exsist. In this case, the deviation of the tensile stress from ROM of the three components composite arises just as that of the two components one.

IV-(2)-4-(ii) Fracture Behaviour

Tensile strength σ_c' of the notched specimens on the basis of the net cross-sectional area nearly obeyed the ROM relation and the change of the notch depth did not affect on σ_c', as stated already. This result means that the fibres and the matrix support the externally applied load up to their full strength, and the brittle zone does not affect on σ_c'. As the brittle zone has been failed by compressive transverse stress or has been spalled from the fibres prior to composites fracture as already shown in the sheet specimens and the extracted fibres, it cannot affect on σ_c'. The major factor affecting on fracture behaviour is the weakness of the brittle zone-matrix bonding. As σ_t is a measure of the interfacial bonding strength, it has been used to predict whether splitting occurs or not in terms of Cook and Gorden's analysis.[34][35] If σ_t/σ_c is smaller than 0.2, splitting will occur.[34][35] As the measured values of σ_t/σ_c of almost all the specimens were smaller than this value, occurring of

splitting can be explained. According to Cook and Gorden's analysis[34], tensile stress perpendicular to the fibres ahead of a crack causes interfacial failure. If the interfacial bonding were strong and therefore σ_t were high, the notched specimens would not exhibit splitting. In such a case, the composite might be fractured by propagation of the transverse crack, and then the values of σ_c' would fall below those predicted by ROM.[36] Thus the weak interfacial bonding plays a role to arrest the transverse crack. The other characteristic behaviour was bridging of the fibres. This will occur under the conditions that (i) the fracture strain of the fibres is greater than that of the matrix and (ii)interfacial bonding is very weak. These conditions are satisfied in the as-pressed composite. In either splitting or bridging, the weak interfacial bonding is a major cause. For the composites used in this work, it is concluded that the fracture mechanism depends strongly upon the weakness of the interface between the brittle zone and the matrix but not upon the brittle zone in itself.

IV-(2)-5 Conclusions

(1)The strength of the fibres was raised as long as the brittle zone with multiple crackings adhered to the fibres and was not fractured in transverse direction by compressive transverse stress, as ascertained in the previous work. Effects of grain size of aluminium fibre on deformation behaviour of aluminium-alumina composite were made clear.

(2)Strengthening effect of the brittle zone on stainless steel-

brittle zone-aluminium composite arised only from the mechanical interaction between the brittle zone and fibres, and the interaction between the brittle zone and the matrix was negligible due to the weak bonding between them.

(3)The brittle zone in itself did not affect on fracture behaviour, due to spalling or fracture by compressive transverse stress prior to composite fracture in the stainless steel-brittle zone-matrix composite. The fracture behaviour depended strongly upon the weak bonding at the interface between the brittle zone and the matrix.

IV-(3) Effects of Interfacial Reaction on Deformation and Fracture Behaviour of Tungsten Fibre-Nickel Matrix Composites

IV-(3)-1 Introduction

Effects of interfacial reaction on tensile properties of composites have been widely investigated[1]-[27], but there are very few studies on relationships between mechanical properties and the extent of interfacial reaction. Furthermore, variations of the effects of the reaction zone due to differences in volume fraction and fibre diameter have seldom been studied. With these facts in mind, the present work was undertaken.

Single tungsten fibre-nickel matrix composite was chosen as a suitable system in this study for the following reasons : (1) it can be readily fabricated by the plating method, (2) it is not necessary to consider the effects of deformation and fracture behaviour of neighbouring fibres[37]-[39] in the case of single fibre-composites and (3) the deformation and fracture behaviour of each component (fibre, matrix and reaction zones) is expected to appear directly in load-elongation curves of single fibre-composites.

Tensile behaviour of the composites which were annealed in vaccum at 900°C for various times to change the interfacial bonding strength and to form the reaction zones with various thicknesses were studied at room temperature and 77°K. This implies that tungsten undergoes a ductile-brittle transition with decreasing temperatures and thereby enables the effects of ductility or notch-sensitivity of tungsten fibres on tensile properties of the

composites to be determined.

IV-(3)-2 Experimental Procedure

Tungsten fibres of 100 or 300μm diameter were cleaned to remove graphite lubricant and oxides by boiling in a saturated sodium hydroxide solution for 30min prior to nickel plating. The solution composition and the oprating condition for nickel plating are summarized in Table 1. The fibre volume fraction was varied by changing the thickness of nickel layers. The specimens were annealed in vaccum at 900°C for 0-100 hr. Murakami's solution and HNO_3 50% + CH_3COOH 50% solution were used as the etchants for tungsten and nickel, respectively.

Tensile tests were carried out at room temperature in air and 77°K in liquid nitrogen with an Instron tensile machine at a constant crosshead speed of 2 mm per min, corresponding to a strain rate 0.05 per min, and load-elongation curves, ultimate tensile strengths and elongations of all the specimens were measured. Observations of the fractured specimens were made by scanning electron and optical microscopy.

IV-(3)-3 Results

IV-(3)-3-(i) Structure of Composites

Photo. 5 shows the structure and X-ray microanalyser line profiles of tungsten and nickel of the transverse section of the 300μm fibre-composite annealed for 100 hr. Two new zones were found in addition to the original two phases i.e. fibre and matrix. As the zone surrounding the fibre was brittle as shown later, this is named `brittle zone' in this paper. Another new zone is called `diffusion zone'. These zones were recognized

Table 1 Solution composition and operatimg condition for nickel plating.

Composition of Electrolyte	$NiSO_4$: 329.2 g/ℓ $NiCl_2$: 44.9 g/ℓ Boric acid: 37.4 g/ℓ in water
Temperature (°C)	60
Current density (mA/mm^2)	0.5
Agitation	Mechanical

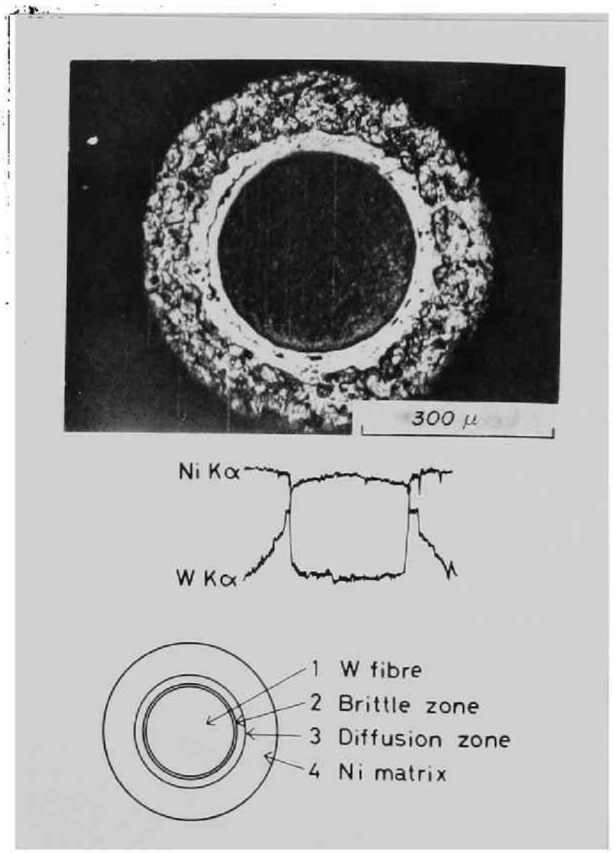

Photo. 5 The structure and X-ray microanalyser line profiles of tungsten and nickel of transverse section of 300μm fibre-composite annealed for 100 hr.

microscopically in the specimens annealed for more than 30 min, though they were not found in the specimens annealed for 1-10 min. The real fibre volume fraction V_f' decreased, and the volume fractions of the brittle zone V_b' and the diffusion zone V_d' increased with increasing annealing time as shown in Fig.7. It should be noted that the diffusion zone and matrix, especially the diffusion zone, contain a fairly large amount of the tungsten element as shown in Photo.5. This result agrees well with the experimental evidence that the solubility of tungsten in nickel is large (about 34 wt %) at 900°C according to the nickel-tungsten phase diagram.(40)

IV-(3)-3-(ii) Tensile Tests

IV-(3)-3-(ii)-(a) 100μm Diameter Fibre-Composites

IV-(3)-3-(ii)-(a)-a Specimens with V_f=0.50 at Room Temperature

Typical load-elongation curves, and the relationships between UTS, σ_c, and annealing time, and between elongation e_c and annealing time of the specimens of 50% by initial fibre volume fraction are shown in Fig.8, Fig.9 and Fig.10, respectively. The values of σ_c and e_c of the specimens annealed for 1-10 min did not vary with annealing time, while those of the specimens annealed for 30 min-3 hr slightly decreased with increasing annealing time. In the specimens annealed for 10-100 hr, the values decreased rapidly with increasing annealing time. Photo.6 shows appearances of the fractured specimens. A separation between the fibre and the matrix was observed in the non-annealed specimen(a). On the contrary, in the specimens annealed for 1-10 min, the fibre was not separated from the matrix, and the specimens failed by necking as a whole (b)(c), and those annealed for 30 min-3 hr also failed

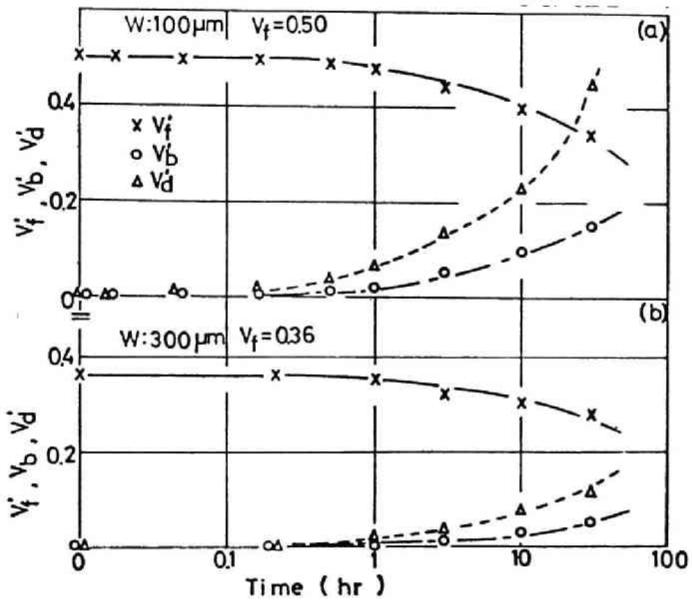

Fig.7 Measured values of V_f', V_b' and V_d' of 100μm fibre-composite with V_f=0.50 and 300μm fibre-composite with V_f=0.36.

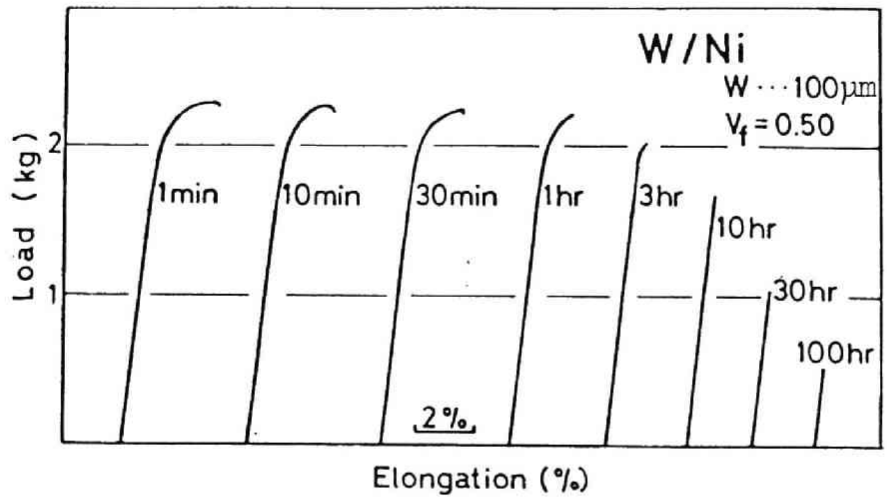

Fig. 8 Typical load-elongation curves at room temperature of 100μm fibre-composites with V_f=0.50, annealed for various times.

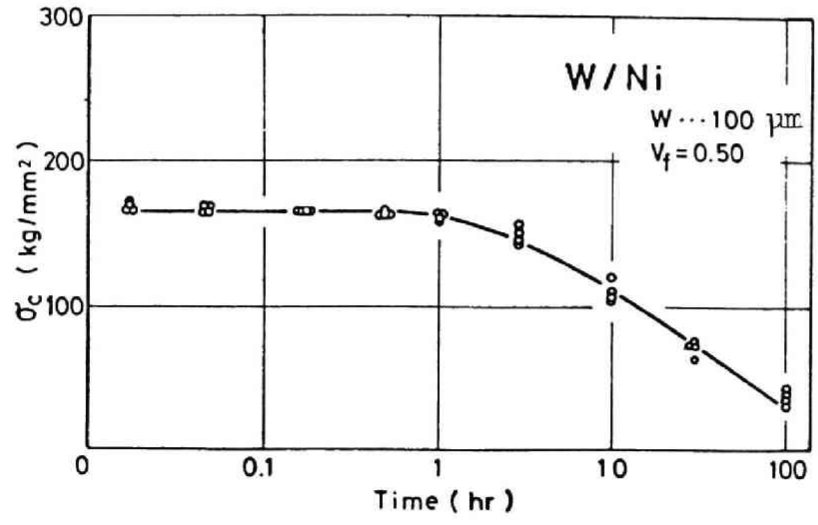

Fig.9 Relationship between tensile strength at room temperature and annealing time in 100μm fibre-composites with V_f=0.50.

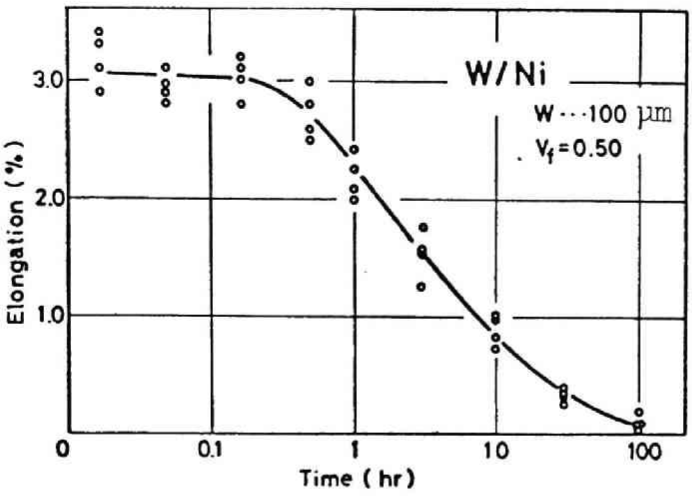

Fig. 10 Relationship between elongation at room temperature and annealing time in 100μm fibre-composites with V_f=0.50.

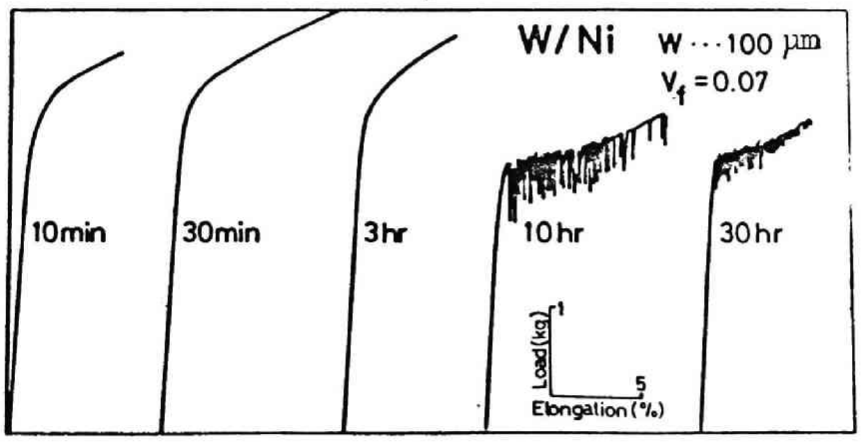

Fig. 11 Typical load-elongation curves at room temperature of 100μm fibre-composites with V_f=0.07, annealed for various times.

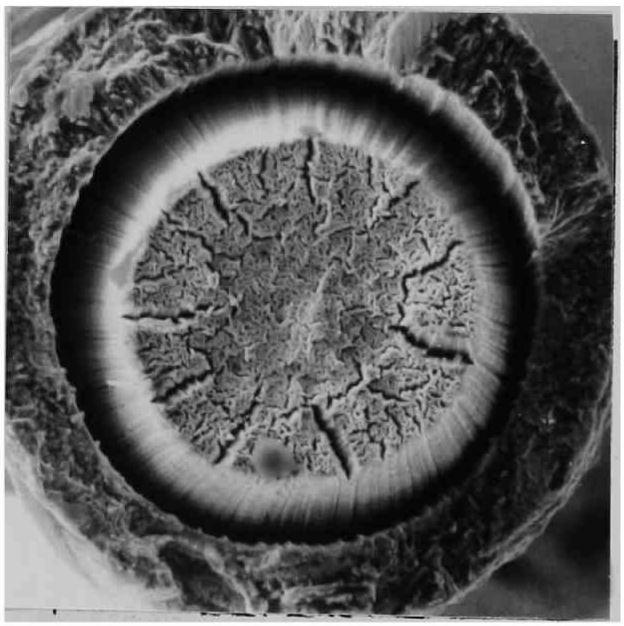

(a) 50 μm

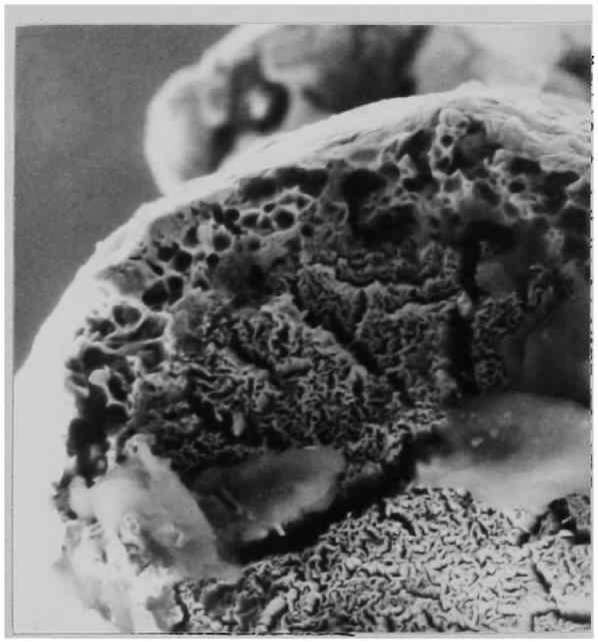

(b) 30 μm

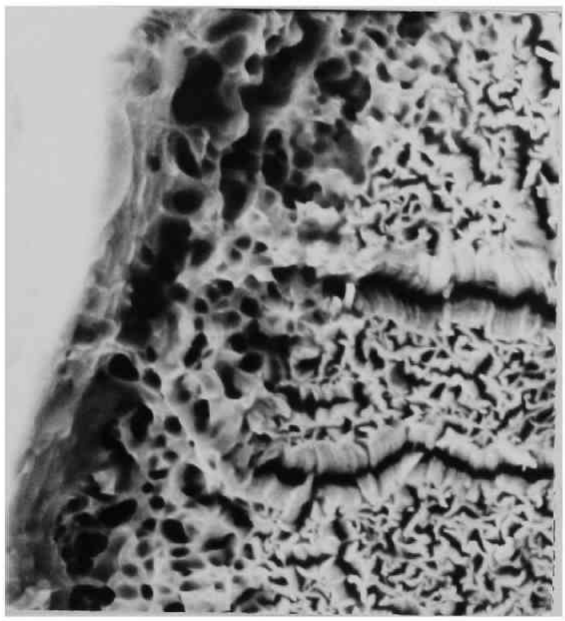

(c) 10 μm

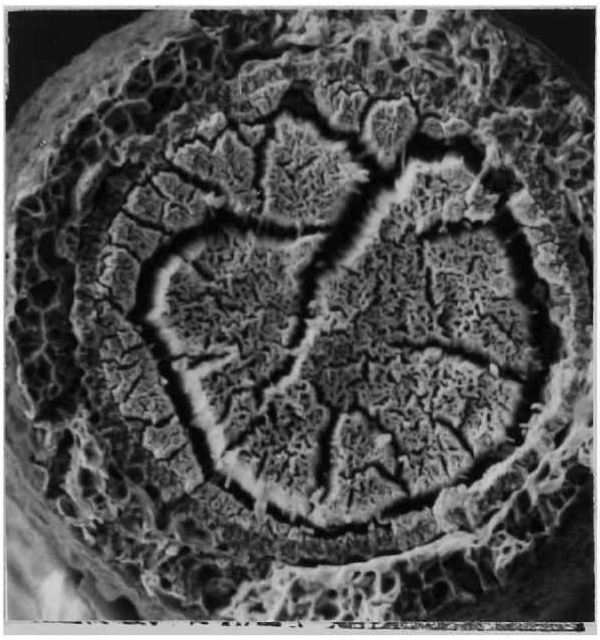

(d) 50 μm

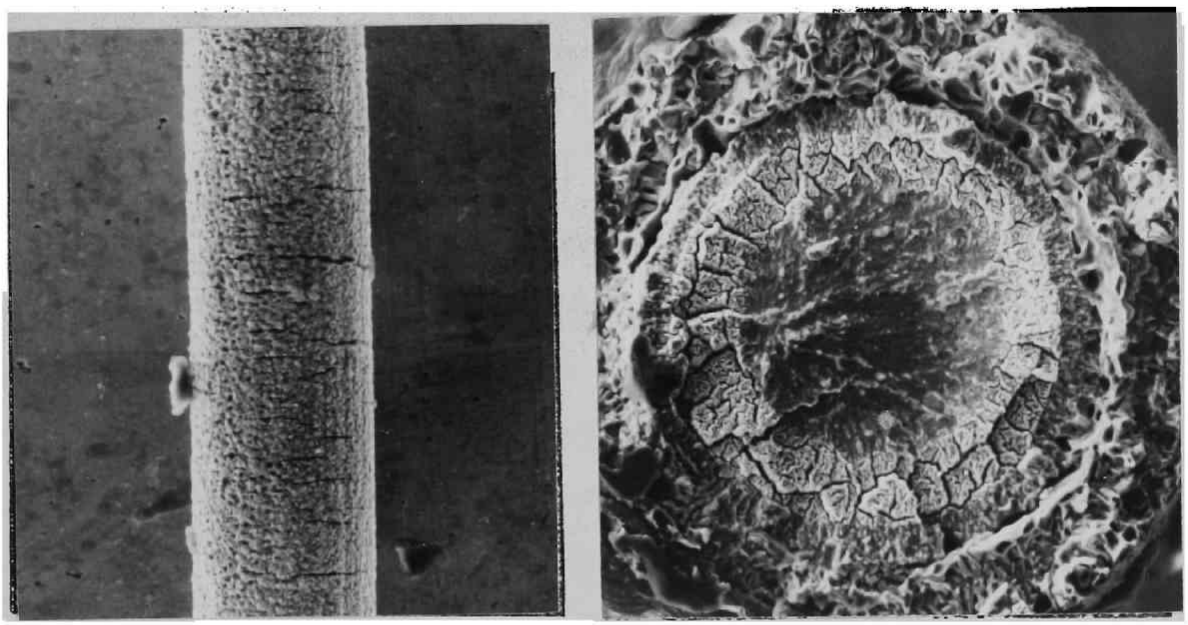

Photo. 6 Appearances of 100μm fibre-composites fractured at room temperature. (a):Fracture surface of the non-annealed specimen (b)(c):Fracture surface of the specimen annealed for 1 min (d):Fracture surface of the specimen annealed for 3 hr (e):Appearance of the brittle zone after tensile test in the specimen annealed for 3 hr (f):Fracture surface of the specimen annealed for 10 hr.

similarly (d). After dissolving away the diffusion zone and matrix from the fractured specimen annealed for 3 hr, some parallel cracks perpendicular to the tensile axis in the brittle zone (namely, multiple crackings of the brittle zone) were found (e). The fibre in the specimen annealed for 10 hr exhibited such a strange fracture surface as shown in (f). The tungsten fibre fractured in a brittle manner in the centre and in a ductile manner in the peripheral zone. If the crack originating from the fracture of the brittle zone propagated into the fibre, a completely brittle appearance would be expected at the fracture surface of the fibre. Photo.6(f) indicates that the values of σ_c and e_c of this specimen annealed for 10 hr were decreased not by a propagation of crack but by a degradation of the fibre itself.

IV-(3)-3-(ii)-(a)-b Specimens with V_f=0.07 at Room Temperature

Fig.11 shows typical load-elongation curves of the specimens with V_f=0.07 annealed for various times. Many drops in load were observed in the specimens annealed for more than 10 hr. This phenomenon is explained as follows, as similarly as in chapter III-(2). In case V_f is smaller than V_{min} which is the minimum fibre volume fraction to reinforce the matrix material, when the fibre breaks in one cross-section, there is a drop in load bearing capacity. In this cross-section,however, the diffusion zone and matrix work-harden and the load bearing capacity rises again. Then, the fibre once broken fails again in another cross-section. With a repitition of this process , the fibre is continually broken into shorter and shorter lengths,finally into $l_c/2$ where l_c is a critical length. The number of drops observed in the load-elongation curves corresponds to the number of breaks of the initially continuou tungsten fibre. The numbers of breaks of the fibres and aspect

ratios of the fractured segments measured from the load-elongation curves are summarized in Table 2. The former increased and the latter decreased with increasing annealing time. This result shows that the tungsten fibres in the specimens become weaker with increasing annealing time, according to the Kelly model.[41] Photo.7(a)(b) shows an appearance of the fractured fibre in the specimen annealed for 30 hr. Crack growth caused by fracture of the initially continuous fibre was observed to be stopped at the diffusion zone (b).

IV-(3)-3-(ii)-(a)-c Specimens with V_f=0.50 at 77°K

Tungsten fibre fails in a ductile manner at room temperature and in a brittle manner at 77°K. In the present study, tensile tests were carried out at 77°K to investigate the effect of non-ductility of the fibre on the fracture behaviour in the presence of the brittle zone surrounding the fibre. Fig.12 shows the measured values of σ_c versus annealing time. It is to be noted that the tensile strength decreased comparatively gradually with increasing annealing time at room temperature, but suddenly at 77°K in the specimens annealed for 3 hr.

IV-(3)-3-(ii)-(b) 300μm Fibre-Composites

Fig.13 shows a relationship between σ_c and annealing time in the specimens containing 36 % of 300μm tungsten fibres. The values of σ_c decreased only slightly with increasing annealing time for 0-100 hr, in contrast to the result obtained in 100μm fibre-composites. Photo.8 shows appearances of the planes parallel to the tensile axis of the fractured specimens. In the 30 hr-annealed specimen whose elongation was about 8 %, a multiple cracking of the brittle zone was found, as in (a). Crack growth in

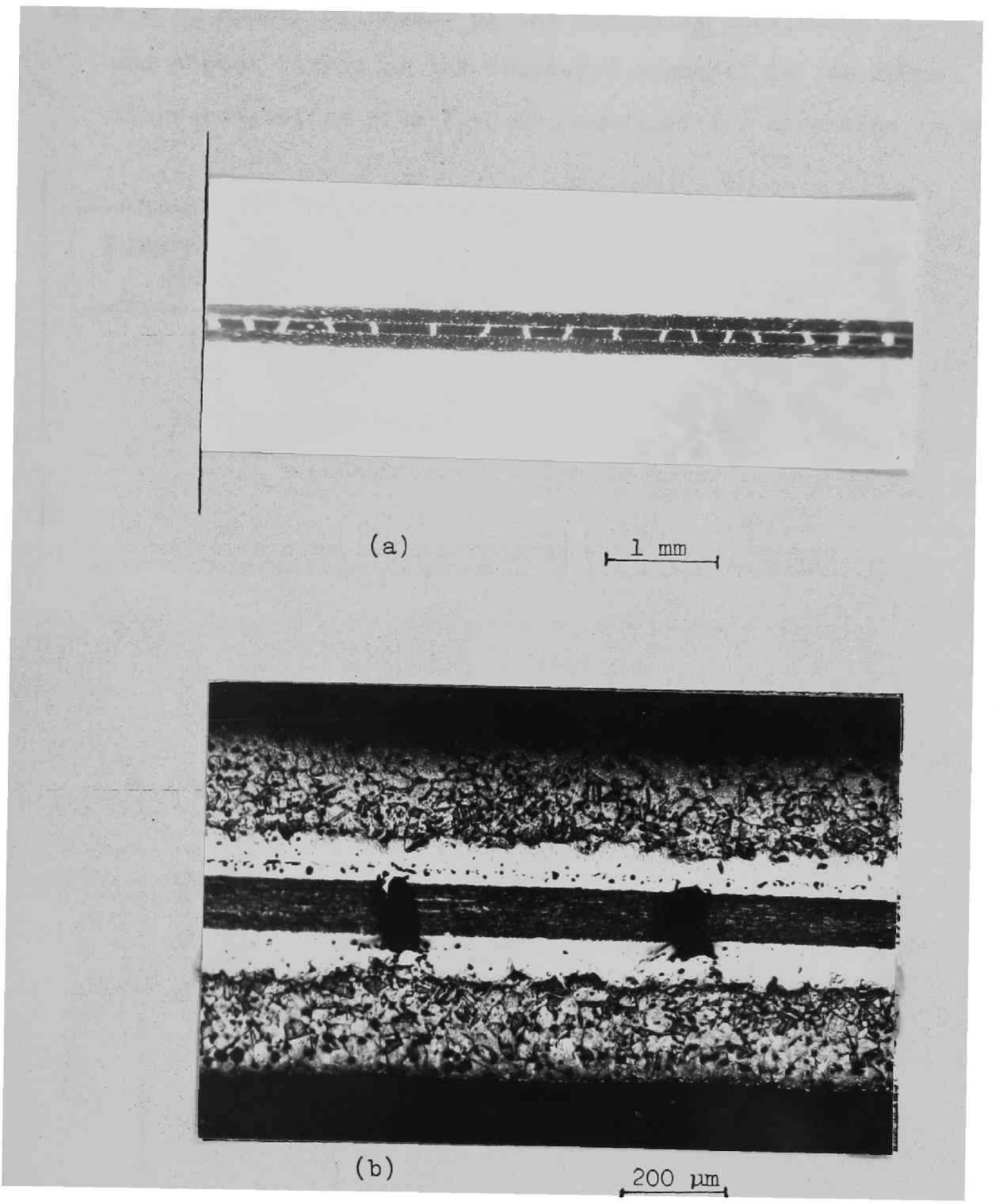

Photo. 7 Appearance of the longitudinal section after tensile test at room temperature of the 100μm fibre-composite with V_f=0.07 annealed for 30 hr.

Table 2 Number of breaks of the initially continuous fibres and aspect ratios of the fractured segments in the 100μm fibre-composites with V_f=0.07, annealed for more than 10 hr.

Annealing time (hr)	Number of breaks (average)	ℓ/d
10	40	10.0
30	65	6.2
100	119	3.4

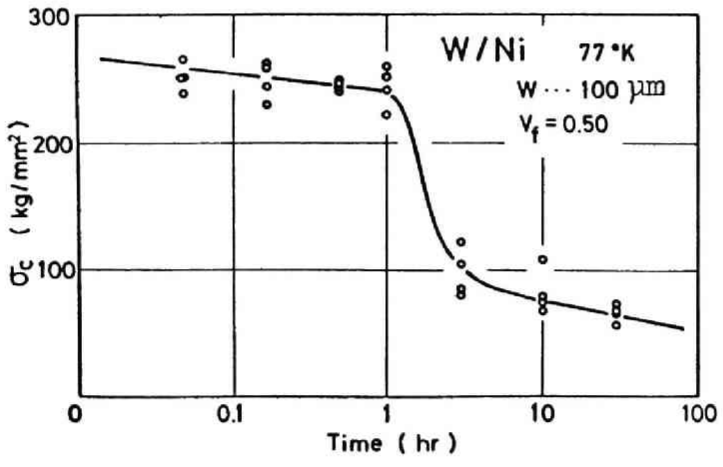

Fig.12 Relationship between UTS at 77°K and annealing time in 100μm fibre-composites with V_f=0.50.

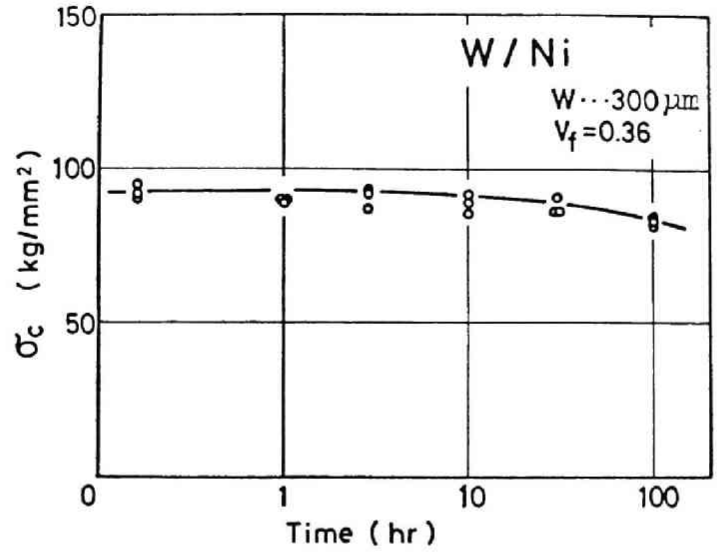

Fig. 13 Relationship between UTS at room temperature and annealing time in the specimens containing 36% of 300μm fibres.

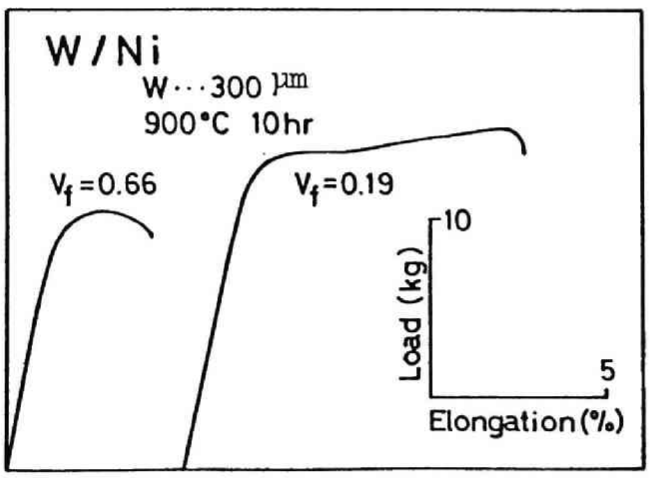

Fig. 14 Typical load-elongation curves at room temperature of the specimens with different fibre volume fractions, annealed for 10 hr.

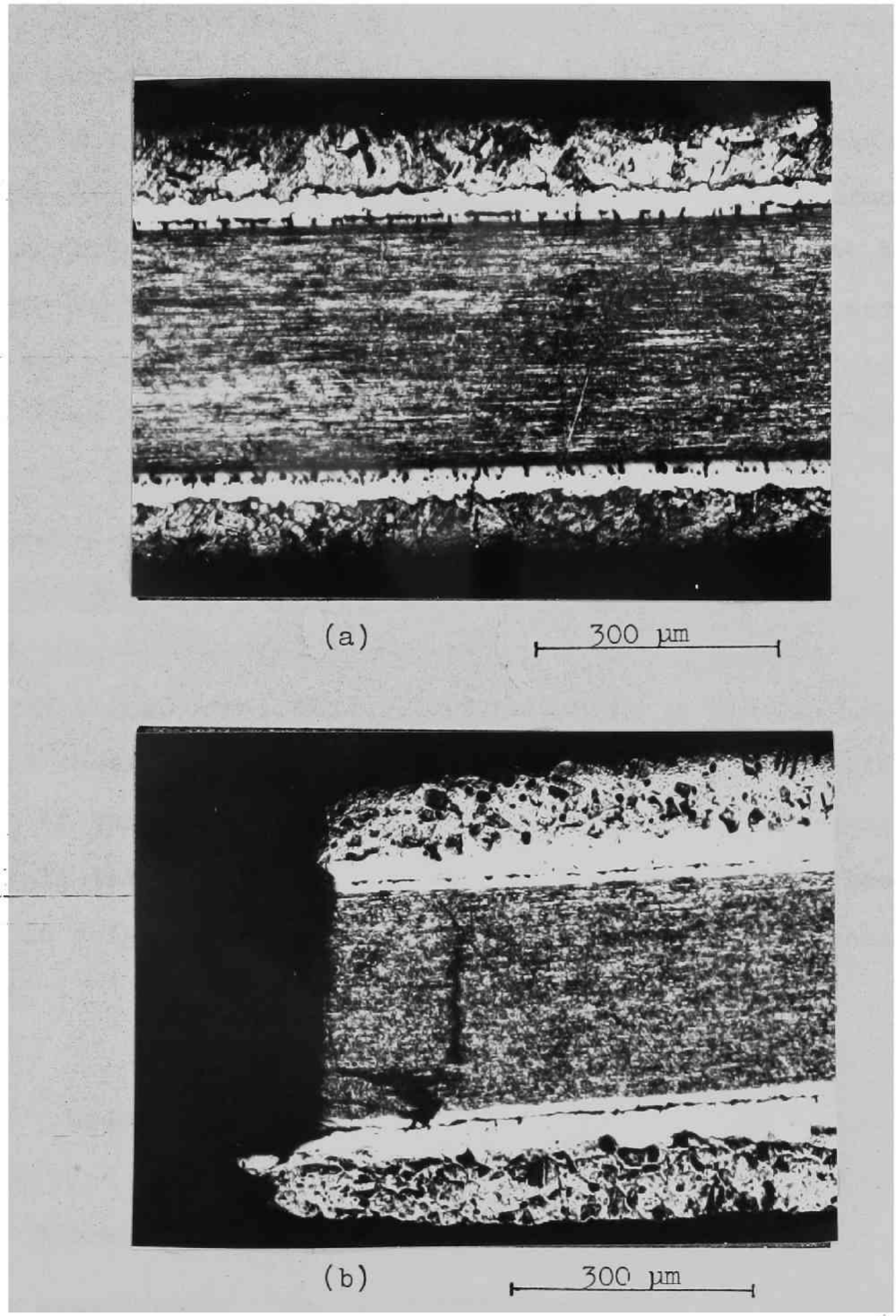

Photo. 8 Appearances of the planes parallel to tensile axis of the specimens with V_f=0.36 fractured at room temperature (a):Annealed for 30 hr (b):Annealed for 100 hr.

the brittle zone was stopped at both the fibre and the diffusion zone. On the contrary, when annealed for 100 hr, the specimen showed a very small elongation. No crack in the brittle zone was found as shown in (b). Fig.14 shows typical load-elongation curves of the two specimens with different fibre volume fractions after annealing for 10 hr. They are so much different in shape from each other. Photomicrographic observations were made to know the reason for the difference. It was found that, in the specimen with V_f=o.19, a severe multiple cracking of the brittle zon was found to occur, but not in the specimen with V_f=0.66. The load-elongation curve of the former exhibited a flat and non-workhardenable stage in the range from 2 to 5 or 6% elongations. From the photomicrographic observation of the specimens stretched to various elongations, the multiple cracking of the brittle zone was found to take place below about 6 % elongation and a further cracking of this zone was seldom observed above 6 % elongation. This result indicates that the brittle zone fractured to become shorter in length up to 6 % elongation where the length became critical.

IV-(3)-4 Discussion

IV-(3)-4-(i) Deformation and Fracture Behaviour of 100μm Fibre-Composites at Room Temperature

The experimental results stated above show that the deformation and fracture behaviour of the specimens varies with the factors such as fibre diameter, fibre volume fraction, annealing time and ductility of the fibre. At first let's discuss the UTS and elongation of 100μm fibre composites at room temperature. In

order to clarify the effects of interfacial reaction, the measured values σ_c were compared with $\sigma_{c,cal}$, the UTS calculated by using the rule of mixtures on the assumption that no interfacial reaction had occurred. Such a comparison will prove useful in explaining the difference between the tensile properties, which the composites actually had after interfacial reaction, and those which composites would have had if interfacial reaction had not occured. The ratios of σ_c to $\sigma_{c,cal}$ are plotted against annealing time in Fig.15. If the ratio is over 1, the reaction is useful to raise the UTS, but if less than unity, it degrades the composite strength.

From the relationships between the rate of the reaction and both values of $\sigma_c/\sigma_{c,cal}$ and e_c, and from the observation of the fractured specimens as stated above, we can classify the deformation and fracture behaviour of the composites into three stages according to the extent of the reaction.

In stage I (1-10 min annealing), the values of σ_c are greater than those of $\sigma_{c,cal}$, and the measured elongations of composites are larger than the fibre elongation tested separately, 2% at most. There are many examples that elongation of the composites is larger than that of the contained fibres tested alone.[41)-(45)] Much discussion on the elongation of various composites has been done to date.[43)-(47)] Piehler[37] showed that necking of fibres is arrested if the interfacial bonding is strong enough. Mileiko[44], and Garmong and Thompson[47] applied the plastic instability approach to tensile behaviour of composites with a strong interfacial bonding, and obtained good results. According to their approach, composites can deform uniformly along the tensile axis through the elongation at which necking would begin in the fibres if they were tensile-tested separately, until necking

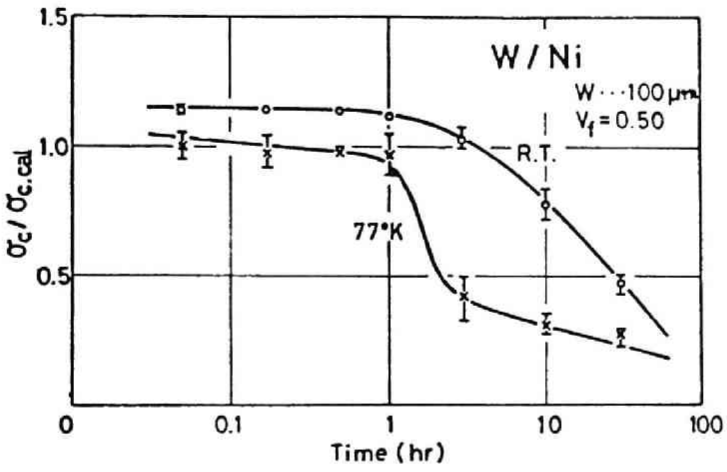

Fig.15 Ratios of the measured tensile strengths to the calculated ones versus annealing time.

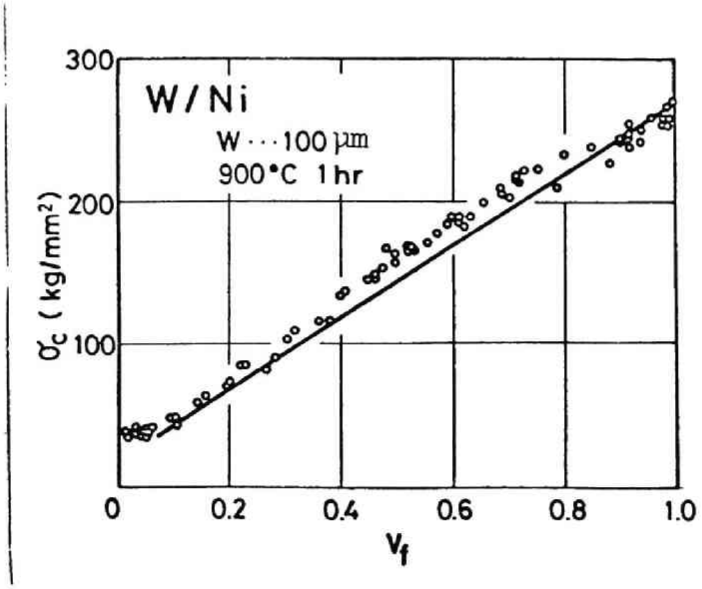

Fig.16 Relationship between UTS at room temperature and fibre volume fraction in the 100μm fibre-composites annealed for 1 hr.

begins in the composites as a whole. From Photo.6(b)(c), we can see that the interfacial bonding is strong and the specimen fails by necking as a whole. Thus, the results in stage I can be explained in terms of strong interfacial bonding. Therefore, a slight degree of the interfacial reaction is useful for the increase of UTS and elongation of composites.

In stage II(30 min-3 hr) where the brittle zone and the diffusion zone exist, the newly formed zones affect the mechanical behaviour of the composites. In this stage, the load bearing capacity of the composites is expected to decrease for the following reasons :

(i) Reduction of cross-sectional area of the fibres

(ii)Multiple cracking of the brittle zone. This causes both (a)reduction of the cross-sectional area which can bear the applied load and (b) stress concentration at the root of the formed notches, which will promote fracture initiation of the fibres and consequently lead to an earlier fracture of composites.

However, the measured values of σ_c were larger than the calculated ones. The same tendency was found for the specimens containing various fibre volume fractions, as in Fig.16. It was deduced that the following factors can compensate for the lowering of the load bearing capacity of the composites:

(i)Contribution of the diffusion zone : This zone is inferred to have ductility from Photo.7(b) and to have a higher strength than nickel matrix from the Vickers hardness(the measured value was 210 on an average, corresponding to about 70 kg/mm^2 in yield stress, while that of the matrix was 70-90).

(ii)Strong bonding strength : The specimens fail by necking as a whole since the fibre-brittle zone-matrix bonding was strong.

(iii)Constraint effect due to circumferential notches formed by earlier fracture of the brittle zone(see chapter II-(2)).

A rough estimation of the effects of mechanical interactions, (ii) and (iii) on UTS of the composites can be made as follows: As the brittle zone breaks before the composite fails, this zone cannot carry the tensile load at composite fracture. Thus the modified rule of mixtures should be written as

$$\sigma_c' = \sigma_{fu}'V_f' + \sigma_d'V_d' + \sigma_m'V_m' \qquad (1)$$

where V_f', V_d' and V_m' are respectively real volume fractions of the fibre, diffusion zone and matrix,which are already shown in Fig.7, σ_{fu}' is UTS of the fibre, and σ_d' and σ_m' are respectively the stresses carried by the diffusion zone and matrix. σ_{fu}' can be inferred from the fracture strain and the Young's modulus. σ_d' is nearly 70 kg/mm^2 since the vickers hardness was 210 on an average. Also σ_m' is about 21 kg/mm^2, which is the yield stress of nickel measured independently. The values of σ_c' calculated by eq.(1) do not include the effects of (i) and (ii). The effects of mechanical interaction between the constituents arising from (ii) and (iii) probably correspond to the difference $\Delta\sigma_c$ between the measured values of σ_c and those of σ_c'. The values of $\sigma_{fu}'V_f'$, $\sigma_d'V_d'$, $\sigma_m'V_m'$, σ_c' , σ_c and $\Delta\sigma_c$ are summarized in Table 3. This result shows a large contribution of the mechanical interactions among the constituents to σ_c.

In stage II, however, the experimental results show that UTS and elongation decrease with increasing annealing time. This tendency indicates that the degrading factors mentioned above become predominant with increasing annealing time.

In stage III where the annealing time is more than 10 hr, the values of σ_c and e_c decrease drastically, although the contribution

Table 3 Effects of mechanical interaction among the constituents on σ_c in stage II (kg/mm^2)

Specimen	$\sigma_{fu}'V_f'$	$\sigma_d'V_d'$	$\sigma_m'V_m'$	σ_c'	σ_c	$\Delta\sigma_c$
30min	132	2	10	144	160	16
1 hr	130	4	9	143	156	13
3 hr	101	9	8	118	145	27

of the diffusion zone with high strength can, to some extent, compensate for the drop in load bearing capacity derived from the embrittlement of the fibre and decrease in real fibre volume fraction. In this stage, $\Delta\sigma_c$ is calculated to be 3.2 and -1.6 kg/mm^2 for the specimens annealed for 10 hr and 30 hr, respectively. Effects of mechanical interactions are negligible. The loss of the mechanical interaction might be derived from the decrease of ductility of the fibre and the lack of multiple-cracking of the brittle zone in this stage.

In this composite, V_{min} is calculated to be 0.06 by assuming that no interfacial reaction takes place. Therefore, at a content of 7% by initial fibre volume fraction, tungsten fibres would not break continually according to Kelly's theory of reinforcement[48], if the reaction did not occur. However, a continuous fracture of the fibre was actually observed in this stage as shown in Fig.11. This result indicates that V_{min} becomes larger than 0.07 as the reaction advances. Thus, an excessive interfacial reaction accompanying degradation of the fibre properties and decrease in fibre volume fraction raises the value of V_{min}.

IV-(3)-4-(ii) Effects of Interfacial Reaction on σ_c at 77°K

From a comparison of the values of $\sigma_c/\sigma_{c,cal}$ at 77°K with those at room temperature, two evident differences between them are found.

(a)The values of $\sigma_c/\sigma_{c,cal}$ at room temperature are always larger than those at 77°K.

(b)Their ratio at room temperature decreases comparatively gradually, but at 77°K it decreases rapidly with prolonged

annealing time.

These two differences indicate that effects of reaction zones on UTS of composites differ depending upon the ductility of the fibre. At room temperature, the brittle zone exhibits a multiple cracking, and the fibre fails by necking in stage II. These results mean that the fracture of the tungsten fibre is not caused by a propagation of the crack formed in the brittle zone. On the contrary, at 77°K, the brittle zone fails at a small strain and the notches thus formed can lead the fibre to fracture because the tungsten fibre is brittle and therefore notch-sensitive. Heitman et al.[12] found, from the tensile test at 78°K of molybdenum fibre-aluminium matrix composites with a compound at the interface, that the fibre stress at fracture is proportinal to $c^{-1/2}$ where c is the maximum penetration depth of the compound. However, the sudden drop in σ_c in Fig.12 cannot be explained only in terms of the thickness of the brittle zone because the thickness of the brittle zone did not increase suddenly in the specimens annealed for 3 hr. This result will be discussed again in IV-(5) and the reason why the sudden drop occured will be made clear.

IV-(3)-4-(iii) Deformation and Fracture Behaviour of 300μm Fibre-Composites at Room Temperature

As compared with 100μm fibre composites, UTS of 300μm fibre-composites decreases very slightly with increasing annealing time. This results shows that the effects of interfacial reaction are different depending upon the fractions occupied by the diffusion and brittle zones since their fractions are much smaller in 300μm fibre-composites than in 100μm fibre-composites when the same heat-treatment is conducted. The deformation and fracture

behaviour of 300μm fibre-composites is also classified into three stages, stage I, stage II and stage III, corresponding to annealing time for 1-10min, 30min-30hr and more than 100 hr, respectively.

Specimens vary in deformation and fracture behaviour with different fibre volume fractions,as shown in Fig.14. This result and observations of the fractured specimens indicate that whether or not the brittle zone can be fractured to a critical length depends on fibre volume fraction(or matrix volume fraction). When the brittle zone breaks in one cross-section, there occures a drop in load bearing capacity. Then, the matrix, the diffusion zone and the fibre work-harden in this cross-section. Therefore, the load bearing capacity of this cross-section rises again so that the drop in load due to a fracture of the zone is compensated for, if the volume fraction of the brittle zone is small. In this case, the zone once broken fails again in another section. With a repetition of this process,the brittle zone undergoes severe mulitple cracking. On the contrary,if the volume fraction of the zone is large,when the zone breaks in one cross-section, work-hardening of the other components cannot necessarily compensate for the drop in load bearing capacity. When the same heat-treatment is conducted on the specimens with various fibre volume fractions, the cross-sectional area of the brittle zone, the diffusion zone and the fibre change similarly in all the specimens. Taking these factors into consideration, it can be concluded that the cross-sectional area of the matrix (which is determined by the fibre volume fraction) governs whether the multiple-cracking of the brittle zone occurs to a critical extent or not when the stress concentration at the root of the fractured brittle zone does not accerate fracture initiation of the fibre and then leads to

an earlier fracture of the composite.

IV-(3)-5 Conclusions

Effects of interfacial reaction on deformation and fracture behaviour of the tungsten fibre-nickel matrix composites were investigated. The main results obtained are summarized as follows.

(1)The deformation and fracture behaviour of the composites in which interfacial reaction occurred varied with the factors such as the extent of interfacial reaction, fibre diameter, fibre volume fraction, and ductility of the fibres.

(2)The deformation and fracture behaviour at room temperature were classified into three stages according to the extent of inetrfacial reaction. The influences of the extent of the reaction on tensile properties of the composites were discussed. The factors causing deviations of the measured tensile strength from that calculated by assuming that the reaction did not take place were pointed out for each stage.

(3)Whether multiple cracking of the brittle zone occurres to a critical extent or not depends on the matrix volume fraction(or fibre volume fraction).

IV-(4) Deformation and Fracture Behaviour of Composites of Copper and Copper-Chromium Alloys Reinforced with Tungsten or Molybdenum Fibres

IV-(4)-1 Introduction

Many investigations have been made on deformation and fracture behaviour of pure metallic matrix composites.[41][42][49]-[52] It is, however, anticipated that most high strength composites to be produced will utilize high strength fibres embedded in alloyed matrices. If age-hardenable alloys can be used as matrix materials, use of age-hardening of matrices together with reinforcement will produce strong composites. Fibres, however, may be damaged by interfacial reaction between fibres and matrix elements and therefore alloyed matrix may degrade properties of composites, even if the base metal does not act on fibres. In this work, as fibre materials, tungsten and molybdenum wires were used, and , as matrix materials, copper which does not act on both the fibres and age-hardenable copper-chromium alloy in which chromium acts on both the fibres[53][54] were used.

In this part, some mechanical interactions between the fibres and the matrix, effects of interfacial reaction on elongation and tensile strength of the composites and effects of age-hardening treatment on strength of composites were investigated by employing multi-fibre-composites.

IV-(4)-2 Experimental Procedure

Tungsten and molybdenum wires of 100μm and 500μm diameters, and, OFHC copper and Cu- 0.40%(or 0.56%)Cr alloy were used as fibre and matrix materials, respectively. The fibres were cleaned to remove graphite lubricant and oxides by boiling in a saturated sodium hydroxide solution for 30min prior to composite fabrication. Continuous wires were loaded into a graphite mould,and OFHC copper or Cu-Cr alloy was placed on the top of it. The assembly was next placed in a quartz tube, which was evacuated to about 10^{-3}mm mercury. The tube and its content were heated to 1160°C, held for 30min and then cooled from the bottom to avoid cavities. Pure copper matrix composites were annealed at 550°C for 30min and then cooled in a furnace. Cu-Cr alloy matrix composites were solution-treated at 1000°C for 1hr , quenched into water and aged at 475°C for 2hr for 0.56% Cr and for 5hr for 0.40% Cr. The thickness of the reaction zone was determined by means of EPMA.

Tensile test was carried out at room temperature. Stress-strain curve was measured by using two strain gages pasted on the opposite sides of a specimen. Young's modulus was obtained from the slope of the stress-strain curve. Yield stress σ_y was taken from the deviation point from stage I to stage II. Observation of the fractured specimens was made by a scanning electron microscope.

IV-(4)-3 Results

IV-(4)-3-(i) Interfacial Reaction

No reaction zone at the interface was detected in copper matrix composites from the electron microprobe examination. This result agrees well with the fact that pure copper and tungsten or molybdenum are mutually insoluble. The addition of chromium in copper matrix resulted in formation of a solid solution layer in a peripheral zone of the fibres. The thickness of the reaction zones were about 3μm and 8μm in W/Cu-Cr and Mo/Cu-Cr composites, respectively.

To know the effects of the solid solution layer on the tensile strength of the fibres, tungsten fibres extracted from the W/Cu-Cr composites were electro-polished in a dilute sodium hydroxide solution in steps of 1.0μm reduction in diameter and then tensile-tested. For each depth of the removed surface layer, tensile strength of more than ten fibres were measured. Fig.17 shows UTS of fibres, σ_{fu}, versus the depth of the removed surface layer, Δr. The as-extracted fibres ($\Delta r=0$) were brittle with low values of σ_{fu}. This brittleness of the fibres is explained as follows ; W-Cr solid solution layer in the peripheral zone of the fibres should fail prior to a failure of the inner portion of the fibres without chromium because strength and toughness of tungsten are reduced by addition of chromium.[55] The earlier failure of the layer leads to formation of circumferential cracks, which hasten failure of fibres. The above explanation is supported by the fact that, at Δr=2-3μm, σ_{fu} recovers to the original strength of tungsten without chromium,as shown in Fig.17; namely the recovery of σ_{fu} stems from a removal of W-Cr layer which is a crack source. On the

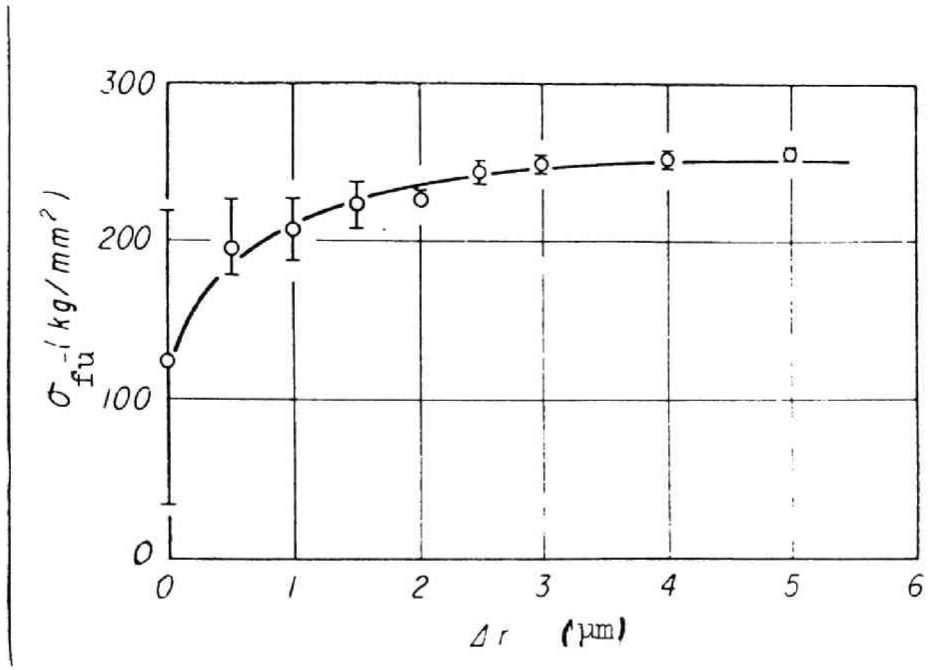

Fig.17 Recovery of the tensile strength of tungsten fibres with a W-Cr solid solution layer in the peripheral zone by electro-polishing. Δr is the depth of the removed surface layer in tungsten fibres.

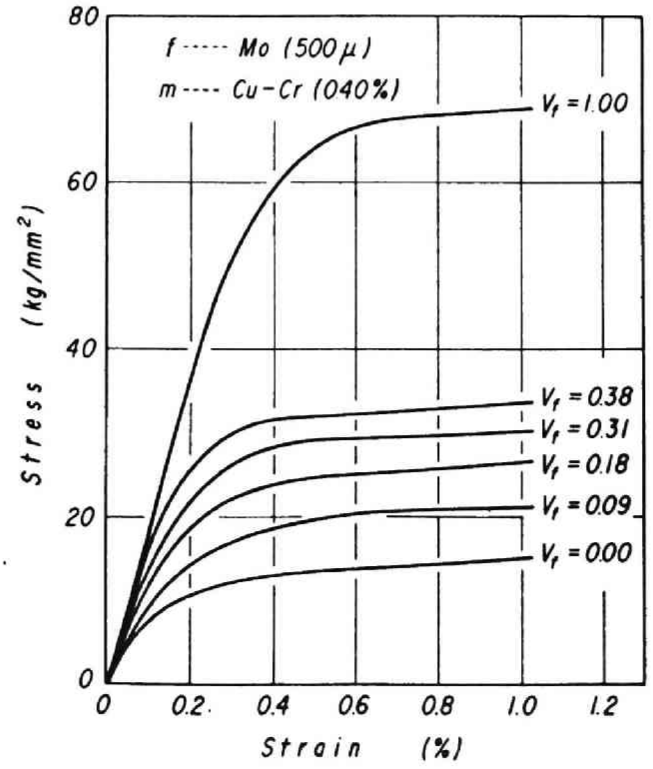

Fig.18 Initial portions of stress-strain curves of age-hardened Mo/Cu-Cr composites.

contrary, Mo-Cr solid solution layer did not degrade the fibre strength, as shown later.

IV-(4)-3-(ii) Tensile Test

Stress-strain curves of W/Cu, Mo/Cu and Mo/Cu-Cr composites were consisted of the four stages , as described in chapter I. W/Cu-Cr ccmposite, however, had not stage III, which means that the fibres in this composite failed in a brittle manner. While primary Young's modulus of all types of composites obeyed ROM, deformation behaviour of these composites showed deviation from ROM in stage II and stage III. Figs.18 and 19 show stress-strain curves of Mo/Cu-Cr and W/Cu-Cr composites, respectively. Composite stress σ_c is predicted by

$$\sigma_c = \sigma_f V_f + \sigma_m V_m \qquad (10)$$

where σ represents stress at any particular value of strain taken from the stress-strain curves of the components and the subscript symbols c,f and m refer to composite,fibre and matrix respectively. The predicted curves of all types of composites studied, however, were below the measured curves, as typically shown in Fig.20. Taking the stress-strain curve of the fibres to be same in the composites as when the fibres are tested separately, we can find actual stress in the matrix, σ_m^* , from the measured values of σ_c and the known V_f and V_m, by using eq.(11),

$$\sigma_m^* = (\sigma_c - \sigma_f V_f)/(1-V_f) \qquad (11)$$

The result is also shown in Fig.20, indicating σ_m^* is higher than σ_m. Kelly and Lilholt[52] made careful measurements of the stress-strain curves of 10μm and 20μm tungsten fibre-copper matrix composites and found the same phenomenon, namely, σ_m^* is higher than σ_m. They found that this phenomenon cannot be explained in terms

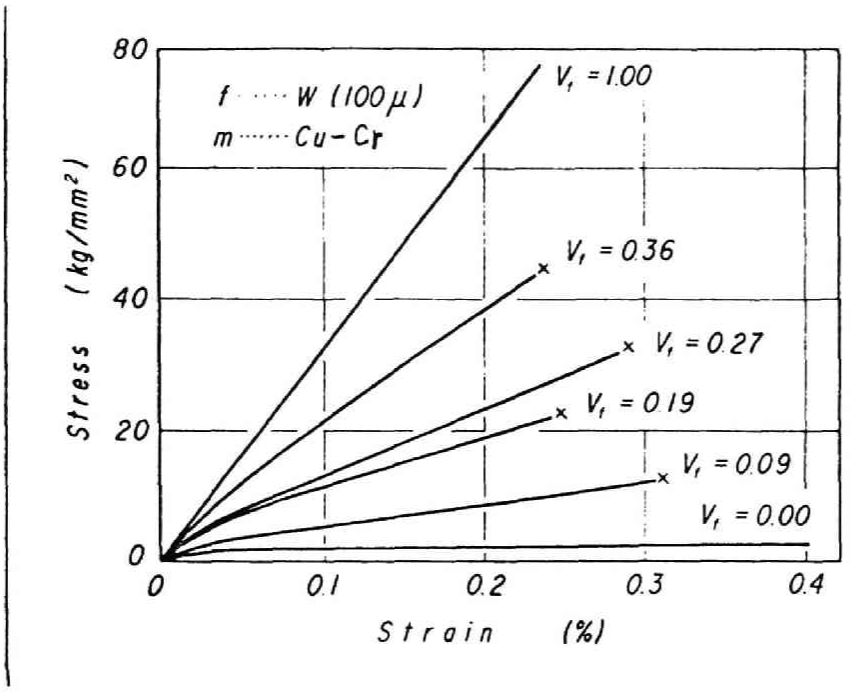

Fig.19 Stress-strain curves of W/Cu-Cr composites whose Cu-Cr **alloy** matrix is a supersaturated solid solution.

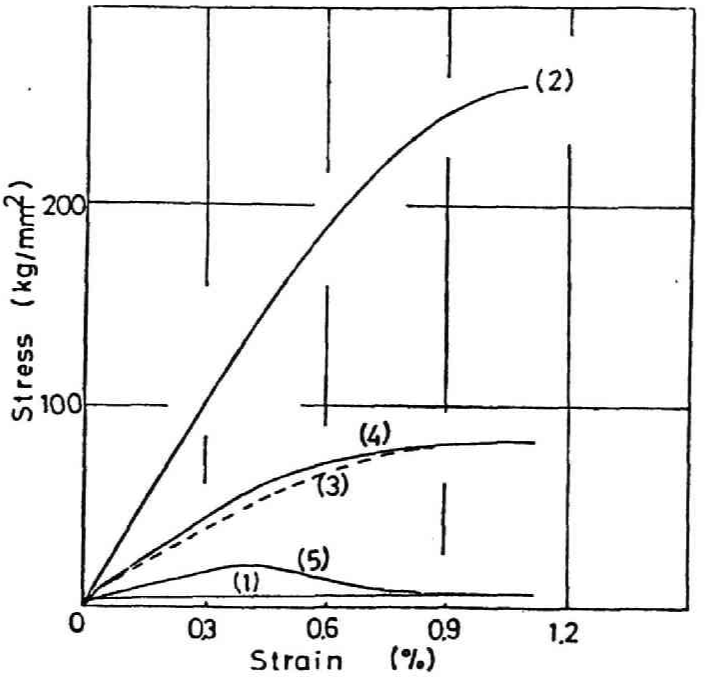

Fig.20 Initial portions of the stress-strain curves of copper matrix (1), tungsten fibre (2), W(100μm)/Cu composites with V_f=0.302 (calculated by the simple ROM), W/Cu composite (measured) (4) and derived matrix stress (5).

of the dislocation pile-up model, and then interpreted this phenomenon to mean that the yield of the copper is gradual, and that during stage II, an appreciable portion of the copper continues to deform elastically due to the constraint of the two components caused by the different lateral contractions. As thicker fibres(100μm and 500μm in diameter) were used in this work in comparison with the Kelly's thinner ones(10μm and 20μm), the pile-up model may be unapplicable to the present result. σ_m^* has a peak at 0.40% strain and then decreases with increasing strain. This phenomenon is explained as follows; As 0.40% is a yield strain of the fibre, transverse contractions of both the fibre and the matrix become same (0.5) over 0.40% and therefore the constraint vanishes. Thus the high stress of σ_m^* disappears. The same phenomenon was also observed in Mo/Cu and Mo/Cu-Cr composites. The strain at which σ_m^* began decreasing was about 0.16%, which was the yield strain of the molybdenum fibres.

The measured values of σ_c , $\sigma_{0.2}$(0.2% off-set proof stress) and σ_y are shown in Fig.21. The σ_c of W/Cu and W/Cu-Cr composites plotted against V_f is shown in Fig.22. The σ_c of W/Cu composite was higher than that of W/Cu-Cr composite. Alloyed matrix degraded composite strength despite age-hardening of the matrix. On the contrary, Mo/Cu-Cr composite had higher σ_c and $\sigma_{0.2}$ than Mo/Cu composite(Fig.23), due to age-hardening of the matrix.

IV-(4)-3-(iii) Observation of Fracture Surface

Appearances of the fractured W/Cu composite are shown in Photo.9. As some fibres failed in a brittle manner near the outer surface, the surface layer of the matrix was removed and

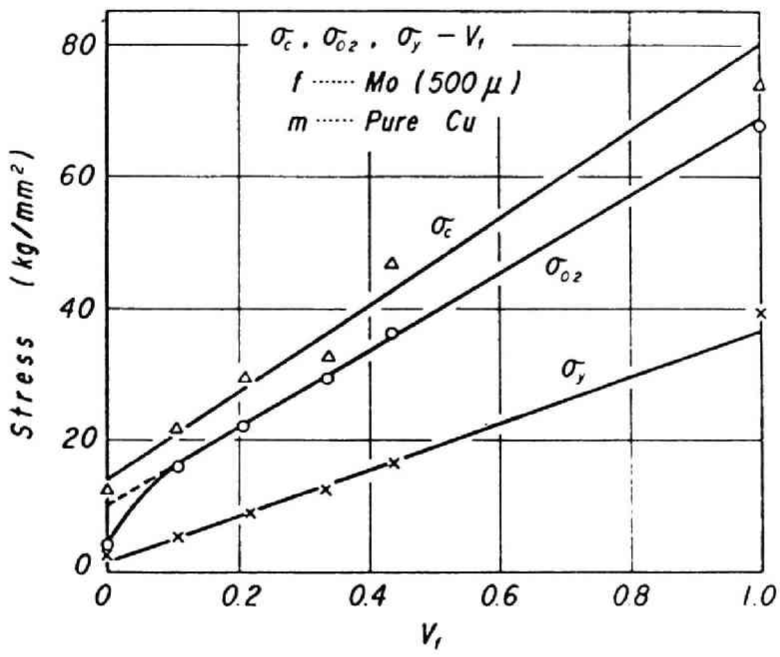

Fig.21 Tensile strength σ_c, yield stress $\sigma_{0.2}$ and true stress σ_y of Mo/Cu composites versus V_f. σ_y is an initial deviation stress from stage I to stage II.

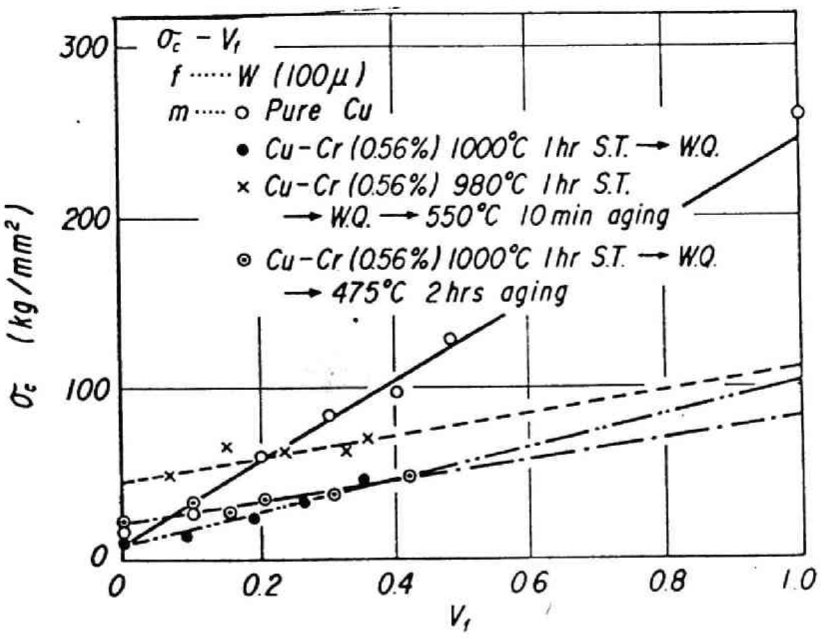

Fig. 22 Tensile strength σ_c of W/Cu and W/Cu-Cr composites versus V_f.

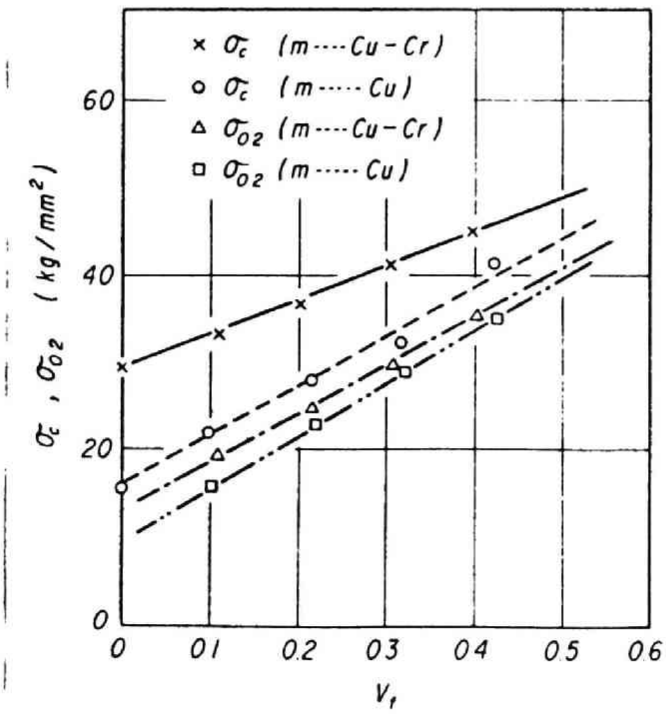

Fig. 23 Tensile- and yield strength σ_c and $\sigma_{0.2}$ of Mo/Cu and age-hardened Mo/Cu-Cr composites versus V_f.

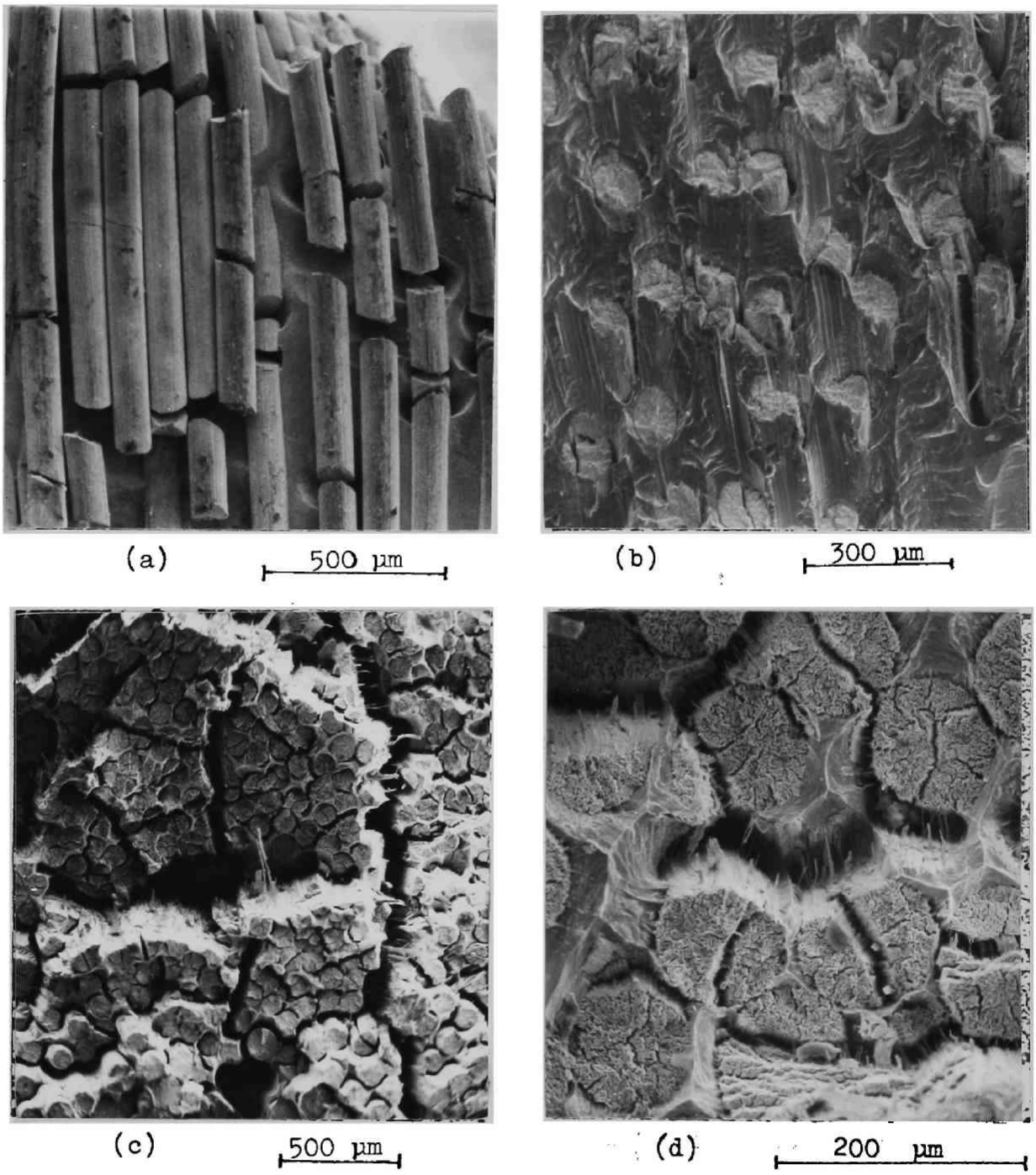

Photo.9 Scanning electron micrographs of fractured W/Cu composite. (a)Appearance of the fractured fibres. Matrix was removed by etching. V_f=0.30 (b)Fracture surface. Fracture occurs in the matrix shear direction. V_f=0.30 (c)Fracture surface. Fracture occurs perpendicularly to the tensile axis and is accompanied by splitting. V_f=0.58 (d)Fracture surface. Transverse fracture occurs in fibres. V_f=0.58.

then appearance of the fractured fibres was observed. On the right side of (a) where inter-fibre spacing is wide locally, fracture of the fibres occurres in the shear direction of the matrix(about 45° from the tensile axis) and on the left side where the inter-fibre spacing is narrow locally, it occurres perpendicularly to the tensile axis. This appearance may correspond to the following observations. When V_f is small, fracture of composite occurs in the shear direction of matrix (b), and when V_f is large, it occurs perpendicularly to the tensile axis(c). Fracture of the composites is accompanied by splitting (c) and transverse fracture in fibres,(c) and (d). Photo. 10 shows multiple necking of the fibres in the composites. The fibres in W/Cu-Cr composite did not exhibit multiple-fracture (Photo.11),being different from those in W/Cu composite. This observation leads to the speculation that, in W/Cu-Cr composite, a crack initiated by a fracture of the weakest fibre grew and caused fracture of the composite. Appearance of the fracture surface is shown in Photo.12 where the fibre surface exhibits herringbone. It is found from the herringbone that the fracture of the fibre was derived from the interface(a), and from the propagation of the crack stemed from the fracture of the neighbouring fibre,(b). Macroscopic fracture surface is shown in (c). Some fibres exhibit transverse fracture. Unlike W/Cu composite, this composite did not exhibit splitting. Mo/Cu-Cr composite showed the fracture surface similar to Mo/Cu one,as in Photo.13. Namely, the fibres failed by necking and the matrix exhibited dimple pattern. Fracture of this composite was also accompanied by splitting.

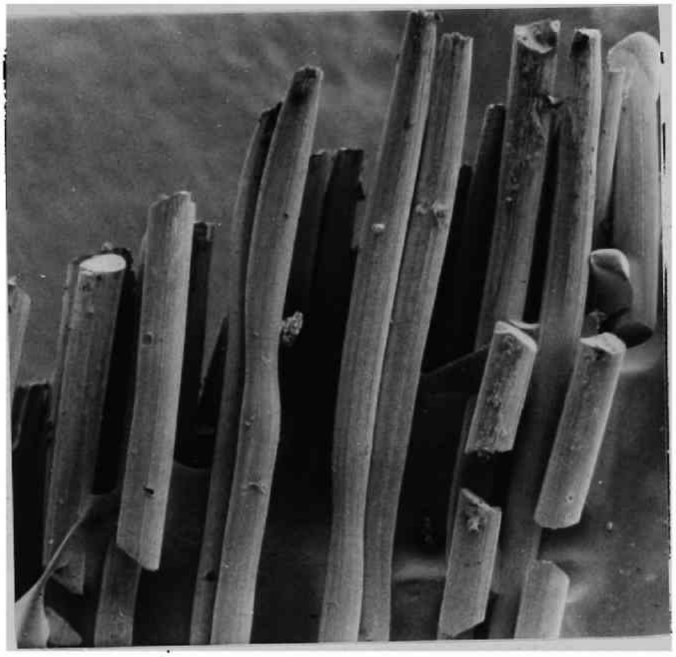

Photo.10 Scanning electron micrograph of multiple necking of fibres in a W/Cu composite. Matrix was removed by etching. V_f=0.10.

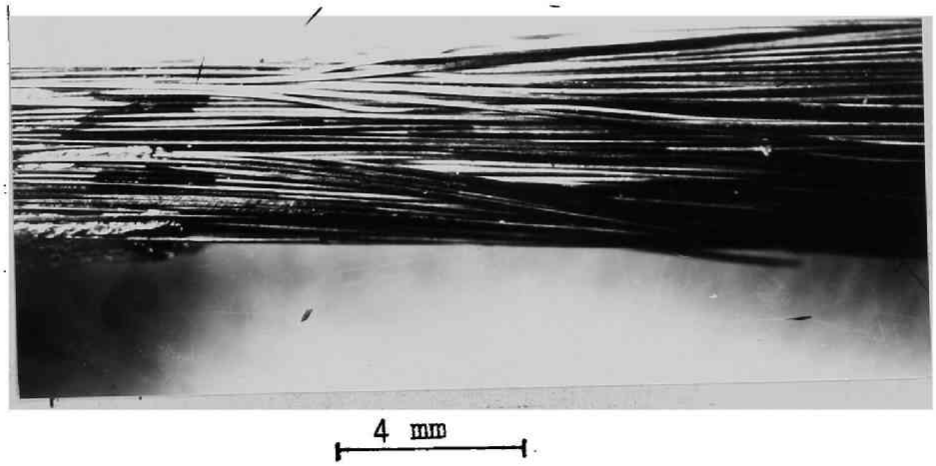

Photo.11 Appearance of unbroken tungsten fibres in a W/Cu-Cr composite after tensile test. Matrix was removed by etching. V_f=0.30.

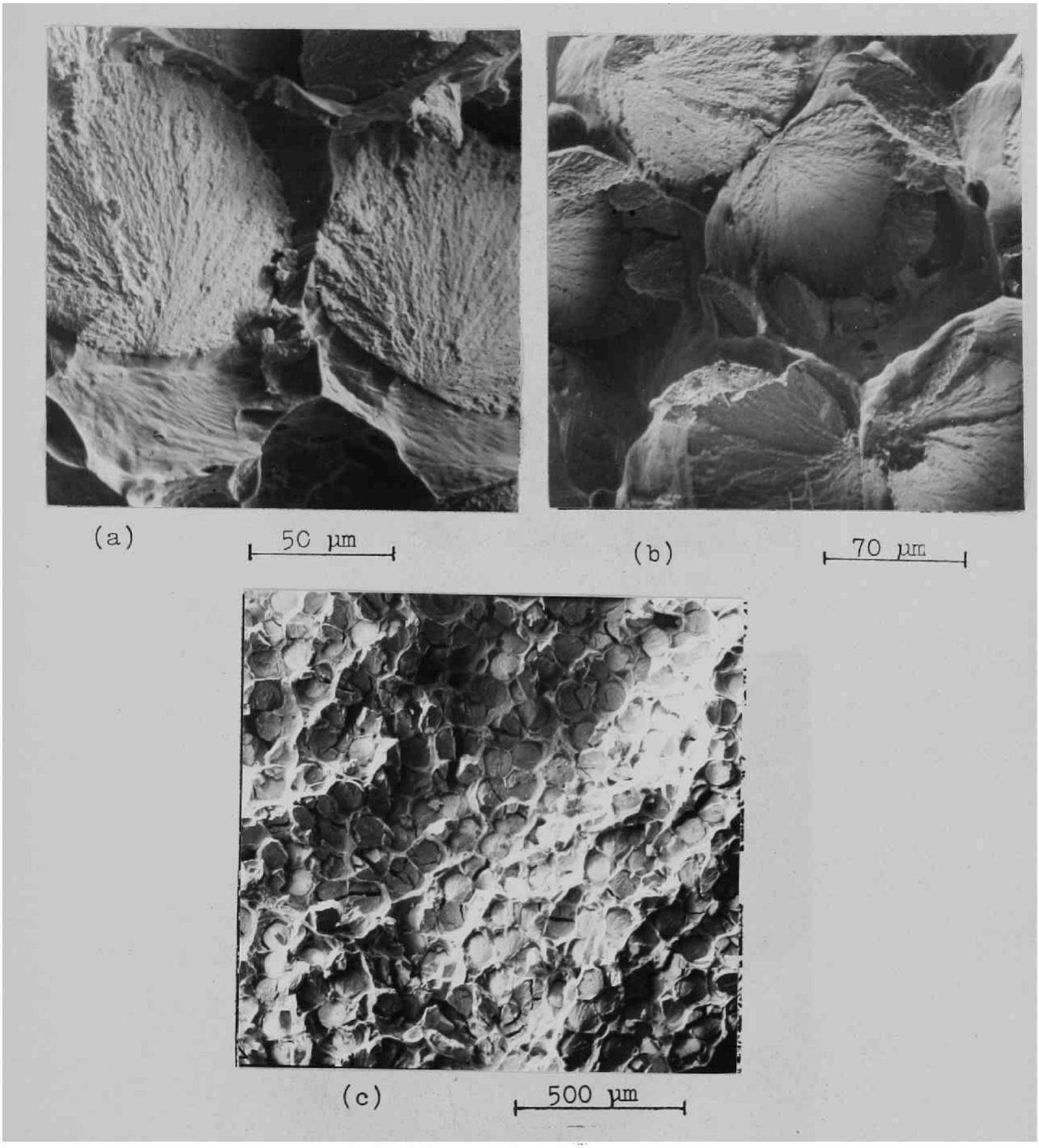

Photo. 12 Scanning electron micrographs of the fracture surface of W/Cu-Cr composite. V_f=0.20.

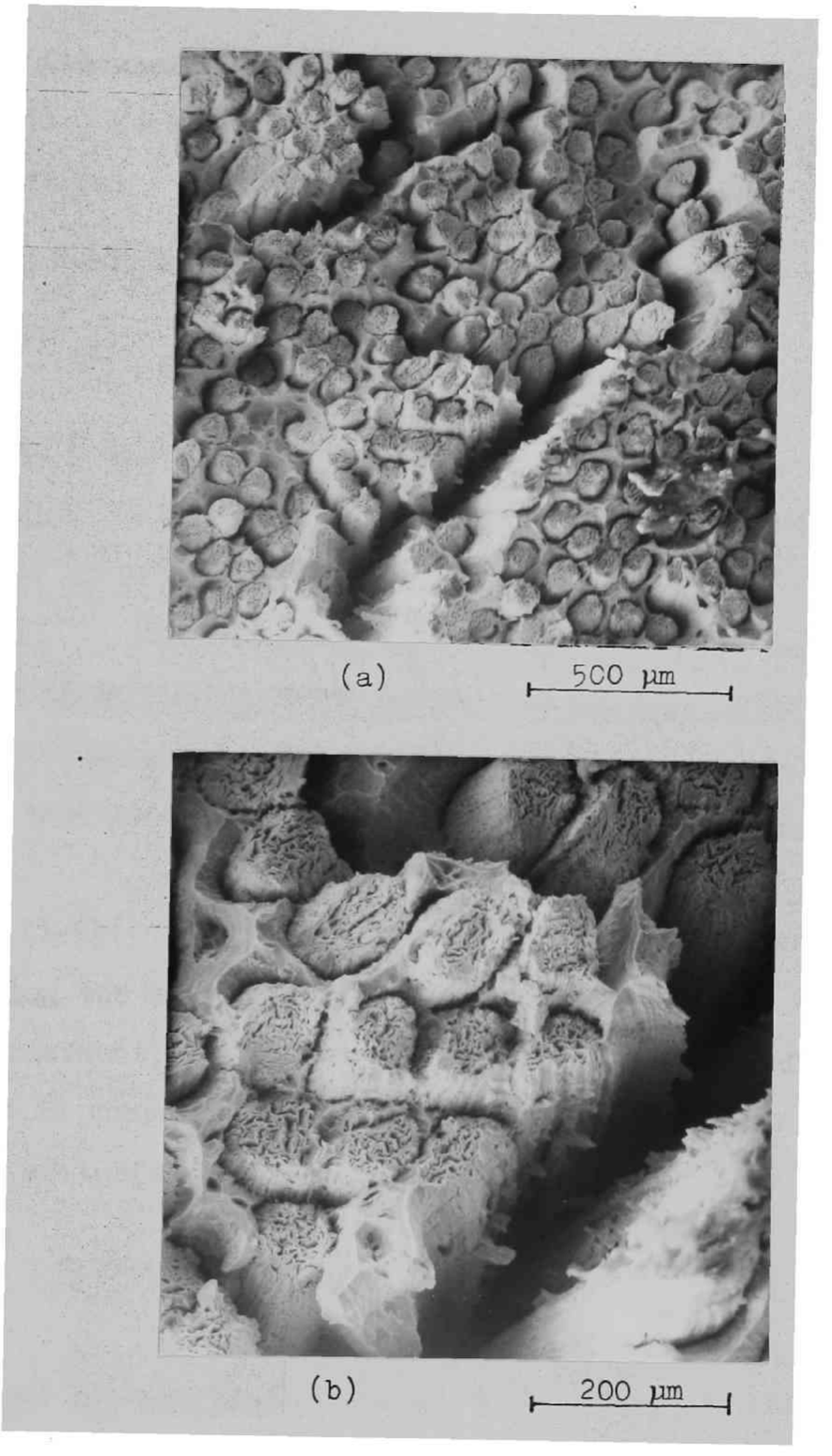

Photo. 13 Scanning electron micrographs of the fracture surface of Mo/Cu-Cr composite. V_f=0.40.

IV-(4)-4 Discussion

IV-(4)-4-(i) Mechanical Interaction between Fibres and Matrix

IV-(4)-4-(i)-(a) Young's Modulus E_c^I

Using Kelly's treatment[56], E_c^I is calculated as

$$E_c^I = E_f V_f + E_m V_m + \frac{4(\nu_f-\nu_m)^2 V_f V_m}{V_f/k_m + V_m/k_f + 1/G_f} \qquad (12)$$

where k and G are plain strain bulk modulus and shear modulus, respectively. Eq.(12) also corresponds to the upper bound of E_c^I obtained by Hill[57]. The deviation from ROM is, however, very small. For instance, E_c^I of W/Cu composite with V_f=0.24 calculated by eq.(12) is 19400 kg/mm^2, while that calculated by ROM is 19300 kg/mm^2. The positive deviation is only 100 kg/mm^2. Thus, why the measured values of E_c^I nearly obey ROM relation is explained.

IV-(4)-4-(i)-(b) The Strain at the Onset of Yielding of Matrix

Knowing the stress components in matrix obtained by Kelly's treatment,[56] the strain at the onset of yielding of the matrix in composites can be obtained as eq.(13) by applying the yield criterion of Von Mises.

$$e_y = e_{my} \frac{E_m}{E_m + \dfrac{2(\nu_f-\nu_m)(1-2\nu_m)V_f}{V_f/k_m + V_m/k_f + 1/G_f}} \qquad (13)$$

where e_y and e_{my} are yield strains of the matrix when contained in composites and when tested separately, respectively. For Mo/Cu ccmposite, e_y is calculated to be 1.007, 1.004 and 1.002 times e_{my} for V_f=0.332, 0.211 and 0.104, respectively. The difference

between e_y and e_{my} is so small that it is difficult to be detected. Also σ_y can be calculated by using

$$\sigma_y = e_y E_c^I \qquad (14)$$

where e_y and E_c^I are already shown in eq.(13) and eq.(12), respectively. As shown already, as E_c^I and e_y were nearly obey ROM relation, σ_y also nearly obeys the same relation. Why the measured values of σ_y in Fig.21 obey ROM is explained. Conclusively, the transition point from stage I to stage II is merely affected by the mechanical interaction between the components.

IV-(4)-4-(i)-(c) Tensile Stress Exerted at Interface

In multi-fibre composites, the interface is subject to tensile stress.[32)(33)(58)] The stress in stage I is not high, as expected by the above consideration. In stage II, the stress becomes high since the difference of Poisson's ratio between the components becomes large. In W/Cu-Cr composite whose fibres fracture in a brittle manner, the effects of this stress in stage II is found, as shown already in Photo.12(c). As tungsten fibres have been deformed severely during the production process, they are composed of fibrous structure, and their transverse strength is very weak. In W/Cu-Cr composite, the interfacial bonding strength is higher than the transverse strength of the fibres.[59)] Then the exerted tensile stress at the interface will cause transverse fracture in the fibres when it exceeds the transverse strength of the fibres.

In stage III, the difference of the Poisson's ratio disappears and the stress exerted at the interface vanishes. However, when the composites are elongated past the strain at which necking

would begin in the fibres if they were elongated separately, the radial and transverse(circumferential) stresses wii be exerted at the interface[37], thus stage III can be divided into two substages : stage III(1) and stage III(2).

Stage III(1):ranging from the onset of plastic deformation of both the components to the strain at which the fibres would begin necking if tested alone. The deformation may be described by the simple ROM since the Poisson's ratios of both the components are 0.5 in this stage and thus no difference in lateral contractions between the components arises for constraint.

Stage III(2) : ranging from the end of stage III(1) to failure of composites. Strain of composites exceeds that of fibres tested alone and thus the deformation behaviour cannot be predicted by the simple ROM. When the fibres fail by necking, the radial stress exerted at the interfaces due to necking of the fibres will cause separation of the interfaces if such a stress exceeds the interfacial bonding strength. In our W/Cu composite, interfacial bonding strength is higher than the transverse strength of the fibres.[59] Then the transverse fracture of the fibres will be predicted. The fracture surface of this composite shown in Photo.9(c) and (d) has two features : (i)transverse fracture of the fibres and (ii) macroscopic splitting of the composite. (i) is explained by the radial stress arising from the difference of Poisson's ratio between the two components as stated already. (ii) is probably derived from the radial stress arising from the necking of the fibres, because (ii) is not found in the fracture surface of W/Cu-Cr composite in which fibres fail in a brittle manner. On the other hand, the fracture surface of

Mo/Cu and Mo/Cu-Cr composites showed (i) separation of the interfaces and (ii) macroscopic splitting, as shown in Photo.13. As a recrystallization of the molybdenum fibres occurred during the preparation of the composite at 1160°C and therefore transverse strength of the fibres are very high, the exerted radial stress at interfaces gives rise to (i). Macroscopic splitting in W/Cu, Mo/Cu and Mo/Cu-Cr composites indicates that the tensile radial stress exerted at interfaces in stage III(2) is much higher than that in stage II.

IV-(4)-4-(ii) Elongation of Composites

Elongation of composites has been reported to be greater than the embedded fibres.[41)-(45)] This has been explained interms of (A) uniform elongation of fibres beyond the failure strain tested alone, (B) multiple necking of fibres and (C) growth of voids between the fractured segments. The conditions which result in (A), (B) and (C) are as follows.

(A)Strong interfacial bonding : it is necessary both to prevent separation of interface against tensile radial stress developed at interface due to necking of fibres and to supress necking.[37)(46)]

(B)Sufficient amount of matrix : multiple necking results from local transfer of load from fibres to surrounding matrix if V_f is smaller than $V_{c,mn}$(see chapter II-(3)) and needs no interfacial bonding.[43)(44)(60)]

(C)Arrestment of cracks :cracks formed by fracture of the weaker fibres should be arrested, otherwise composites will fail by propagation of the formed cracks. Concerning with an ability to arrest cracks, the next four factors should be taken into consideration. (i)If the interfacial bond is strong enough to

transfer the applied load from matrix to fibre, no more strength is necessary, otherwise, fracture of the fibres immediately causes that of matrix. Therefore ,excessive interfacial strength causes fracture of neighbouring fibres one after another.[61] However little the interfacial bonding strength may increase, the possibility of a propagation of the cracks formed by the fracture of fibres into matrix will increase. (ii)If a notch-sensitive material is used as matrix, cracks will propagate easily. (iii) When the fibre diameter is large, the cracks formed by the fracture of fibres are large and therefore propagate easily. Namely the conditions for actualizing (C) are weak interfacial bonding, notch-insensitive matrix, small V_f and small diameter of fibres. However, for instance, even if the interfacial bond is excessively strong, notch-insensitive matrix will cause (C). All of the aforementioned four factors need not simultaneously exist to cause (C). When a reaction zone is formed at the interface, two possibilities will be found. (1)The bonding strength will increase and therefore (A) will be expected. (2)Decrease in toughness of matrix due to alloying and increase in interfacial bonding strength will make the cracks propagate easily and then hasten the fracture of composites, and therefore reduce the composite elongation. Furthermore, if the formed reaction zone is brittle, it breaks in early stage and thus formed notch will hasten the initiation of failure of fibres. In such a case, the composite elongation will also decrease.

Let's discuss on the present results, taking the aforementioned

factors into consideration. Elongation of Mo/Cu composite and W/Cu one with small V_f was greater than that of the embedded fibres tested alone, though interfacial debonding occurred. They are explained in terms of (B) and (C). Some of W/Cu composites with large V_f exhibited smaller elongation than the fibres tested separately. This results from the decrease in the matrix amount. Mo/Cu-Cr composite exhibited greater elongation of molybdenum fibres tested separately , as similarly as Mo/Cu composite, which is also explained by (B). The Mo-Cr solid solution layer does not degrade composite strength as is inferred by Photo.13 in which molybdenum fibres containing chromium element fail by necking. The fracture strain of W/Cu-Cr composite ranged from 0.23 to 0.34% while that of W/Cu composite was more than 1%. The decrease in fracture strain due to alloying the matrix may be explained in terms of (a) notch effect derived from the earlier fracture of W-Cr solid solution layer, (b) decrease in ability to arrest cracks stemmed from increase in interfacial bonding strength, and (c) decrease in ability to arrest cracks due to exchange of matrix from copper to copper-chromium alloy. However, (c) can be disputed since toughness of copper-chromium alloy(especially when solution-treated) is not so much different from that of copper. (a) hastens the fracture of the fibre and (b) makes cracks propagate easily. In conclusion, W-Cr solid solution layer breaks at first, which causes the fibre fracture. The formed cracks can comparatively easily propagate into matrix and then neighbouring fibres since the strong interfacial bonding is produced by interfacial reaction.

IV-(4)-4-(iii) Tensile Strength of Composites

When elongation of composites is smaller than that of the embedded fibres, the fibres fail before they show full load bearing capacity. In such a case, tensile strength of composites also decrease. The reasons why tensile strength of W/Cu-Cr composite is smaller than that of W/Cu composite are explained by the aforementioned discussion.

If cracks are not formed during deformation, tensile strength of W/Cu-Cr composite will be predicted by ROM in which lateral constraints are taken into consideration. On the other hand, if many cracks are formed during deformation and the rate of crack propagation is slow, the tensile strength of the composite will be smaller than that predicted by ROM. Now, by the following treatment, we will see whether or not any decrease in tensile strength of the composite is caused by the presence of the cracks. Assuming lateral constraints are equal between W/Cu-Cr and W/Cu composites (this assumption is valid since the mechanical properties such as E_m and ν_m are not different between copper and copper-chromium alloy especially when solution-treated), σ_c of W/Cu-Cr composite will be calculated by eq.(15).

$$\sigma_c = \sigma_f(e)V_f + \sigma_m^*(e)V_m \qquad (15)$$

where $\sigma_f(e)$ is a stress of the fibres with peripheral zones containing chromium element, at a strain e where the composite fails. $\sigma_f(e)$ is taken from the stress at a strain e in the stress-strain curve of the fibres extracted from W/Cu-Cr ccmposite. σ_m^* is the matrix stress at the strain e, which is taken from the measured value of σ_m^* of W/Cu composite with the same V_f. Table 4 shows a comparison of the calculated and measured values

Table 4 Comparison of the calculated and measured tensile strength of W/Cu-Cr composite whose matrix is super-saturated solid solution.

V_f	e	σ_m^*(kg/mm^2)	σ_c(kg/mm^2) (cal.)	σ_c(kg/mm^2) (meas.)
0.19	0.0024	11	24	23
0.36	0.0023	27	44	45

of σ_c of W/Cu-Cr composite whose matrix was solution-treated. This result means that the effects of cracks on deformation behaviour merely exist and the cracks propagate rapidly at the fracture of the composite. As tensile strength of the fibres extracted from W/Cu-Cr composite ($\Delta r=0$ in Fig.9) are scattered, weaker fibres shoud fracture at early stage of deformation. The formed cracks, however, do not grow until stress state is favorable for them to grow, and then they grow rapidly, which results in composite fracture. Conclusively, deformation behaviour obeys the ROM in which mechanical interactions between fibres and matrix are taken into consideration,while fracture behaviour obeys growth of cracks.

IV-(4)-5 Conclusions

Deformation and fracture behaviour of W/Cu, Mo/Cu, W/Cu-Cr and Mo/Cu-Cr composites prepared by a vaccum infiltration method was investigated. Interfacial reaction occurred in the latter two composites but not in the former two composites.
The main results obtained are summarized as follows:
(1)Mechanical interaction between fibres and matrix occurred in all stages of deformation. The effect of it on the primary modulus and yield stress of composites was small, while it was large in stage II and stage III due to large difference of Poisson's ratio between the fibres and the matrix, and derived stresses by necking of the fibres, respectively.
(2)The fracture of W/Cu-Cr composite occurred in an elastic range of the tungsten fibres, and the elongation and tensile strength

of this composite were lower than those of W/Cu composite. This mode of fracture was explained in terms of a notch effect on tugsten fibres caused by the earlier fracture of the W-Cr solid solution layer formed in the peripheral zone and a poor notch resistance of the composite arising from the increased bonding. Moreover, the deformation was confirmed to obey the rule of mixtures in which the constraint arising from the different lateral contractions between the fibres and the matrix is taken into consideration.

(3)The tensile- and yield-strengths of age-hardened Mo/Cu-Cr composite were found to show higher values than those of Mo/Cu one by the ageing treatment, because of the hardening of the matrix and the absence of detrimental effects of the Mo-Cr solid solution layer formed during preparation.

IV-(5) Tip Radius of Cracks Formed by Earlier Fracture of Brittle Reaction Zones in Fibre-Composites

IV-(5)-1 Introduction

The formation of brittle zones by chemical reaction weakens composites through (i) notch effect on fibres derived from earlier fracture of the zones[12][14] or (ii) reduction of effective cross-sectional area bearing applied load due to earlier fracture of the zones.[5][12] The magnitude of the degrading effect of the brittle zones on fibres depends upon notch-sensitivity of fibres.[12] When fibres are brittle, (i) will occur, resulting in a severe reduction in fibre strength. On the other hand, when fibres are ductile, (ii) will occur, resulting in a relatively minor degradation.

However, it has been found in this chapter that both of (i) and (ii) can occur in tungsten fibre reinforced composites in accordance with the type of brittle zones ; namely tungsten fibres in W/Cu-Cr composite prepared by a vaccum infiltration method failed in a brittle manner owing to the circumferential notch formed by the earlier fracture of the W-Cr solid solution layer in the peripheral zone of the fibres. On the contrary, the same tungsten fibres in W/Ni composite prepared by a plating method and then annealed at 900°C for more than 30 min failed in a ductile manner and the newly formed brittle zone surrounding the fibre exhibited multiple fracture.

From the facts described above, we can draw the following inference. When W-Cr solid solution layer in the peripheral zone of the fibre fractures, the formed circumferential crack can propagate easily since the crack exists in the

fibre in itself. On the other hand, when the newly formed brittle zone surrounding the fibre fractures, the formed crack is not directly connected with the fracture of the fibre. There will be a important key in a difference of degree of stress concentration at the crack tip bwteen them. The degree of stress concentration is closely related with the radius of curvature ρ at the crack tip. The value of ρ for both composites can be calculated as follows.

IV-(5)-2 Calculation of Tip Radius of Cracks

IV-(5)-2-(i) Tungsten-Copper Chromium Alloy Composite

According to the Griffith theory of brittle fracture,[62] fracture strength σ_f of a brittle body containing a crack with a length 2c is

$$\sigma_f = \sqrt{\frac{2E\gamma_S}{\pi Lc(1-\nu^2)}} \qquad (16)$$

where E and ν are respectively Young's modulus and Poisson's ratio, and γ_S is the true surface energy. For plastically relaxed crack, γ_S is replaced by the effective surface energy γ_E which means the work done per unit area of fracture surface. Also γ_E is represented by

$$\gamma_E = \gamma_S \cdot \rho/3a \qquad (17)$$

for an elliptical crack where a is the lattice spacing.[63]

The fracture strength of the tungsten fibre with W-Cr layer was 130 kg/mm^2 on an average and c is inferred to be 3μm since the notch depth in the fibre will be equivalent to the depth of the reacted layer.[64] Substituting E=42000 kg/mm^2,[65] ν=0.28[65], σ_f=130 kg/mm^2 and c=0.003 mm into eq.(16), γ_E is calculated to be 1.74 x 10^{-3} kg/mm

(17000 ergs/cm^2). This value is similar to the calculated values of 13600 ergs/cm^2 of niobium[66] and 12000 ergs/cm^2 of molybdenum[67]. Then ρ is calculated to be 34.2Å by substituting γ_S=4700 ergs/cm^2[68] and a=3.16Å into eq.(17).

IV-(5)-2-(ii) Tungsten-Nickel Composite

At room temperature, tungsten fibre with brittle zone fails in a ductile manner, suggesting occurence of blunting of the crack tip due to plastic deformation of the fibre. If the fibre is brittle, such a blunting will not occur. σ_c versus $c^{-1/2}$ at 77°K, where the bare fibre fails in a brittle manner, is represented in Fig.24 which is reproduced from Fig.12 in this chapter. If σ_f is given by eq.(16), σ_c will be of the form

$$\sigma_c = \sqrt{\frac{2E\gamma_S}{\pi c(1-\nu^2)}} \cdot V_f + \sigma_m^* V_m \qquad (18)$$

where V_f and V_m are respectively volume fractions of the fibre and the matrix, and σ_m^* is the matrix stress at the fracture of the fibre. Assuming each of γ_S and σ_m^* has a unique value for all the composites, σ_c should decrease linearly with decreasing $c^{-1/2}$. Though γ_S and σ_m^* might not be constant for all the composites due to interfacial reaction, the sudden drop in σ_c shown in Fig.24 should be noted since γ_S and σ_m^* might not vary so suddenly. The sudden drop in σ_c for increasing c from 1.5 μm to 3.1 μm is inferred to indicate that degree of stress concentration enough to fracture the fibre was satisfied for 3.1 μm but not for 1.5 μm.

Assuming the theoretical strength of the tungsten fibre is equal to $\sqrt{E\gamma_S/a}$ [70], the observed strength of the bare

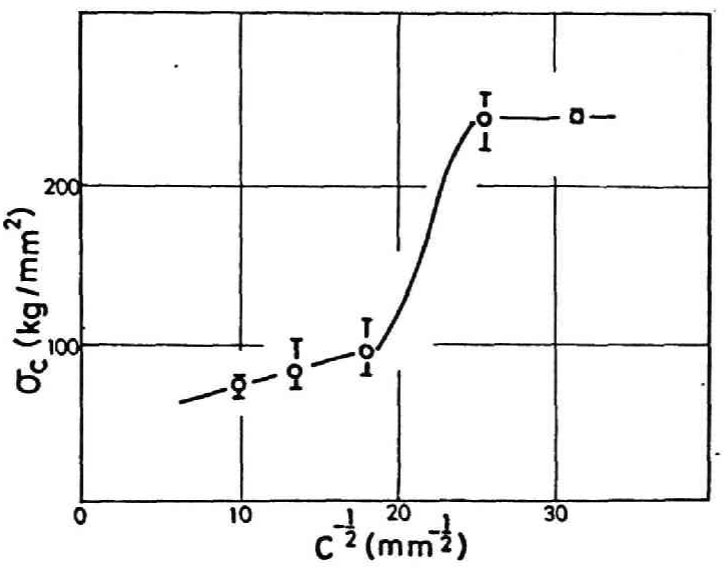

Fig. 24 σ_c versus $c^{-1/2}$ of W/Ni composite at 77°K.

fibre requires defects with stress concentration factor $K_1=\sqrt{E\,\gamma_S/a}\,/\sigma_f$. On the other hand, the stress concentration factor K_2 for a surface crack is of the form

$$K_2 = 1 + k\sqrt{c/\rho} \qquad (19)$$

where k is a proportionality constant.[71] For $K_1 > K_2$, the predominant source of the fracture of the fibre will be intrinsic defects in the fibre. For $K_2 > K_1$, fracture of the fibre will be caused by the notch formed by the brittle zone. This consideration leads to

$$\sqrt{E\,\gamma_S/a}\,/\sigma_f > 1 + k\sqrt{c/\rho} \qquad (20)$$

for c=1.5 μm where σ_c is nearly equal to the theoretical strength calculated by the rule of mixtures, and

$$1 + k\sqrt{c/\rho} > \sqrt{E\,\gamma_S/a}\,/\sigma_f \qquad (21)$$

for 3.1 μm where σ_c drops suddenly. A rough evaluation of ρ may be made by setting k=2 which corresponds to a elliptical crack.[72] Substituting the known values of E, σ_f(420 kg/mm^2), γ_S and c into eqs.(20) and (21), ρ is calculated as 180 Å < ρ < 380 Å.

At room temperature, ρ will increase due to increase in the ability of plastic deformation.

IV-(5)-3 Conclusions

Comparing ρ of W/Cu-Cr composite with that of W/Ni one, the former is smaller than the latter. Conclusively, the difference in type of interfacial reaction leads to difference in ρ or stress concentration.

IV-(6) Summary

Mechanical behaviour of the indivudial composite with interfacial reaction has been investigated and been made clear to some extent. Let's summarize effects of the reaction on the mechanical behaviour of composites in view of the following four points : (i) characteristics of reaction zone , (ii) bonding among fibre, reaction zone and matrix, (iii) thickness of reaction zone, and (iv) reaction time.

(i)-(a)Brittle Reaction Zone

When the reaction zone is brittle, its effect becomes different one depending upon whether the fibre is brittle or ductile. If fibre is brittle, it fails due to a propagation of the crack formed by the earlier fracture of the reaction zone, while the radius at the crack tip is different between the two cases ; i.e. the case where the reaction zone is formed in the peripheral zone of the fibre, corresponding to a small tip radius, and the case where the reaction zone is newly formed on the surface of fibre, corresponding to a large tip radius. It should be noted that the formed crack will not break the fibre if the stress concentration at the crack tip is lower than that at the intrinsic defects in the fibre.

If the fibre is ductile, the composite will fail in an early stage of deformation when the volume fraction of the reaction zone is so high that a decrease in load bearing capacity due to an earlier fracture of the brittle zone cannot be compensated by the work-hardening of the fibre and the matrix. When the volume fraction of the brittle zone is low,the brittle zone exhibits multiple crackings. In this case, a constaraint

effect arises at the formed notches so long as the brittle zone adheres to the fibre for thick zone and is not fractured by the compressive transverse stress for the thin zone. Then the stress in the composite can be raised in comparison with that predicted by ROM. After a spalling or fracture of the brittle zone, the usual ROM is applicable.

(i)-(b)Ductile reaction zone

When the reaction zone is ductile, the strength of the composite depends upon that of the reaction zone. If the reaction zone is stronger than the matrix,the strength of the composite will be raised in comparison with that of the identical composite without interfacial reaction. If the reaction zone is weaker than the matrix, the strength of the composite will decrease. When the fibre and the reaction zone are ductile, the composite can deform past the elongation at which necking would begin in the less ductile phase between the fibre and the reaction zone if they were tested separately, until necking begins in the composite as a whole, if the interfacial bondings among the three phases are strong.

(i)-(c)Thin film effect

If the reaction zone is thin and therefore includes no defects, the reaction zone will exhibit high strength such as whiskers. However, this case is merely found.

(ii)Bonding among fibre,reaction zone and matrix.

(ii)-(a)Bonding between fibre and reaction zone

If the bonding between fibre and reaction zone is strong, machanical interaction will arise between them. Then, when the reaction zone fails in a earlier stage, the formed crack propagates easily for brittle fibre or constraint effect arises for ductile

fibre as stated in (i)-(a). On the other hand, if the bonding is weak, the formed crack does not propagate into matrix, and the constraint effect does not arise.

(ii)-(b)Bonding between reaction zone and matrix

If the bonding between the reaction zone and the matrix is strong, mechanical interaction between them will arise. If the bonding is weak, splitting will occur if the transverse strength of the composite is less than one-fifth of the longitudinal strength. However,in some composites with weak interfacial bonding, the mechanical behaviour shows deviations from the ROM relation owing to the mechanical interaction among the phases. For instance, multiple necking of the fibre requires no interfacial bonding. Also, even if the bonding is so weak that debonding occurres during deformation, some mechanical interactions among the phases may arise after debonding owing to the differences in deformation amount and Poisson's ratio among them. For instance , multiple fracture of the brittle fibre contained in the composite with weak interfacial bonding is caused by the mechanical interaction after debonding. Concerning with the relation between interfacial bonding and mechanical interaction among the phases, there exist much uncertainties.

(iii)Thickness of reaction zone

(iii)-(a)Brittle reaction zone

If the fibre is ductile, the following three cases will occur in accordance with the thickness of the reaction zone. If the reaction zone is extremely thick, the fracture of the zone leads to an earlier fracture of the fibre and

the composite due to a decrease in load bearing capacity of the composite. If the zone is thick (but not extremely thick), spalling of the zone from the fibre will occur when the bonding is weak. If the zone is thin, the zone will be failed by the compressive transverse stress.

If the fibre is brittle, the strength of the fibre depends upon the crack tip radius and the thickness of the zone. If the crack tip radius is small enough to break the fibre, the strength of the fibre will be inversely proportional to the square root of the thickness of the zone. If the crack tip radius is large, and therefore the stress concentration at the crack tip is lower than that at the intrinsic defects in the fibre, the strength of the composite will decrease linearly with increasing the volume fraction of the zone.

(iii)-(b)Ductile reaction zone

The strength of the composite depends upon that of the reaction zone. If the reaction zone is stronger than the matrix, the strength of the composite will increase with increasing thickness of the zone. If the zone is weaker than the matrix, the strength of the composite will decrease with increasing thickness of the zone.

(iv)Reaction time

Changes of the characteristics of the fibre and the matrix due to softening, recrystalization , strengthening derived from alloying by diffusion and so on affect on the strength of the composite.

It should be noted that the bonding strength is controlled by a volume change occuring during the formation of the reaction

zone. If the reaction zone is dense compared with the fibre and the matrix, the growth of the reaction zone stops at some stage of the interfacial reaction, and the interfacial bonding is weak. On the other hand, the reaction zone is less dense than the fibre and the matrix, the reaction zone grows with increasing reaction time, and the bonding is strong.

References

(1)W.I.Stuhrke : Metal Matrix Composite, ASTM, (1969), p.76.

(2)P.W.Jackson : Metals Eng. Quarterly , ASM , 9(1969),22.

(3)R.B.Barclay and W.Bonfield : J. Mat. Sci., 6(1971), 1076.

(4)P.W.Jackson and J.R.Majoram : J. Mat. Sci., 5(1970),9.

(5)D.W.Petrasek and J.W.Weeton : Trans..Met. Soc. AIME,230(1964),977.

(6)D.M.Braddick, P.W.Jackson and P.J.Walker : J. Mat. Sci., 6(1971),419.

(7)D.W.Petrasek : Trans. Met. Soc. AIME, 236(1966),887.

(8)R.L.Mehan and M.J.Noone : Composite Materials, ed. by K.G.Kreider, vol.4, (1974),p.159.

(9)R.A.Signorell : Composte Materials , ed. by K.G.Kreider, vol.4, (1974), p.159.

(10)Y.Umakoshi, K.Nakai and T.Yamane : Met. Trans., 5(1974),1250.

(11)W.H.Sutton and E.Feingold : General Electric Space Sci. Lab. Rep. R65SD39, (1965), p.54.

(12)P.W.Heitman, L.A.Shepard and T.H.Courtney : J. Mech. Phys. Solids, 21(1973),75.

(13)K.Akamatsu and K.Kamei : Read at the Autumn Meeting of Japan Inst. Metals, 1975.

(14)E.Friedrich and W.Pompe : J. Mat. Sci., 9(1974),1911.

(15)A.G.Metkalfe : Composite Materials , ed. by K.G.Kreider, vol.4, (1974), p.159.

(16)A.Pattnaik and A.Lawley : Met. Trans., 5(1974),111.

(17)Y.Umakoshi and T.Yamane : Trans. JIM, 17(1976),25.

(18)E.G.Kendall : Composite Materials , ed. by K.G.Krieder , vol.4, (1974), p.319.

(19)A.Kitamura and K.Kobayashi : Read at the Autumn Meeting of Japan Inst. Metals, 1973.

(20)M.Morita and A.Baba : J. Japan. Inst. Metals, 37(1973),315.

(21)I.Shiota and O.Watanabe : J. Japan Inst. Metals, 38(1974),788.

(22)Ibid., 794.

(23)E.Ignatowitz : Aluminium, 50(1974),335.

(24)A.J.Perry, E. de Lamotte and K.Phillips : J. Mat. Sci., 5(1970),945.

(25)D.L.Harrod and R.T.Begley : SAMPE, 10(1966),E1.

(26)D.W.Petrasek, R.A.Signorelli and J.W.Weeton : NASA TN D-4187.

(27)J.W.Weeton and R.A.Signorelli : NASA TN D-3530.

(28)Chapter II-(2)

(29)J.S.Thornton and A.D.Thomas, Jr : Met. Trans., 3(1972),637.

(30)T.Heumann and S.Dittrich : Zs. Metallkunde, 50(1959),617.

(31)A.K.Kurakin : Fiz. Metal. Metalloved., 30(1970),432.

(32)L.J.Ebert and J.D.Gradd : Fiber Composite Materials, ASM, Ohio, (1964), p.89.

(33)Y.Murakami, S.Ochiai, K.Shimomura and S.Okuda : Read at the Autumn Meeting of Japan Institute of Metals, 1975.

(34)J.Cook and J.E.Gorden : Proc. Roy. Soc., 282A(1964),508.

(35)W.W.gerberich : J. Mech. Phys. Solids, 19(1971),71.

(36)G.A.Cooper and A.Kelly : J. Mech. Phys. Solids, 15(1967),279.

(37)H.R.Piehler : Trans. Met. Soc. AIME, 233(1965),12.

(38)R.W.Hertzberg : Fiber Composite Materials, ASM, Ohio, (1964), p.77.

(39)S.Ochiai, M.Mizuhara, M.Kawasaki and Y.Murakami : Trans. JIM, 15(1974),66.

(40)M.Hansen : Constitution of Binary Alloys, McGraw-Hill, (1958), p.1057.

(41)A.Kelly and W.R.Tyson : J. Mech. Phys. Solids, 13(1965),329.

(42)D.L.McDanels, R.W.Jech and J.W.Weeton : Trans. Met. Soc. AIME, 233(1965),636.

(43)R.M.Vennet, S.M.Volf and A.P.Levitt : Met. Trans., 1(1970),1969.

(44)C.Schone and E.Scara : Met. Trans., 1(1970),3466.

(45)I.Ahmad and J.M.Barranco : Met. Trans., 1(1970),989.

(46)S.T.Mileiko : J. Mat. Sci., 4(1969),974.

(47)G.Garmong and R.B.Thompson : Met. Trans., 4(1973),863.

(48)A.Kelly : Proc. Roy. Soc., 282A(1964),63.

(49)S.Bhattacharyya and N.M.Parik : Met. Trans.,1(1970),1437.

(50)I.Miura and H.Honma : J. Japan Inst. Metals, 31(1967),475.

(51)H.P.Cheskis and R.W.Heckel : Met. Trans., 1(1970),1931.

(52)A.Kelly and H.Lilholt : Phil. Mag., 20(1969),311.

(53)M.Hansen : Constitution of Binary Alloys, McGraw-Hill, (1958),570.

(54)Ibid., 537.

(55)H.Braun and K.Sedlatschek : Niobium, Tantalum, Molybdenum and Tungsten, Ed. by A.G.Quarrel, Elsevier, (1961), p.347.

(56)A.Kelly : Strengthening Methods in Crystals , Ed. by A.Kelly and R.B.Nicholson, Elsevier, (1971), p.439.

(57)R.Hill : J. Mech. Phys. Solids, 12(1964),199.

(58)G.S.Holister and C.Thomas : Fibre Reinforced Materials, Elsevier, (1966), p.49.

(59)Y.Murakami and S.Ochiai : Read at the Spring Meeting of Japan Institute of Metals, 1976.

(60)Chapter II-(3)

(61)A.H.Cottrell : Proc. Roy. Soc., 221A(1964),2.

(62)A.A.Griffith : Phil. Trans. Roy. Soc., 221A(1920),163.

(63)A.S.Tetelman and A.J.McEvily, Jr : Fracture of Structural Materials, John Wiley and Sons, (1967), p.38.

(64)R.A.Signorelli : Composite Materials, ed. by K.G.Kreider, Vol.4, (1974), p.229.

(65)C.J.Smithelles : Metals Reference Book, Vol.3, Butterworth, London, (1967), p.608.

(66)M.A.Adams, A.C.Roberts and R.E.Smallman : Acta Met., 8(1960),328.

(67)A.A.Johnson : Phil. Mag., 4(1959),194.

(68)J.J.Gilman : Fracture of Solids, Interscience, New York, (1963), p.541.

(69)D.T.Hurd : Metals Handbook, ASM, Metals Park, Ohio, (1961), p.1225.

(70)E.Orowan : Reps. Prog. Phys., XII(1948),185.

(71)J.Friedel : Electron Microscopy and the Strength of Crystals, John Wiley and Sons, New York, (1963), p.119.

(72)R.E.Peterson : Stress Concentration Design Factors, John Wiley and Sons, New York, (1953), p.136.

Chapter V

Cold Rolling Characteristics of Ductile Fibre-Composites

V- 1 Introduction

Fibre-reinforced composites promise significant improvements in properties over conventional materials. For practical use, it will be necessary to understand the rolling or drawing characteristics and the effects of them on mechanical properties of composites. Cold rolling and drawing behaviour of composites have been investigated in some composite systems[1]-[4] but there are few studies on relationships between tensile strength and extent of deformation. Moreover, effects of interfacial reaction on the above relationships have not yet been studied.

This investigation was undertaken to know how ductile fibre-reinforced composites with or without interfacial reaction respond to rolling and to know effects of rolling on tensile strength. Rolling was selected as the deformation process because of the directionality of deformation and the ease of control. The specimens used were Mo/Cu composite without interfacial reaction and age-hardened Mo/Cu-Cr one with interfacial reaction.[5]

V-2 Experimental Procedure

The apparatus and procedure for preparing specimens and heat-treatment were described in chapter IV-(4). Specimen dimension was 40 x 20 x 2 mm, and volume fraction of the fibre, V_f , was 25% and 40%. Rolling was accomplished using a four-high rolling mill at a speed of 20 m per min. The rolling direction was either parallel or perpendicular to the direction of the fibre alignment. Samples were rolled in steps of about 10 % reduction of the original

thickness per one pass. Tensile test was carried out at a speed of 0.025 per min under the condition where tensile axis was parallel to the fibre alignment. Observation of the fractured specimens was made by a scanning electron microscope.

V-3 Results

V-3-1 Deformation Behaviour

Photo.1 shows cross-sectional plane of Mo(500μm)/Cu composite rolled 70% parallel to the fibres. The shape of the cross section of the fibres which was originally circular became elliptical. The fibres in the deformed composites showed the same cross-sectional area to each other at a given reduction. In these composites, not only matrix but also fibres were deformed. This feature is discerned from that of B/Al composite in which boron fibres undertake not plastic deformation but breakage. Changes of cross-sectional area of Mo/Cu and Mo/Cu-Cr composites colled rolled parallel or perpendicular to fibres are shown in Fig.1, in which the original area is taken as 1. Perpendicular rolling caused spreading of width (perpendicular direction to fibres) and therefore cross-sectional area of the composites did not vary so much. On the other hand, parallel rolling caused much longitudinal (parallel direction to fibres) stretching and a little transverse one. Fig.2 shows changes of fibre cross-sectional area S_f, major axis a and semiminor one b. It is notable that fibres exhibited no transverse stretching. V_f did not vary with rolling in the case of perpendicular rolling, which was consistent with the observation stated above. On the contrary, as shown in Fig.3, parallel rolling caused a

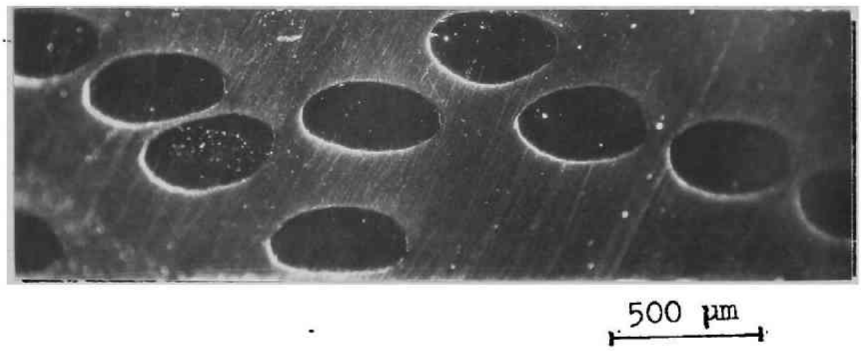

Photo.1 Cross-sectional plane of Mo/Cu composite cold rolled 70% parallel to fibres

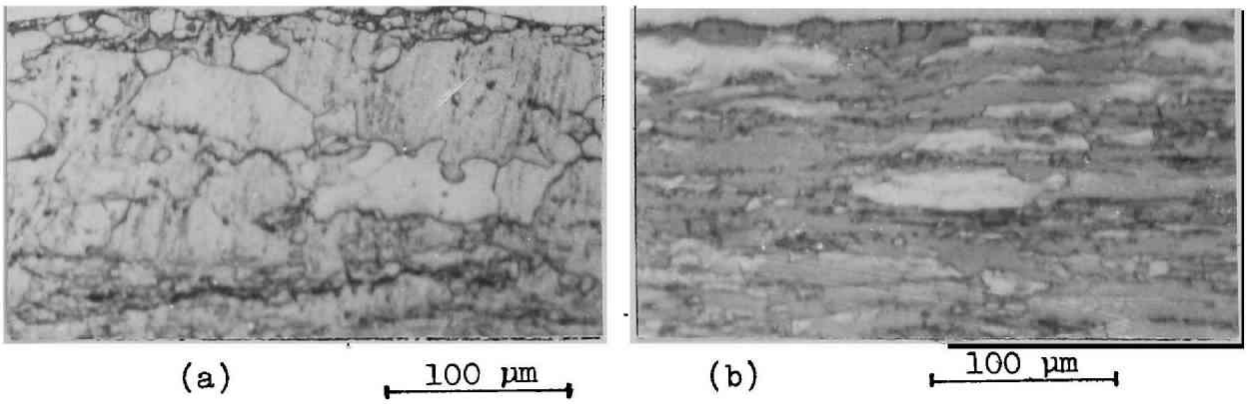

Photo.2 Grain structure of Mo fibres in the cold rolled Mo/Cu composites. (a)Cold rolled 70% perpendicular to fibres. (b)Cold rolled 90% parallel to fibres.

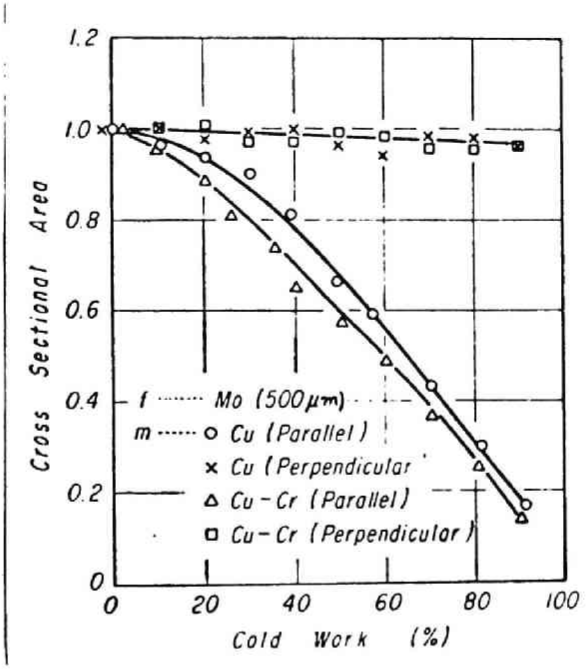

Fig.1 Change of cross-sectional area of Mo/Cu and Mo/Cu-Cr composites caused by cold rolling parallel or perpendicular to fibres.

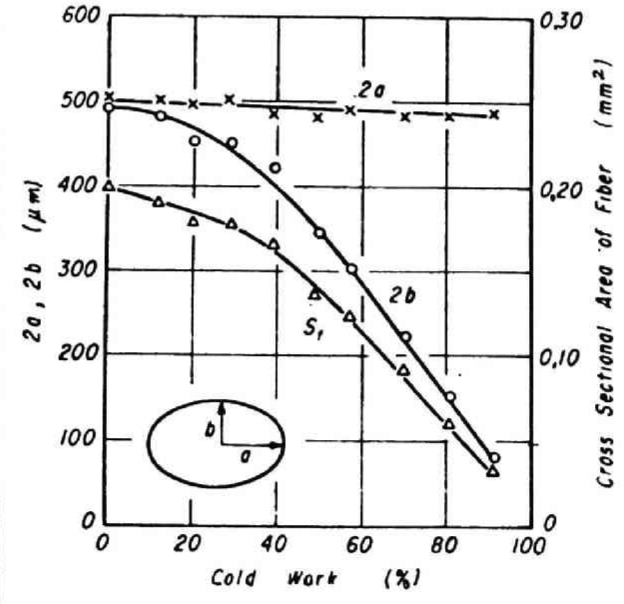

Fig.2 Effect of cold rolling parallel to fibres on the shape and cross-sectional area of fibres in Mo/Cu composites.

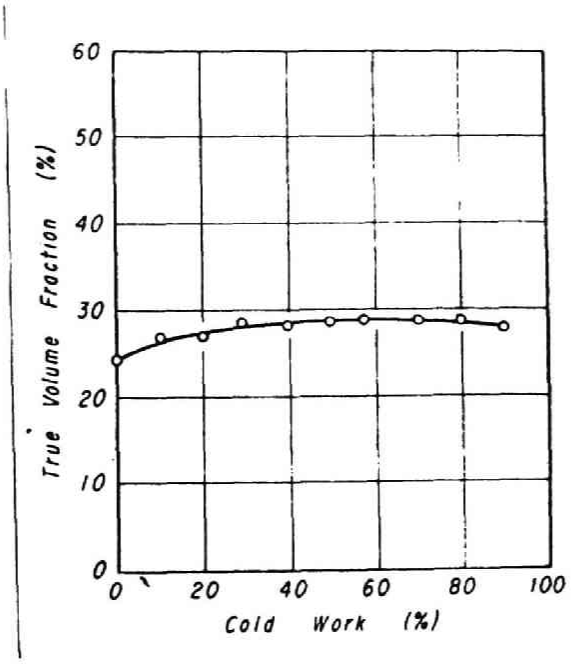

Fig.3 Change of volume fraction of fibres in Mo/Cu composites cold rolled parallel to fibres.

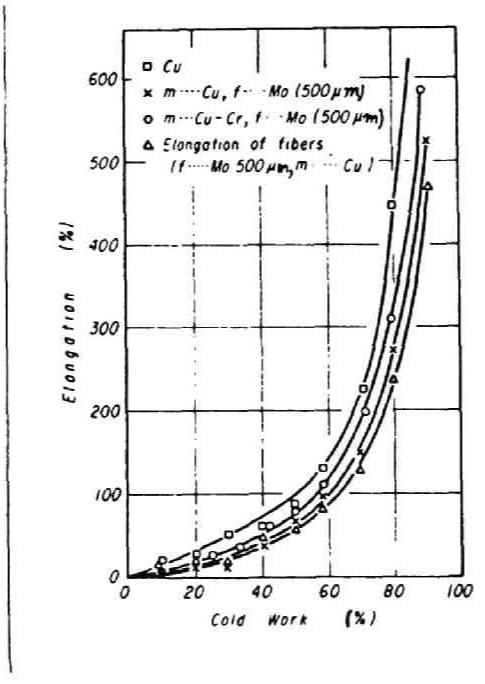

Fig.4 Elongation of composites caused by cold rolling parallel to fibres.

little increase in ν_f , which derived from the difference of transverse stretching between fibre and matrix. Fig.4 shows longitudinal elongation caused by parallel rolling. The difference among the each type of the composites was explained by the difference of transverse stretching. Elongation of fibres, which was calculated on the basis of cross-sectional area of fibres, was smaller than that of composites. This fact means that growth of voids between the fractured fibres contributes to the elongation of the composites. For Mo/Cu composite, the contribution is represented by the difference of the elongations between the composite(x) and the fibres(Δ) in Fig.4.

V-3-2 Tensile Test

Tensile strength of Mo/Cu and Mo/Cu-Cr composites versus cold work were shown in Figs. 5 and 6. In Mo/Cu composite, tensile strength σ_c increased with increasing cold work for both parallel and perpendicular rolling. On the other hand, in Mo/Cu-Cr composite, the measured values of σ_c were scattered, but they increased with increasing cold work up to 30%. The reason will be discussed later. Whether matrix is copper or copper-chromium, parallel rolling produced higher strength than perpendicular rolling.

V-3-3 Structure and Fracture Surface

Grains of molybdenum fibres were not so much deformed by perpendicular rolling, whereas they were deformed in parallel direction by parallel rolling, as shown in Photo.2. Typical fracture surface of Mo/Cu-Cr composite is shown in Photo.3.

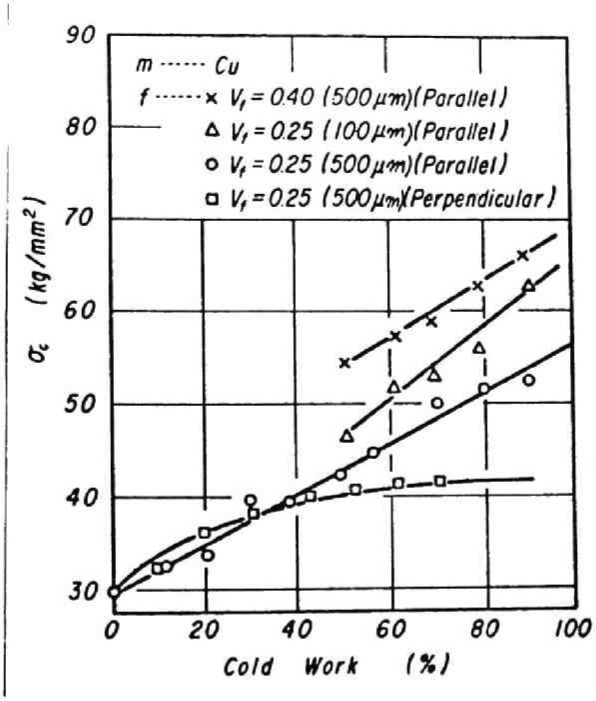

Fig.5 Effect of cold rolling parallel or perpendicular to fibres on the tensile strength of Mo/Cu composites.

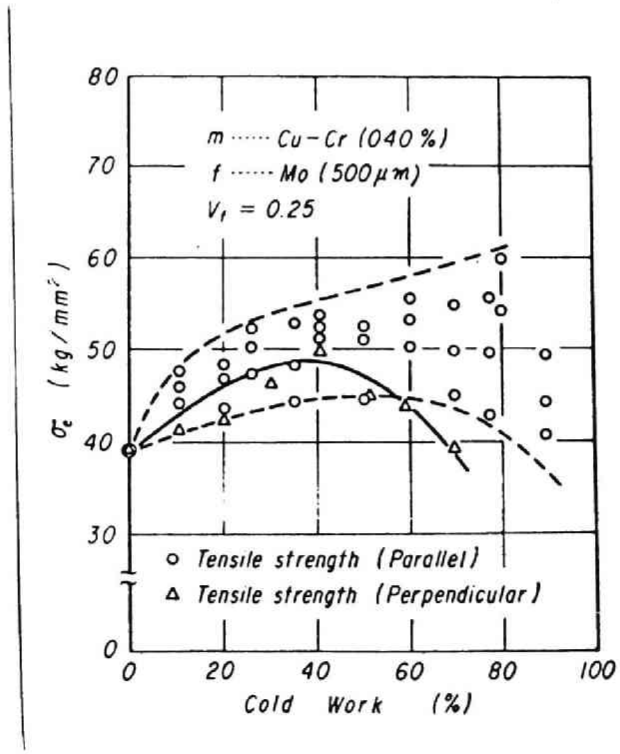

Fig.6 Effect of cold rolling parallel or perpendicular to fibres on the tensile strength of Mo/Cu-Cr composites with V_f=0.25.

The fibres failed by necking. In the case of 100μm fibre-composite, the shape of the cross-section of the fibres was not necessarily elliptical since the inter-fibre spacing was narrow in comparison with that of 500μm fibre-composite.

V-4 Discussion

V-4-1 Deformation Behaviour

Strength of the fibres was different between parallel and perpendicular rolling. Taking the case of Mo/Cu composite, parallel rolling produced higher tensile strength of the fibres than perpendicular rolling as shown in Fig.8 and Fig. 9 in which the symbol x represents tensile strength of the fibres estimated by Vickers hardness. Taking into account this fact and the difference in the deformed grain structure as already shown in Photo.2 , deformation behaviour of the fibres and matrix depends upon rolling direction. In the case of parallel rolling, major axis in the cross-section of the fibres did not vary but spreading of the width of the composite occured. This means that deformation amount of the matrix is greater than that of the fibres. The transverse spreading was,however, about 1/10 of the longitudinal elongation and therefore, to a first approximation, deformation amount of the fibres was nearly equal to that of the matrix and thus V_f did not so much change. As the deformation resistance of the fibres is higher than that of the matrix, tensile stress exerts on the fibres and compressive one on the matrix during rolling.[6] Existence of these stresses are ensured by strong interfacial bonding in the composites studied. These stresses

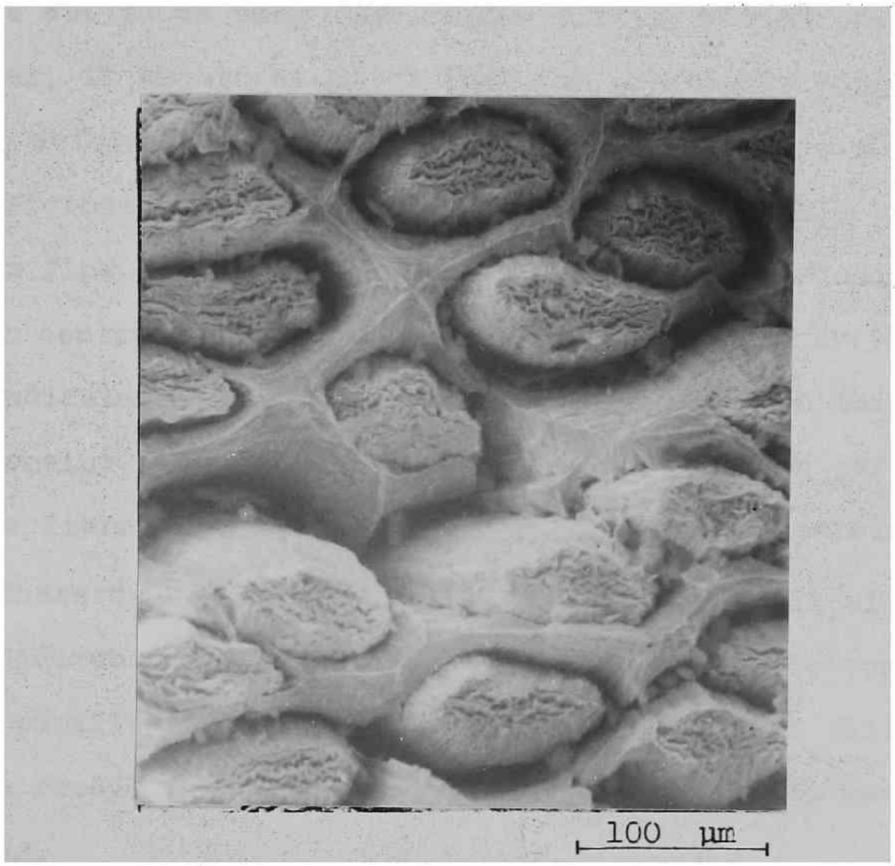

Photo.3 Appearance of fracture surface of Mo/Cu-Cr composite cold rolled 50% parallel to fibres.

will make the components deform to produce nearly same deformation amounts. This deformation behaviour of composites is very similar to the behaviour of composites in a normal tensile test. On the other hand, in the case of perpendicular rolling, deformation amount of the matrix is larger than that of the fibres due to an easy flow of the matrix between the fibres.[2] However, it should be noted that the molybdenum fibres were deformed as shown in Fig. 9. This means that the deformation behaviour cannot be explained only by the matrix flow between the fibres, although the predominant factor controlling deformation of the composite by the perpendicular rolling is the matrix flow. In this case, V_f remains nearly constant in the cross-section perpendicular to the fibre alignment, as similarly as in the parallel rolling.

These deformation behaviours correspond well with those of the unidirectionally solidified Al-Al_3Ni eutectic composite where parallel rolling causes crackings in Al_3Ni while cold work can be readily achieved without cracking in Al_3Ni by perpendicular rolling.

V-4-2 Tensile Strength

Following factors can be mentioned as affecting ones on tensile strength of the cold rolled composites.

(a)Work-hardening of the fibres

(b)Work-hardening of the matrix

(c)Reduction in tensile strength of the fibres due to damage introduced during rolling

(d)Reduction in effective V_f due to breakage of the fibres

(e)Stress concentration at the damaged or broken portions in the fibres

(f)Increase in V_f due to different deformation amounts between the fibres and the matrix

(g)Reduction in notch resistance of severely deformed matrix

(h)Mechanical relief of residual stresses introduced during preparation

(i)Residual stresses introduced during rolling

(j)Texture

At first we will consider (a) and (b). If we can estimate (a) and (b) in the rolled composite, we can deduce tensile strength of the composite assuming the rule of the mixtures. Tensile strength of the composite is given by

$$\sigma_c = \sigma_f V_f + \sigma_m^* V_m \qquad (1)$$

where σ_m^* is a matrix stress at a failure of composite and V_m is a volume fraction of matrix. As the change of V_f due to rolling is very small in both the cases of parallel and perpendicular rolling as stated already, we can calculate σ_c as follows.

If the stress-strain curve expressed in true co-ordinate, σ(true stress) and $\bar{\varepsilon}$(true strain), is approximated by a power function

$$\sigma = F(\bar{\varepsilon})^n \qquad (2)$$

where F is a constant and n is a strain (true) at necking, we can obtain equivalent stress-equivalent plastic strain relationship by setting $\bar{\varepsilon}$ as equivalent plastic strain introduced by rolling. As shear deformation of the specimen surface caused by frictional resistance during rolling was found very small in this work, it is neglected in the following treatment. As normal tensile strength σ_u is expressed by

$$\sigma_u = F(n/e)^n \qquad (3)$$

where e is the base of natural logarithm, F can be calculated by inserting the measured values of σ_u and n. As the normal tensile strength and normal plastic strain at necking of molybdenum fibre, copper and copper-chromium are 74.5 kg/mm^2 and 20%, 14 kg/mm^2 and 35%, and 29.5 kg/mm^2 and 26% on an average respectively, true stress- true strain curves are expressed by

$$\sigma_{Mo} = 121.9(\bar{\varepsilon})^{0.182} \qquad (4)$$

$$\sigma_{Cu} = 26.7(\bar{\varepsilon})^{0.300} \qquad (5)$$

$$\sigma_{Cu-Cr} = 51.9(\bar{\varepsilon})^{0.231} \qquad (6),$$

Then, when total strains of equivalent plastic strain introduced during rolling and plastic strain introduced during tensile test are $\bar{\varepsilon}_f$ and $\bar{\varepsilon}_m$ for the fibres and the matrix, respectively, true tensile stress $\sigma_{C,Cu}$ of Mo/Cu composite in the cross-section perpendicular to the fibres is

$$\sigma_{C,Cu} = 30.5(\bar{\varepsilon}_f)^{0.182} + 20.0(\bar{\varepsilon}_m)^{0.300} \quad \text{for } V_f=0.25 \qquad (7)$$

$$\sigma_{C,Cu} = 48.8(\bar{\varepsilon}_f)^{0.182} + 16.0(\bar{\varepsilon}_m)^{0.231} \quad \text{for } V_f=0.40 \qquad (8)$$

True tensile stress, $\sigma_{C,Cu-Cr}$ of Mo/Cu-Cr composite is

$$\sigma_{C,Cu\text{-}Cr} = 30.5(\bar{\varepsilon}_f)^{0.182} + 38.9(\bar{\varepsilon}_m)^{0.231} \quad \text{for } V_f = 0.25 \quad (9)$$

$$\sigma_{C,Cu\text{-}Cr} = 48.8(\bar{\varepsilon}_f)^{0.182} + 31.1(\bar{\varepsilon}_m)^{0.231} \quad \text{for } V_f = 0.40 \quad (10)$$

In the treatment above, the stress-strain behaviour of the fibre with interfacial reaction layer was assumed to be identical to that of the fibre without reaction layer. By eqs.(7)-(10), the relationships between total deformation amount introduced by rolling and tensile test, and true tensile stress are expressed. As tensile test was carried out on the rolled composites, normal tensile strength should be calculated based on the cross sectional area of the rolled composites. Here, as tensile strain is much smaller than the equivalent strain introduced by rolling, it can be neglected. Then, we can calculate tensile strength of composites by inserting equivalent strains into $\bar{\varepsilon}_f$ and $\bar{\varepsilon}_m$. As, in this work, parallel rolling produced nearly equal deformation amounts in the fibres and the matrix, equivalent plastic strain of the composite, $\bar{\varepsilon}_c$, is substituted into $\bar{\varepsilon}_f$ and $\bar{\varepsilon}_m$. $\bar{\varepsilon}_c$ is calculated by eq.(11) using the measured plastic strains in three axes, $\bar{\varepsilon}_1$, $\bar{\varepsilon}_2$ and $\bar{\varepsilon}_3$.

$$\bar{\varepsilon}_c = \sqrt{2}/3\sqrt{(\bar{\varepsilon}_1 - \bar{\varepsilon}_2)^2 + (\bar{\varepsilon}_2 - \bar{\varepsilon}_3)^2 + (\bar{\varepsilon}_3 - \bar{\varepsilon}_1)^2} \quad (11)$$

In the case of perpendicular rolling, $\bar{\varepsilon}_f$ is not equal to $\bar{\varepsilon}_m$. However, as $\bar{\varepsilon}_f$ and $\bar{\varepsilon}_m$ were not measured in this work, eqs.(7)-(10) are unapplicable. Now, we deduce σ_f from Vickers hardness and take the tensile strength of the matrix σ_{mu} as σ_m^* . Thus we can calculate σ_c by eq.(12).

$$\sigma_c = \sigma_f V_f + \sigma_{mu} V_m \quad (12)$$

Let's compare the calculated values with the measured ones.

(1)Mo/Cu composite

Fig.7 shows eqs.(4)(5)(7)(8) represented by the dotted curves and the measured curves represented by the solid curves in the case of parallel rolling versus hypothetic normal elongation e_c which was calculated by eq.(13)

$$\bar{\varepsilon}_c = \ln(1 + e_c) \qquad (13)$$

Figs.8 and 9 show the measured and calculeted strengths plotted against cold work for the cases of parallel and perpendicular rollings, respectively. The measured values agree well with the calculated ones on the basis of the rule of mixtures, whether the rolling direction is parallel or perpendicular. In this composite, fracture of the fibres during rolling gives no serious damage on tensile strength.

(2)Mo/Cu-Cr composite

The measured tensile strength of Mo/Cu-Cr composite showed lower values than the calculated ones for both of the rolling directions. In Fig.10, the measured and calculated values in the case of parallel rolling versus cold work above 40 % are shown, together with $\sigma_m^* V_m (=\sigma_{mu} V_m)$ for comparison. The lower bound of the measured values are lower than $\sigma_m^* V_m$ when cold work is over 80 %. This fact means that, in the severely rolled Mo/Cu-Cr composite, the existence of the fibres reduces the tensile strength of the composite.

Now, let's deduce which factor among (c)-(k) reduced the tensile strength of Mo/Cu-Cr composite. As the rolling behaviour of this composite is nearly same as that of

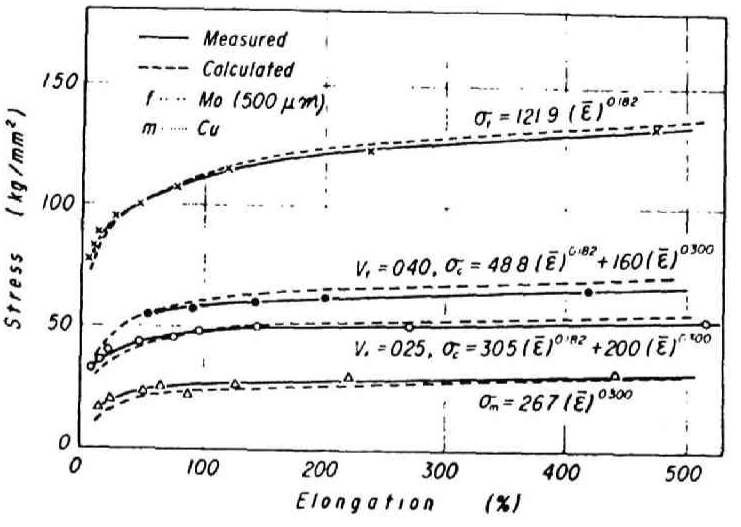

Fig.7 Hypothetic stress-strain curves. Equivalent plastic strain caused by cold rolling parallel to fibres is assumed to be identical to that caused hypothetically by tensile test.

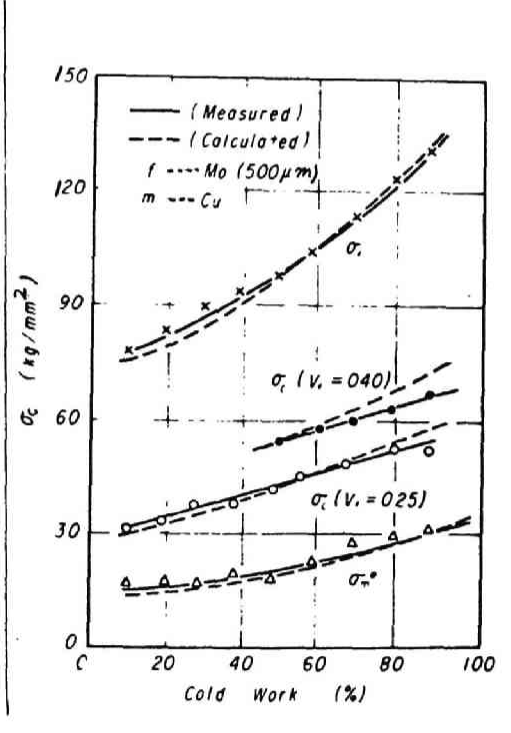

Fig.8 Comparison of the measured tensile strength of Mo/Cu composites cold rolled parallel to fibres with the strength calculated by eqs.(7) and (8).

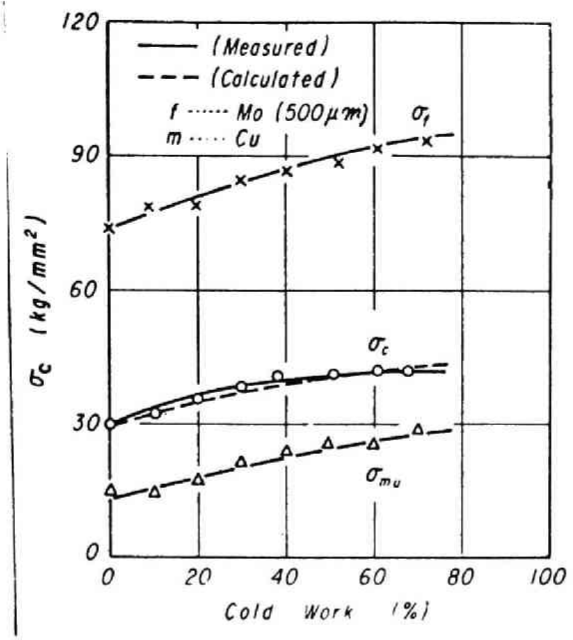

Fig.9 Comparison of the measured tensile strength of Mo/Cu composites with the strength calculated by eq.(12), for perpendicular rolling.

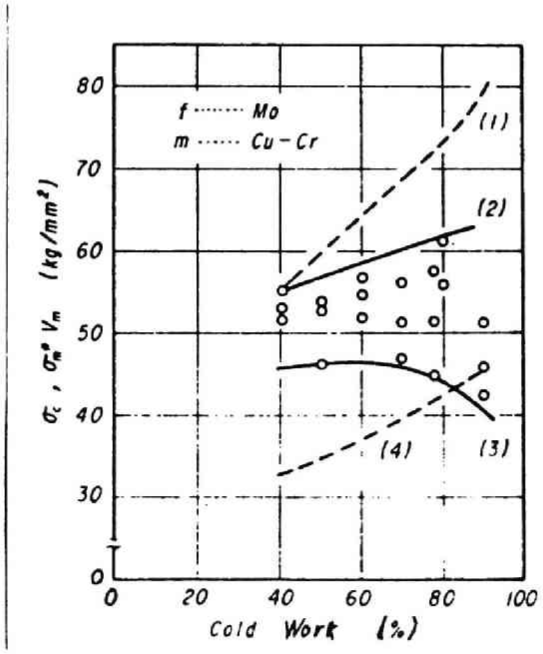

Fig.10 Comparison of the measured tensile strength of Mo/Cu-Cr composites cold rolled parallel to fibres with the calculated σ_c and $\sigma_m^* V_m$. (1), (2), (3), and (4) refer to σ_c calculated by eq.(9), upper bound of the measured σ_c, lower bound of the measured σ_c and $\sigma_m^* V_m$, respectively.

Mo/Cu composite, the factors of (d), (h), (i) and (j) can be excluded. One of the difference between Mo/Cu-Cr composite and Mo/Cu one is that Mo-Cr sloid solution layer is formed during preparation in the former composite, while no reaction layer is found in the latter one. This layer will be broken prior to the failure of the non-reacted part in the fibres. Stress concentration at the formed notches in the peripheral zone of the fibres will hasten the failure of the fibres. Furthermore, strong interfacial bonding will make the cracks formed by the fracture of the fibres propagate easily into the heavily deformed matrix. Such a situation may be seen in Photo 4 in which the matrix seems not to have arrested the cracks. Conclusively, the interfacial reaction reduces the tensile strength of the composite in the case of cold rolling , while it does not degrade the tensile properties in the case of the normal tensile test.

V-5 Conclusions

The cold rolling characteristics of ductile fibre-reinforced Mc/Cu and Mo/Cu-Cr composites prepared by a vaccum infiltration technique have been investigated. The main results obtained are summarized as follows:

(1)Tensile strength of Mo/Cu composite agreed well with those calculated based on the rule of mixtures in which work-hardening of the fibres and the matrix was taken into consideration.

(2)In Mo/Cu-Cr composite, tensile strength showed lower value than that calculated by the rule of mixtures,probably, due

Photo.4 Appearance of fracture surface of Mo/Cu-Cr composite cold rolled 80% parallel to fibres.

to damages by cold rolling of Mo-Cr solid solution layer formed at the interface during preparation.

References

(1)J.R.Getten and L.J.Ebert : Trans. ASM, 62(1969),869.

(2)M.Salkind, F.George and W.Tice : Trans. Met. Soc. AIME, 245(1969),2339.

(3)B.P.Strauss and R.M.Rose : Phys. Letters, 25A(1967),362

(4)H.E.Cline , B.P.Strauss, R.M.Rose and J.Wulff : Trans. ASM, 59(1966),132

(5)Chapter IV-(4)

(6)A.G.Atkins and A.S.Weinstein : Inter. J. Mech. Sci., 12(1970),641.

Chapter VI

Conclusions

In chapter II, deviations of behaviour of composites from the rule of mixtures, such as strengthening effect of the brittle zones and multiple necking of fibres were investigated. In the former part of the chapter , it was suggested that the fibre can be strengthened by the constraint effect of the notched regions formed by micro-crackings of the brittle zone, as long as the brittle zone adheres to the fibre and is not fractured by compressive transverse stress. The suggested theory satisfactorily explained the experimental results. After spalling or fracture of the brittle zone , the constraint effect was not able to exsist, and the usual rule of mixtures was applicable. In the latter part of the chapter, mechanisms of multiple necking and deformation processes of composites were studied. It was concluded that multiple necking was caused by the local transfer of load from fibre to surrounding matrix. Processes of plastic deformation of the composites at various stages were discussed, and the characteristics of each stage were described. Multiple necking occurred when the fibre volume fraction was smaller than a critical value. The critical value determined for each composite indicates that stronger matrix yields larger critical value.

In chapter III, the two important parameters for stress transfer from matrix to fibre, i.e. critical aspect ratio and shear stress at the interface were measured both by the multiple-fracture test and by the pull-out test on the composites with various interfacial conditions. The experimental results showed that the most efficient stress transfer corresponds to the case where interfacial

bonding strength is higher than the matrix shear stress, while the externally applied stress is transferred through the interface even when the interfacial bonding is almost zero. An appropriate coating and a favourable interfacial reaction produced high interfacial shear strength. The meanings of the shear stress at the interface determined by the pull-out and multiple-fracture tests were clearly understood. Namely, in the pull-out test, the shear strength of the interface was measured. On the other hand, in the multiple-fracture test, the frictional shear stress at the interface was measured when the shear strength of the interface was so weak that debonding occurred at the interface, while the shear stress in the matrix was measured when the shear strength of the interface was higher than the shear stress in the matrix.

In chapter III, effects of interfacial reaction on deformation and fracture behaviour of composites were studied. In chapter III-(2), effects of the brittle zone with multiple crackings on deformation and fracture behaviour of ductile fibre-composites were investigated by employing composites consisting of two components of aluminium-alumina as well as three components of stainless steel-brittle zone-aluminium. The strength of the fibres was raised as long as the brittle zone adhered to the fibres and was not failed in a transverse direction by compressive transverse stress as ascertained in chapter II-(2). The effects of grain size of ductile aluminium fibre on the deformation behaviour of the binary aluminium-alumina composite was clearly understood by using the strengthening theory suggested in chapter II-(2). The strengthening effects of the brittle zone on the ternary

composite arised only from the mechanical interaction between the brittle zone and the fibre. The mechanical interaction between the brittle zone and the matrix was negligible since the interfacial bonding between them was very weak. In chapter III-(3), the behaviour of W/Ni composite at room temperature was classified into three stages according to the extent of interfacial reaction. The influence of the extent of the reaction on tensile strength and elongation was discussed, and then factors, whick make the tensile strength deviate from the value calculated on the assumption that no reaction had occurred, were pointed out for each stage. Effects of interfacial reaction on the behaviour of the composite were confirmed to be dependent upon the ductility and the size of the fibre. In chapter IV-(4),the results obtained on Mo/Cu and W/Cu composites without the reaction agreed with the previous reports. The fracture of W/Cu-Cr composite with interfacial reaction occurred in an elastic range of the fibre, and the elongation and tensile strength of the composite showed lower values than those of W/Cu composite. This mode of fracture was explained in terms of a notch effect caused by the breakage of the reaction layer and a poor notch resistance of the composite arising from the increased bonding between the fibre and the matrix owing to the reaction. On the other hand, the tensile- and yield strengths of age-hardened Mo/Cu-Cr composite with interfacial reaction showed higher values than those of Mo/Cu one without the reaction. This result was explained in terms of the hardening of the matrix and the absence of detrimental effects of the Mo-Cr solid solution layer formed in the peripheral zone of

the fibre. Effects of the mechanical interaction between the constituents on the primary Young's modulus and the onset of yielding of the matrix were relatively small, but those on the behaviour in stages II and III were large. The tensile stress exerted at the interface causes transverse fracture in fibre in stage II for W/Cu-Cr composite and splitting in stage III for W/Cu, Mo/Cu and Mo/Cu-Cr composites. In chapter IV-(5), the tip radius of cracks formed by the earlier fracture of the reaction zones was calculated for W/Cu-Cr and W/Ni composites. The calculated results showed that the difference in type of interfacial reaction leads to different tip radius or stress concentration on the fibre.

In chapter V , the cold rolling characteristics of ductile fibre-reinforced Mo/Cu and Mo/Cu-Cr composites were studied. Deformation behaviour of the fibres and matrix in composites was made clear. The fibre volume fraction did not vary so much with rolling in both the cases of transverse and parallel rollings. Tensile strength of the rolled Mo/Cu composite agreed well with that calculated from the rule of mixtures in which work-hardening of the fibres and the matrix was taken into account. In the rolled Mo/Cu-Cr composite, the measured tensile strength was lower than the calculated one, probably due to the damages caused by breakage of the reaction zone during cold rolling.

On a macroscopic scale, effects of interface on deformation and fracture behaviour of composites have been widely investigated and been made clear in some detail in this work. However, on a microscopic scale, many problems such as mechanisms of bonding and dislocation behaviour in

composites remain still unsolved. Very careful and detailed studies are required to solve these problems at microscopic level. Microscopic and macroscopic studies, making up for each other, will establish interfacial characteristics which are the most important plblems for composite materials.

Finally, tests using single fibre-composites have proved to be very useful to study interface characteristics. This approach makes it possible to understand the independent role of interfaces on mechanical behaviour of composites in a relatively simple fashion. This approach is expected to be applied to a wide range of interface problems in composites.

Acknowledgements

The author would like to express his greatest appreciation to Professor Yotaro Murakami who guided the author to the study of this problem and has given the constant encouragement, discussions and suggestions through the course of this study.

The author wishes to express his gratitude to the following persons, since without any help of them, this study could not have the present form.

To Professor Moriya Oyane for helpful discussions on chapter V.

To Assistant Professor Kozo Osamura for the observation using scanning electron microscope, the constant encouragement and helpful discussions.

To Dr. Satoru Yamamoto for helpful discussions.

To Mr. Hajimu Yamanaka for his assistance in various aspects of the experimental work.

To Mrs. Makoto Mizuhara, Masafumi Kawasaki, Kensuke Shimomura, Shigeru Okuda and Hidemasa Tanaka for the cooperation in the experiments.

To Dr. Minoru Umemoto for his help in preparing the manuscript.

To all the members of Murakami's Laboratory for the hospitality and encouragement.

To his parents for the hospitality and encouragement.

The List of Published Papers

1. Shojiro Ochiai, Makoto Mizuhara and Yotaro Murakami : Deformation and Fracture Behaviours of Composites of Copper and Copper-Chromium Alloys Reinforced with Tungsten or Molybdenum Fibres
   Journal of the Japan Institute of Metals, 37(1973),208-215.

2. Shojiro Ochiai, Makoto Mizuhara and Yotaro Murakami : Deformation Behaviour and Deviation from the Simple Rule of Mixtures for Ultimate Tensile Strength in the Colled Rolled Fibre-Reinforced Composites.
   Journal of the Japan Institute of Metals, 37(1973),579-588.

3. Shojiro Ochiai, Makoto Mizuhara, Masafumi Kawasaki and Yotaro Murakami : The Room and Elevated Temperature Tensile Properties of a Unidirectionally Solidified Quasi-Binary Al-S($Cu_2Mg_2Al_5$) Eutectic Composite Alloy.
   Transactions of the Japan Institute of Metals, 15(1974),66-74.

4. Yotaro Murakami, Shojiro Ochiai and Makoto Mizuhara : Studies on Composites of Copper and Copper Alloys Reinforced with Metallic Fibres.
   Journal of the Japan Copper and Brass Research Association, 13(1974),104-119.

5. Shojiro Ochiai, Makoto Mizuhara, Kensuke Shimomura and Yotaro Murakami : Effects of Interfacial Conditions on Critical Aspect Ratio of Fibres in Single-Fibre Composites.
   Transactions of the Japan Institute of Metals,16(1975),345-352.

6. Shojiro Ochiai, Kensuke Shimomura, Makoto Mizuhara and Yotaro Murakami : Effects of Interfacial Reaction on Deformation and Fracture Behaviour of Tungsten fibre-Nickel Matrix Composite.
   Transactions of the Japan Institute of Metals,16(1975),463-471.

7. Shojiro Ochiai, Kensuke Shimomura and Yotaro Murakami : Multiple Necking of Fibre in Single Tungsten Fibre Composites.
   Metal Science, 9(1975),535-540.

8. Shijiro Ochai, Shigeru Okuda, Kensuke Shimomura and Yotaro Murakami : Effects of Interfacial Conditions on Shear Strength of Interface and Critical Aspect Ratio in Tungsten-Copper Composites.
Transactions of the Japan Institute of Metals, 17(1976),649-654

9. Shojiro Ochiai and Yotaro Murakami : The Strengthening Effects of Brittle Zones on Ductile-Fibre Composites.
Metal Science, 10(1976),401-408.

10. Shojoro Ochiai and Yotaro Murakami : Deformation and Fracture Behaviour of Composites with Brittle Zones on Fibre Surfaces.
Transactions of the Japan Institute of Metals, 18(1977),384-392.

11. Shojiro Ochiai, Makoto Mizuhara and Yotaro Murakami : Mechanical Properties of Carbon Fibre Reinforced Copper Matrix Composites.
Journal of the Japan Institute of Metals, (in press)